THE QUANTUM HAMILTON-JACOBI FORMALISM APPROACH TO ENERGY SPECTRA OF POTENTIAL PROBLEMS

A Thesis

Submitted In Partial Fulfilment

For The Degree Of

DOCTOR OF PHILOSOPHY

By

R.S.BHALLA

SCHOOL OF PHYSICS

UNIVERSITY OF HYDERABAD

HYDERABAD - 500 046

INDIA

JULY 1996

To,
My Grandparents

CERTIFICATE

This is to certify that, I, Ramandip Singh Bhalla, have carried the research embodied in this Ph.D. thesis titled *"The quantum Hamilton-Jacobi formalism, approach to energy spectra of potential problems"* under the supervision of Prof. A.K. Kapoor, for the full period prescribed under the Ph.D. ordinances of the University of Hyderabad.

It is further declared to the best of my knowledge, that no part of the research work presented in this thesis was submitted for the award of research degree, of any other university.

RSBhalla

(Ramandip Singh Bhalla)
School of Physics,
University of Hyderabad.

AKKapoor

(Prof. A.K. Kapoor)
Thesis Supervisor,
School of Physics,
University of Hyderabad

KNSh

Dean
School of Physics,
University of Hyderabad

Prof. K.N. Shrivastava
DEAN
SCHOOL OF PHYSICS
University of Hyderabad.

Table of Contents

1 Introduction **1**

References **4**

2 The Hamilton-Jacobi Formalism **6**

2.1 The classical Hamilton-Jacobi Formalism 6

2.2 The quantum Hamilton-Jacobi Formalism 13

2.3 Harmonic oscillator. **19**

References **23**

3 Solvable examples from quantum mechanics **24**

3.1 Harmonic oscillator on the half-line 24

3.2 Morse oscillator 28

3.3 The infinite well 35

3.4 Three Dimensional case 38

References **52**

4 Supersymmetry in quantum mechanics **53**

4.1 Operator method for the harmonic oscillator and SUSY algebra 54

4.2 Eigenvalues of shape invariant potentials 59

4.3 Broken and unbroken SUSY and Gozzi Index 61

References **64**

5 Examples from SUSY quantum mechanics **65**

5.1 Eckart Potential 66

5.2 Other SUSY potentials 72

References 78

6 Analyses of phases of supersymmetry in quantum mechanics 79

6.1 Generalized Poschl-Teller potential 80

6.2 Scarf I (trigonometric) potential 92

6.3 Other potentials with supersymmetry 99

References 103

7 Exactness Of The SWKB Formula **104**

7.1 Comparison of J_{SWKB} and $J(E)$ 107

7.2 Analysis of potentials of the type $V(x) = \omega^2(x) + \hbar\beta\omega'(x)$ 114

7.3 Analysis of non-exact SWKB approximation cases 117

7.4 Conclusions 119

References **127**

Acknowledgements

I take pleasure in expressing my deep sense of gratitude to my supervisor and mentor, Prof. A.K. Kapoor, for his valuable guidance, constant encouragement and inspiration throughout the course of the present investigation.

I am thankful to Dr. Prasanta K. Panigrahi for his keen interest and valuable suggestions which went a long way in helping me complete my work.

I thank Prof. V. Srinivasan and Prof. S. Chaturvedi, Dr. Hindu A. Bambah, Dr. P. Anantha Lakshmi, Dr. C. Nagaraja Kumar and other faculty members for the cooperation and advice extended to me from time to time.

I thank Dr. C. Mukku, dept. of mathematics, Univ. of Hyderabad, Dr. Ranjan Shrivastava and Sanjai Verma, MRI, for their expert advice and ready help, at the computer.

I thank, Prof. K.N. Shrivasata, Dean and Prof A.P. Pathak, former Dean, School of Physics, for permitting me to avail the facilities at the School of Physics.

I am also thankful to Prof. G.S. Agarwal and Prof. A.K. Bhatnagar, coordinator, SAP for providing financial assistance for a part of my work at Hyderabad.

I thank Dr. U.K. Gupta, Director, N.G.R.I and his colleagues, for their help and advice.

My sincere thanks are due to Prof. H.S. Mani, Director, Mehta Research Institute of Mathematics and Mathematical Physics, Allahabad, for extending facilities and providing financial assistance during my stay at MRI.

I thank all my colleague's and friends at University of Hyderabad as well as at MRI, for the memorable time they have given me.

I am grateful to my grand parents and parents, sister and brother in law, uncles, aunts and other family members, for their blessings and concern.

Last but not the least, I owe special thanks to Ms. Sumira Singh, who was instrumental in giving me the requisite motivation to complete my work.

Chapter 1

Introduction

The Hamilton-Jacobi theory is well developed in classical mechanics and has been useful in providing an independent and often useful route for solving dynamical equations [1]. In particular, for periodic motion, the action variable enables one to obtain the frequencies of a given system directly without having to solve the equations of motion completely. The quantum Hamilton-Jacobi (QHJ) formalism has been developed along the lines of the classical Hamilton-Jacobi theory since the inception of quantum mechanics, by the pioneers of the field [2]. It has been recently shown that, analogous to the classical periodic systems, the quantum action variable can be profitably employed to arrive at the *exact* energy eigenvalues for potential problems, without obtaining the corresponding wave functions provided boundary conditions are applied judiciously [3, 4]. This is to be contrasted with the standard procedure to tackle bound state problems, where, the Schrodinger equation is solved both for the eigenvalues and eigenfunctions. In a series of papers [5-10], we have applied the quantum Hamilton-Jacobi (QHJ) formalism [3, 4], to the following:

a) To solve the bound state problems in quantum mechanics [5], to demonstrate the power of this method.

b) Examples from supersymmetric (SUSY) quantum mechanics where exact energy eigenvalues are arrived at, demonstrating the working of this method making use of

properties of SUSY quantum mechanics [6, 11, 12].

c) To analyze cases of broken and unboken SUSY within this framework [8, 9].

d) To gain a better understanding of the working of the semi-classical approximation schemes like SUSY WKB which is exact in certain potentials, where as fails to give exact results for certain cases, and are able to quantify the difference between the exact answer and the SUSY WKB approximation scheme [7, 13]. We see how the QHJ formalism helps give the exact answers, for cases where SUSY WKB fails to give exact answers [10].

In this thesis, the Hamilton-Jacobi formalism in context of quantum mechanics is studied and applied to a whole set of potential problems in supersymmetric and ordinary quantum mechanics and exact energy eigenvalues are obtained.

In Chapter II the Hamilton-Jacobi formalism is briefly reviewed both in the context of classical as well as quantum mechanics [3-5]. Chapter III deals with the application of the quantum Hamilton-Jacobi (QHJ) formalism to some solvable examples in quantum mechanics, to elucidate the power of this method. Chapter IV deals with supersymmetric (SUSY) quantum mechanics and includes concepts of shape invariance, exactness of SUSY WKB [11, 12], broken and unbroken SUSY quantum mechanics [15, 14] and the Gozzi Index [16]. The evaluation of the SUSY WKB approximation quantization condition using complex integration technique which is similar to the evaluation of the action integral in the QHJ formalism [5-7] is also discussed. Chapter V contains one dimensional potential problems where the Hamiltonians are factorizable. We show how the energy eigenvalues are computed for these examples making use of the above properties [6]. In Chapter VI unbroken

and broken phases of SUSY are analyzed, making use of the QHJ formalism and we are able to show that the boundary conditions as will be discussed in the following chapters, implies a set of conditions on the parameters that appear in the potential, and allows us to determine if SUSY is exact or broken for a given range of values of the parameters [8]. We briefly discuss the Gozzi index which can be used to differentiate between spontaneously broken and unbroken SUSY, and its relationship with the QHJ formalism. Chapter VII deals with a detailed analysis of the exactness of SUSY WKB approximation, using QHJ and the complex integration technique. We also discuss why SUSY WKB fails to give exact answers in other examples. It is shown as to how QHJ gives exact answers for cases where SUSY WKB fails and conditions under which SUSY WKB would give exact answers are discussed [7, 10]. We finally end with our conclusions in Chapter VII with a brief summary on further directions and applications of this work.

References

[1] H. Goldstein, *Classical Mechanics* (Addison-Wesley, New York, 1980).

[2] P.A.M. Dirac, *The Principles of Quantum Mechanics* (Oxford University Press, London, 1958); for some original articles and references see, J. Schwinger, *Quantum Electrodynamics* (Dover, New York, 1958).

[3] R.A. Leacock and M.J. Padgett, Phys. Rev. Lett. **50**, 3 (1983).

[4] R.A. Leacock and M.J. Padgett, Phys Rev. D28, 2491 (1983).

[5] R.S. Bhalla, A.K. Kapoor and P.K. Panigrahi *Quantum Hamilton-Jacobiformalism and the bound state spectra*, (quant-ph/9512018), to appear in Am. Jour. Phys. (1997).

[6] R.S. Bhalla, A.K. Kapoor and P.K. Panigrahi, *Energy eigenvalues for a class of one dimensional potentials via quantum Hamilton-Jacobi formalism* (hep-th/9507154), under consideration for publication in Jour. Phys. A.

[7] R.S. Bhalla, A.K. Kapoor and P.K. Panigrahi, *Exactness of the super-symmetric WKB approximation scheme* (quant-ph/9512019), to appear in Phys. Rev. A, (1996).

[8] R.S. Bhalla, A.K. Kapoor and P.K. Panigrahi, *Quantum Hamilton-Jacobianalysis of phases of supersymmetry in quantum mechanics* submitted to Int. Jour. Mod. Phys. A.

[9] R.S. Bhalla, A.K. Kapoor and P.K. Panigrahi, *Quantum Hamilton-Jacobiformalism and broken SUSY WKB approximation scheme,* submitted to Phys. Lett. A.

[10] R.S. Bhalla, A.K. Kapoor and P.K. Panigrahi, *Isospectral Hamiltonians and quantum Hamilton-Jacobi formalism* (under preparation).

[11] R. Dutt, A. Khare, and U.P. Sukhatme, Am. Jour. of Phys. **56**, 163 (1988)

[12] F. Cooper, A. Khare and U.P. Sukhatme, Phys. Rep. **251,** 267 (1995).

[13] K. Raghunathan, M. Seetharaman and S.S. Vasan, Phys. Lett. **B188,** 351 (1987).

[14] R. Dutt, A. Gangopadhyaya, Avinash Khare. A. Pagnamenta and U. Sukhatme, Phys. Lett. **A174**, 363 (1993).

[15] R. Dutt. A. Gangopadhyaya, Avinash Khare, A. Pagnamenta and U. Sukhatme, Phys. Rev. D48, 1845 (1993).

[16] E. Gozzi, Phys. Rev. D12, 3665 (1986).

Chapter 2

The Hamilton-Jacobi Formalism

This thesis would be dealing with the time independent Hamiltonian. In what follows, we briefly discuss the Hamilton Jacobi formalism in context of classical mechanics in section 2.1. In section 2.2 we develop this formalism in context of quantum mechanics. This formalism is applied to the harmonic oscillator, in both the classical (section 2.1) and to quantum (in section 2.3) approach for comparison and to elucidate the working of this method.

2.1 The classical Hamilton-Jacobi Formalism

In classical mechanics, the Hamilton Jacobi theory is well developed and provides an independent and often a powerful method of solving the dynamical equations [1]. We first consider the general approach wherein, the Hamiltonian $H(q, p, t)$is any general function of q, p and t. A canonical transformation from the coordinate and momenta (q, p) at time t, to a new set of constant quantities, (such as the 2n initial values (q_0, p_0), at $t = 0$) is sought such that the new coordinate system, of the transformed Hamiltonian, K; Qi and P_i are constants in time. This is automatically ensured by requiring that the transformed Hamiltonian K is identically zero. We then have,

$$\frac{\partial K}{\partial P_i} \equiv \dot{Q}_i = \{Q_i, K\} = 0 \ , \tag{2.1}$$

$$-\frac{\partial K}{\partial Q_i} \equiv \dot{P}_i = \{P_i, K\} = 0 \ . \tag{2.2}$$

The equations of transformation relating the old and the new canonical variables,

$$\begin{aligned} q &= q(q_0, p_0, t) \ , \\ p &= p(q_0, p_0, t) \ , \end{aligned} \tag{2.3}$$

are then exactly the solution of the problem, as they give the coordinates and momenta as a function of their initial values and time.

K is related to the old Hamiltonian, using canonical transformation; given by

$$K = H(q, p, t) + \frac{\partial F}{\partial t} \ . \tag{2.4}$$

K is required to be zero and F, the generating function, is then taken as a function of the old coordinates q_i, the new constant momenta P_i and time t. i.e., $F_2(q_i, P_i, t)$, which is one of the possible forms for the generating functions involving canonical transformations. Therefore,

$$p_i = \frac{\partial F_2}{\partial q_i} \ , \tag{2.5}$$

$$Q_i = \frac{\partial F_2}{\partial P_i} \ , \tag{2.6}$$

$$\tag{2.7}$$

We then have (2.4) as

$$H(q_1, q_2, \cdots, \frac{\partial F_2}{\partial q_n}, \cdots \frac{\partial F_2}{\partial q_n}, t) + \frac{\partial F_2}{\partial t} = 0 \quad . \tag{2.8}$$

This is the Hamilton-Jacobi equation, and constitutes a partial differential equation, in (ft + 1) variables, $q_1, \cdots, q_n, t$, for the generating function F_2. A complete solution 5, for this first order partial differential equation involves $n + 1$ variables involving $n + 1$ constants of integration. The momenta P_i which have not been specified, are required to be constants. We therefore take these n independent constants of integration α_i *to* be the new (constant) momenta. This generating function $F_2 = S$, is called the Hamilton's principal function, and is denoted by, $S(q_1, q_2, \cdots, q_n, \alpha_1, \cdots, \alpha_n t)$. Therefore (2.5) and (2.6) can now be written as,

$$p_i = \frac{\partial S(q_i, \alpha_i, t)}{\partial q_i} \quad , \tag{2.9}$$

$$Q_i = \beta_i = \frac{\partial S(q_i, \alpha_i, t)}{\partial \alpha_i} \quad . \tag{2.10}$$

At $t = t_0$, from (2.9) we have 'n'equations involving 'n'α's, with the initial values of q_i and p_i which are known; and one is able to calculate these constants in terms of the initial values of the problem. Similarly the constant β_i can be obtained from the initial conditions. Therefore,

$$q = q(\alpha_i, \beta_i, t) \quad , \tag{2.11}$$

which solves the problem, by giving the coordinates as function of time and initial conditions.

It is seen that the above approach is applicable only when S could be separated into two parts, one involving q and the other time. Such a separation is always

possible whenever the Hamiltonian does not involve time explicitly. We then have the Hamilton-Jacobi equations for 5 as,

$$\frac{\partial S}{\partial t} + H(q_i, \frac{\partial S}{\partial q_i}) = 0 \quad . \tag{2.12}$$

From the above equation we see that the first term involves only dependence on t, while the second one depends only on q_i. The time variation can therefore be separated by assuming a trial solution

$$S(q_i, \alpha_i, t) = W(q_i, \alpha_i) - \alpha_1 t \quad . \tag{2.13}$$

We thus have

$$H\left(q_i, \frac{\partial W}{\partial q_i}\right) = \alpha_1 \tag{2.14}$$

which no longer involves time. One of the constants of integration, appearing in 5, namely α_1, is thus equal to this constant value of H. This time independent function W appears merely as a part of the original generating function (the characteristic function) when H is constant, and becomes the new generating function, denoted by $W(q, P)$ and is termed as the Hamilton's characteristic function in literature; We then have the equations of transformation as in (2.5) and (2.6) given by,

$$p_i = \frac{\partial W}{\partial q_i} \ , \quad Q_i = \frac{\partial W}{\partial P_i} = \frac{\partial W}{\partial \alpha_i} \quad .$$

and the condition that determines W is that H is equal to the new momentum α_1. Therefore,

$$H\left(q_i, \frac{\partial W}{\partial q_i}\right) = H(q_i, p_i) = \alpha_1 \quad . \tag{2.16}$$

Since W does not involve time, the new and the old Hamiltonians are equal, it follows that

$$K = \text{a}, \quad ,$$

and W generates a canonical transformation in which, all the new coordinates are cyclic. The canonical equations for P give,

$$\dot{P}_i = -\frac{\partial K}{\partial Q_i} = 0 \quad , P_i = \alpha_i \quad , \tag{2.17}$$

$$\begin{aligned} \dot{Q}_i &= \frac{\partial K}{\partial P_i} = 1 \quad , i = 1, \\ &= 0 \, , \qquad i \neq 1, \end{aligned} \tag{2.18}$$

as the new Hamiltonian depends only on one of the momenta α_i. For (2.18) we have the following solutions;

$$\begin{aligned} Q_1 &= t + \beta_1 \equiv \frac{\partial W}{\partial \alpha_1} \quad , \\ Q_i &= \beta_i \equiv \frac{\partial W}{\partial \alpha_i} \qquad i \neq 1. \end{aligned} \tag{2.19}$$

So the only coordinate that is not simply a constant of motion is Q\. It is not necessary for one to choose α_1 and the **constants of integration in W, as** the new **constant momenta. In general one can make use of a particular set of n independent functions of the α_i's as the transformed momenta. Given 7,'s are these constants, we have**

$$\dot{Q}_i = \frac{\partial K}{\partial \gamma_i} = \nu_i \quad , \tag{2.20}$$

where ν_i's are functions of γ_i's. Therefore,

$$Q_i = \nu_i t + \beta_i \ . \tag{2.21}$$

When the Hamiltonian does not involve time explicitly, both these methods are suitable, and the generating functions are then related to each other according to the formula

$$S(q, P, t) = W(q, P) - \alpha_1 t \ . \tag{2.22}$$

The Hamilton-Jacobi theory is applicable to periodic systems where one defines the action variable J_i, given by

$$J_i = \oint p_i dq_i \ , \tag{2.23}$$

as the transformed (constant) momentum P, where the integration is carried over a complete period. So one has $H = H(J)$ and the characteristic function $W = W(q_i, \cdots q_n, J_1 \cdots J_n)$. The corresponding generalized coordinate Q_i conjugate to J_i is defined as the angle variable $w_i = \frac{}{\partial J}$ and the equation of motion for this is given by

$$\dot{w}_i = \frac{\partial H(J_1 \cdots J_n)}{\partial J_i} = \mu_i(J_1 \cdots J_n) \ ,$$

where μ_i's are a set of constant functions, which implies,

$$w_i = \mu_i t + \beta_i \ , \tag{2.24}$$

as arrived at earlier in (2.21). Now the change in w for a complete cycle of q_j is,

$$\triangle w_i \ = \ \oint \frac{\partial w_i}{\partial q_j} dq_j = \oint \frac{\partial^2 W}{\partial q_j \partial J_i} dq_j = \frac{d}{dJ_i} \oint \frac{\partial W}{\partial q_j} dq_j \ ,$$

$$= \frac{d}{dJ_i} \oint p_j dq_j = 1 \quad . \tag{2.25}$$

Therefore,

$$\triangle w_i = \frac{\partial J_j}{\partial J_i} = \delta_{ij} \quad .$$

From (2.24) we have,

$$\triangle w = 1 = \nu\tau \quad , \tag{2.26}$$

where r is period for a complete cycle of q and v is the reciprocal of the period r and is therefore the frequency associated with the periodic motion of q. Thus, one is able to arrive at the frequencies of a periodic system without having to completely solve the equations of motion. Let us apply the above technique to the classical harmonic oscillator for elucidating the power of this method, for which the action variable is given by,

$$J = \oint pdq = \oint \sqrt{2mE - m^2\omega^2 q^2} dq \quad . \tag{2.27}$$

where E is the total energy and $\omega^2 = k/m$. The substitution,

$$q = \sqrt{\frac{2\alpha}{m\omega}} \sin\theta \quad , \tag{2.28}$$

in (2.27) along with some further simplification gives

$$\begin{aligned} J &= \frac{2\pi E}{\omega} \quad , \\ \Rightarrow E \equiv H &= \frac{Jw}{2\pi} \quad . \end{aligned} \tag{2.29}$$

Therefore.

$$\frac{\partial H}{\partial J} \equiv \nu = \frac{w}{2\pi} = \frac{1}{2\pi}\sqrt{\frac{k}{m}} \quad , \tag{2.30}$$

which is the standard formula for the frequency of the harmonic oscillator problem. Applying the Hamilton- Jacobi formalism, one is thus able to directly arrive at the frequencies of periodic systems, without having to solve the equations of motion.

2.2 The quantum Hamilton-Jacobi Formalism

The quantum Hamilton-Jacobi (QHJ) formalism is built on lines of the classical Hamilton-Jacobi theory and has been studied since the inception of quantum mechanics [2]. In fact, this approach was christened as the "Royal road to quantization" in the early days of quantum mechanics [3]. It has recently been shown that, in analogy to the classical periodic systems, the quantum action variable can be profitably employed to arrive at the energy eigenvalues for potential problems, without the necessity of obtaining the corresponding wave functions [4]. This is to be contrasted with the standard procedure for tackling bound state problems, where the Schrodinger equation is solved both for the eigenvalues and eigenfunctions [6].

The quantum equivalent of the Hamiltonian is the Schrodinger (representation of the Hamiltonian) equation wherein x and p are operators rather than mere observables and this is given as

$$\hat{H} = \frac{\hat{p}^2}{2m} + V(x) \tag{2.31}$$

where

$$\hat{p} = \frac{\hbar}{i}\frac{\partial}{\partial x} \quad \text{and} \quad \hat{x} = x \ .$$

A quantum canonical transformation to a new set of coordinates Q and P is done such that the new Hamiltonian is independent of Q; Although, a complete operator formalism can be given an equivalent formulation in terms of the eigenvalues $(x, p, Q, P$ and $E)$ of $\hat{x}, \hat{p}, P, Q$ and H respectively, is pursued here to avoid the complication arising from operator ordering. Parallel to the classical case, the corresponding "quantum" characteristic function $W(<r\ P\backslash$ yields:

$$p = \frac{\partial W(x, E(P))}{\partial x} \ ,$$

and

$$Q = \frac{\partial W(x, E(P))}{\partial P} \ ,$$

where $W(x,E(P))$ is the corresponding "quantum" characteristic function and the "quantum" Hamilton-Jacobi equation for the characteristic function is given as

$$\frac{\hbar}{i}\frac{\partial^2 W(x, E)}{\partial x^2} + \left(\frac{\partial W(x, E)}{\partial x}\right)^2 = E - V(x) \ . \tag{2.32}$$

$W(x,E)$ is required to satisfy certain boundary conditions associated with its definition and will be discussed a little later in this section. The new momentum P, is defined only in terms of only E, $P = P(E)$ and the QHJ equation for Hamilton's principal function is postulated as in the classical case as

$$\frac{\hbar}{i}\frac{\partial^2 S}{\partial x^2} + \left(\frac{\partial S}{\partial x}\right)^2 = -\frac{\partial S}{\partial t} - V(x) \quad . \tag{2.33}$$

For the time independent case one can use either approach and can arrive at (2.32) from (2.33), by writing

$$S = W - Et \ .$$

This is seen in the classical case also. We can thus say that the time-independent Hamilton Jacobi theory based upon Hamilton's characteristic function W is the required quantum theory for stationary states.

Once again, taking the classical case as a guide, on lines of the classical action variable, the quantum action variable in context of quantum mechanics is written by assuming that $V(x)$ allows periodic motion. One is thus required to define a quantum momentum function $p(x, E)$ in terms of the quantum characteristic function $W(x,E)$ by

$$p(x, E) \equiv \frac{\partial W(x, E)}{\partial x} \quad , \tag{2.34}$$

and on substituting this in (2.32), one arrives at the QHJ equation in $p(x, E)$, given by

$$\begin{aligned} \frac{\hbar}{i}\frac{\partial p(x, E)}{\partial x} + p^2(x, E) &= E - V(x) \\ &= p_c^2(x, E) \ . \end{aligned}$$

Here $p_c(x, E) = (E - V(x))^{\frac{1}{2}}$ is the classical momentum function and this is used to calculate the physical turning points, between which, the classical motion takes

place, are defined as the points where $p_c(x,E)$ vanishes. $p_c(x,E)$ has a branch cut enclosing these physical turning points, in the complex x plane in which $p_c(x,E)$ is defined by taking that branch of the square root as positive at a point just below the cut. This helps in determining the sign of $p_c(x,E)$ through out the complex plane by analytical continuation. Also note that

$$p(x,E) \stackrel{\hbar\to 0}{\to} p_c(x,E) \quad . \tag{2.35}$$

This can be thought of as a manifestation of the *correspondence principle* or as a *boundary condition* on the QMF. As will be seen explicitly later, the above condition helps in determining $p(x,E)$ unambiguously. The quantum characteristic function $W(x,E)$ is related to the energy eigenvectors in the coordinate representation as,

$$\psi(x,E) = < x|E > = e^{\frac{iW(x,E)}{\hbar}} \quad , \tag{2.36}$$

and in the same representation,

$$\begin{aligned} < x|\hat{p}|E > = -i\hbar\frac{\partial}{\partial x} < x|E > &= \frac{\partial W}{\partial x} < x|E > \\ &= p(x,E) < x|E > \end{aligned} \tag{2.37}$$

Thus, one gets

$$p(x,E) = \frac{\hbar}{i}\frac{1}{\psi}\frac{\partial\psi(x,E)}{\partial x} \quad . \tag{2.38}$$

It is straightforward to check that the Schrodinger equation goes over to the corresponding quantum H-J equation under the above substitution and vice versa.

The quantum analog of the classical action variable is defined as

$$J(E) \equiv (1/2\pi) \oint_C dx\, p(x, E) \quad . \tag{2.39}$$

Here, C is a counterclockwise contour in the complex $x-$plane enclosing the real line between the classical turning points. The wave function is known to have nodes between the classical turning points. These nodes correspond to poles of the quantum momentum function. To see this clearly, near a zero of the wave function, located at x_0, we write,

$$\psi = (x - x_0)\phi(x) \quad . \tag{2.40}$$

This implies,

$$p \approx \frac{\hbar}{i} \frac{1}{x - x_0} + \cdots \tag{2.41}$$

It is thus seen that, $p(x, E)$ has a first order pole at x_0 with residue $-i\hbar$. One can also verify the correctness of Eq. (2.41) directly from the quantum H-J equation. Substituting Eq. (2.41) in the QHJ equation, one sees that the contributions of these poles from $p^2(x, E)$ and $-i\hbar\partial p(x, E)/dx$ cancel each other only if they are of first order, each having the residue $-i\hbar$. The first order poles are of quantum mechanical origin and their positions are energy dependent, being the same as the zeros of the energy eigenfunction. Just as the zeros of the wave function change their positions with energy, so do the location of the corresponding poles in the QMF. These poles will be referred to as the moving poles.

The quantum H-J equation shows that, $p(x, E)$ can have singularities in the complex x plane, other than the moving poles on the real axis. These singular points correspond to the singular points of the potential term $V(x)$. The locations of these

singularities are, quite obviously, independent of energy; these poles will be called fixed poles.

For a given energy level, the quantum number 'n'equals the number of nodes of the wave function and hence it counts the number of moving poles of $p(x, E)$ inside the contour C appearing in the definition of the quantum action variable given by Eq. (2.39). The residue of each of these poles is $-i\hbar$.Hence, we have

$$J(E) = n\hbar \quad , \tag{2.42}$$

as an exact quantization condition.

Even though this approach appears similar to that of the familiar WKB scheme, it is worth pointing out that Eq. (2.42), when inverted for E, reproduces the *exact* quantized energy eigenvalues.

Although , the location and the number of the moving poles are not known *a priori*, a suitable deformation of the contour in the complex plane and change of variables allows one to compute $J(E)$,for many potentials, in terms of the fixed poles whose locations and residues are known. In what follows, the QHJ formalism is applied to the harmonic oscillator problem in quantum mechanics both for comparison with the classical harmonic oscillator problem as well as to show the working of the formalism.

2,3 Harmonic oscillator

The QHJ equation for the harmonic oscillator problem with $V(x) = m\omega^2 x^2/2$ is,

$$p^2 + \frac{\hbar}{i}\frac{\partial p(x,E)}{\partial x} = 2m(E - \frac{m\omega^2 x^2}{2}) \equiv p_c^2 \ . \tag{2.43}$$

The turning points, determined from $p_c^2(x,E) = 0$, are $-x_1 = x_2 = +\sqrt{2E/(m\omega^2)}$. The quantization condition is given by

$$J(E) = (1/2\pi)\oint_C p(x,E)dx = n\hbar \ . \tag{2.44}$$

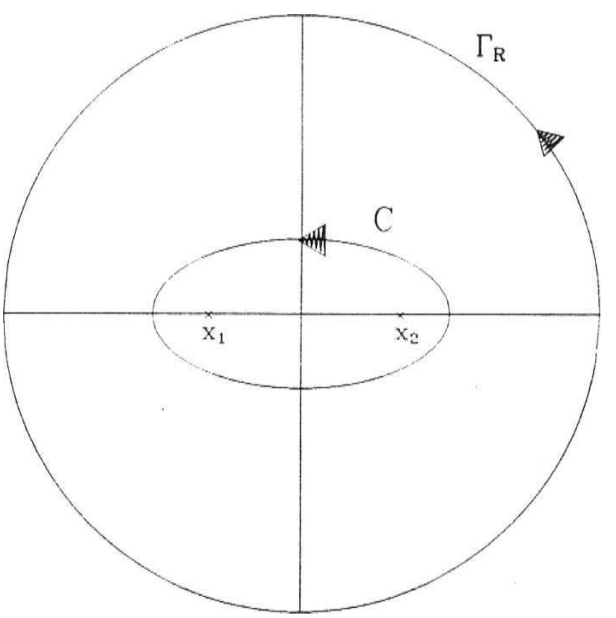

Figure 2.1: Contours for the harmonic oscillator problem.

Here C is the contour enclosing the moving poles between the two turning points x_1 and x_2 (see Fig. 2.1). Noticing that, there is only one fixed pole of $p(x,E)$ at

$x \to \infty$, to evaluate $J(E)$,one considers an integral I_{Γ_R} over a circular contour Γ_R having radius R and oriented in the anti-clockwise direction. The QMF has no other singular points. Hence, for this case, *J(E)* coincides with I_{Γ_R}:

$$I_{\Gamma_R} = J(E) \quad . \tag{2.45}$$

For the evaluation of the contour integral I_{Γ_R}, one makes a change of variable $x = 1/y$ to get,

$$\begin{aligned} I_{\Gamma_R} &= (1/2\pi) \oint_{\Gamma_R} dx p(x, E) \\ &= (1/2\pi) \oint_{\gamma_0} dy \tilde{p}(y, E)/y^2 \quad . \end{aligned} \tag{2.46}$$

Here, $\tilde{p}(y, E) = p(1/y, E)$and the counter clockwise contour γ_0 encloses only one singular point in the y plane, i.e., the pole at $y = 0$. The corresponding contour integral can be straightforwardly calculated. Note that there is no negative sign before the integral; the direction of the contour changes sense under this mapping, which is compensated by the negative sign coming from the integration measure. In this example *J(E)* and I_{Γ_R} are equal, though the relation between *J(E)* and I_{Γ_R} will change from one example to another as will be discussed in the following chapter; the method of computing I_{Γ_R} however remains the same for all the examples.

The QHJ equation written in the y variable becomes

$$\tilde{p}^2(y, E) + i\hbar y^2 \frac{\partial \tilde{p}(y, E)}{\partial y} = 2m(E - \frac{m\omega^2}{2y^2}) = \tilde{p}_c^2 \quad . \tag{2.47}$$

To calculate the contribution of the pole at $y = 0$, $\tilde{p}(y, E)$ is expanded in a Laurent series as,

$$\tilde{p}(y, E) = \sum_{n=0}^{\infty} a_n y^n + \sum_{q=1}^{k} \frac{b_q}{y^q} \quad . \tag{2.48}$$

Making use of the above expansion of *p{y,E)* in Eq. (2.46), one notices that, the only non-vanishing contribution comes from the coefficient a_1 of the linear term in y.

In the next step, substituting $\tilde{p}(y, E)$ in the QHJ equation and comparing the left and right hand sides, it is found that, $b_q = 0$ for $q > 1$. On equating the coefficients of the different powers of y, we have,

$$b_1^2 = -m^2\omega^2 \quad , \tag{2.49}$$

$$2a_0 b_1 = 0 \quad , \tag{2.50}$$

$$-i\hbar b_1 + 2a_1 b_1 + a_0^2 = 2mE \quad . \tag{2.51}$$

From Eq. (2.49), one finds $b_1 = \pm im\omega$. This ambiguity in sign for b_1 can be removed, if we apply the boundary condition given by Eq. (2.35). In the convention followed here, the classical momentum function is defined such that $p_c(x, E) = +i|p_c|$ on the positive real axis [4]. In the limit $y \to 0$, $(x \to \infty)$, $p_c \sim im\omega/y$ and therefore from Eq. (2.48) it follows that $b_1 = im\omega$. From Eq. (2.50), we then have $a_0 = 0$. Substituting the value of b_1 in Eq. (2.51) one gets $a\backslash = (2E - \hbar\omega)/(2i\omega)$. Plugging Eq. (2.48) in Eq. (2.46) and noting Eq. (2.45) gives,

$$J(E) = I_{\Gamma_R} = ia_1 = \frac{2E - \hbar\omega}{2\omega} \quad . \tag{2.52}$$

Thus the quantization condition $J(E) = n\hbar$ when inverted for E, gives

$$E = \left(n + \frac{1}{2}\right)\hbar\omega \ . \tag{2.53}$$

References

[1] H. Goldstein, *Classical Mechanics* (Addison-Wesley Publishing Company Inc. New York, 1950).

[2] P.A.M. Dirac, *The Principles of Quantum Mechanics* (Oxford University Press, London, 1958); for some original articles and references see,
J. Schwinger, *Quantum Electrodynamics* (Dover, New York, 1958).

[3] See pages 306 and 315, of Ref. 1.

[4] R.A. Leacock and M.J. Padgett, Phys. Rev. Lett. 50, 3-6 (1983); R.A. Leacock and M.J. Padgett, Phys. Rev. D 28, 2491-2502 (1983).

[5] R.S. Bhalla, A.K. Kapoor and P.K. Panigrahi, preprint (quant-ph/9512018) (1995), to appear in Am. Jour. of Physics, (1997).

[6] L.D. Landau and E.M. Lifshitz *Quantum Mechanics Non Relativistic Theory* (Pergamon Press, New York, 1958).

Chapter 3

Solvable examples from quantum mechanics

In this chapter, we apply the quantum Hamilton-Jacobi (QHJ) formalism developed in the preceding chapter, to the harmonic oscillator on the half-line, the Morse potential, the infinite well and the three dimensional Coulomb problem, to elucidate this powerful method of arriving at the energy eigenvalues in a simple and straightforward manner[1, 2]. The standard procedure, followed to tackle the bound state problems in quantum mechanics, requires solving the Schrodinger equation for both the eigenvalues and eigenfunctions[3, 4]; this can be contrasted with the QHJ formalism, which proves quite elegant for obtaining energy eigenvalues, using complex analysis.

3.1 Harmonic oscillator on the half-line

The potential for the harmonic oscillator on the half-line is given by (see Fig. 3.1).

$$V(x) = m\omega^2 x^2/2 \text{ for } x > 0 \tag{3.1}$$

$$= \infty \text{ for } x < 0 \ . \tag{3.2}$$

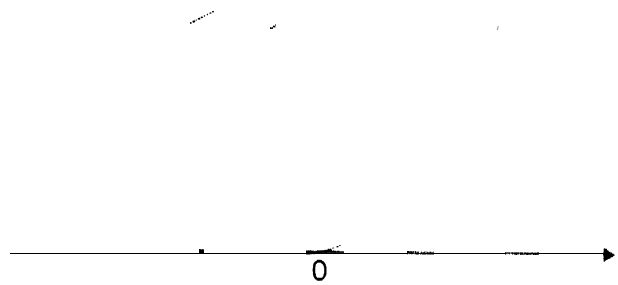

Figure 3.1: The harmonic oscillator potential on the half line.

The QHJ equation for this case is obviously the same as that of the harmonic oscillator example considered in chapter II:

$$p^2 + \frac{\hbar}{i}\frac{\partial p(x,E)}{\partial x} = 2m(E - \frac{m\omega^2 x^2}{2}) \equiv p_c^2 \ , \qquad \text{(for } x > 0\text{)} \ . \qquad (3.3)$$

ror tins potential, the wave function satisfies the boundary condition $\psi(x)|_{x=0} = 0$. This forces us to assume a fixed pole for $p(x, E)$ in the complex x plane at $x = 0$ and this point is also required to serve as one of the turning points. The other turning point is located at $x_2 = \sqrt{2E/(m\omega^2)}$. We then have the quantization condition given by,

$$J(E) = \frac{1}{2\pi} \oint_C p(x)dx = n\hbar \quad , \tag{3.4}$$

where C is the contour enclosing the moving poles between zero and $\sqrt{2E/(m\omega^2)}$. To evaluate $J(E)$.we consider a contour integral I_{Γ_R} over a circle c the complex plane; R is taken large enough to enclose all the singular QMF inside it. This contour integral.

$$I_{\Gamma_R} \equiv \frac{1}{2\pi} \oint_{\Gamma_R} p(x)\, dx \quad , \tag{3.5}$$

gets contributions from the singular points of $p(x, E)$inside Γ_R. These are.

(i) fixed pole at x = 0.

(ii) moving poles between 0 and $x_2 = \sqrt{2E/(m\omega^2)}$, and.

(iii) moving poles on the negative real axis between 0 and $x_1 = -\sqrt{2E/(m\omega^2)}$.

These moving poles on the negative real axis arise due to the symmetry $x \longrightarrow -x$of the problem. Hence.

$$I_{\Gamma_R} = J(E) + I_{C_1} + I_{\gamma_1} \quad . \tag{3.6}$$

where I_{γ_1} is the contour integral for the contour γ_1 that takes into account the additional pole at $x = 0$ and $I_{\Gamma_R}$is the contour integral for the contour Γ_R enclosing all the moving and fixed poles of $p(x, E)$. I_{C_1} is the contour integral for the counter clockwise contour C_1, enclosing the moving poles on the negative side of the real axis (see Fig. 3.2).

However, under $x \rightarrow -x$. the turning points x_1 and x_2 and the moving poles get

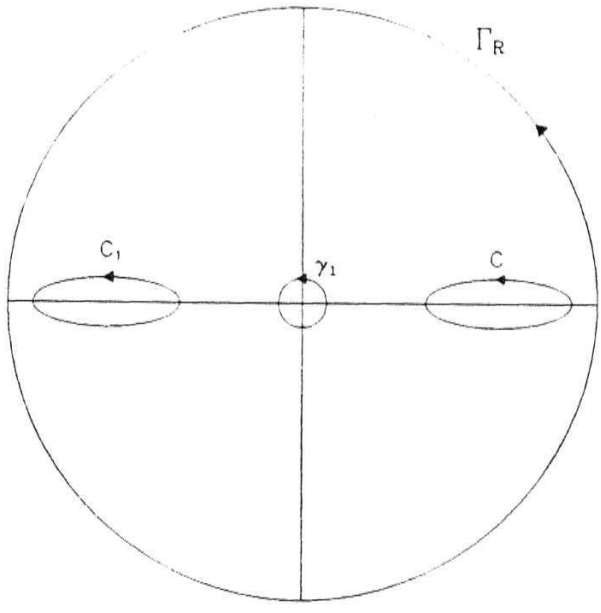

Figure 3.2: Contours for the harmonic oscillator problem on the half line.

interchanged. Thus,

$$I_{C_1} = J(E) \quad . \tag{3.7}$$

Substituting the above in (3.6) we have,

$$I_{\Gamma_R} = 2J(E) + I_{\gamma_1} \quad . \tag{3.8}$$

To compute I_{γ_1}, one needs the residue of $p(x, E)$ at $x = 0$. This can be computed by expanding $p(x, E)$ in Laurent expansion,

$$p(x, E) = \frac{b_1}{x} + \sum_{n=0}^{\infty} a_n x^n \quad . \tag{3.9}$$

We see that, it is only the b_1/x term in the Laurent expansion of $p(x, E)$ that contributes to the contour integral I_{γ_1}, the relevant relation involving b_1 following

from the QHJ equation is,

$$b_1^2 - \frac{\hbar}{i} b_1 = 0 \ . \tag{3.10}$$

From the two solutions b_1 = 0; − $i\hbar$, the former is discarded, **since it does not** give rise to the required singularity at $x = 0$. Hence, using the second value,

$$I_{\gamma_1} = \hbar \ . \tag{3.11}$$

I_{Γ_R} is evaluated as in the previous chapter, for the harmonic oscillator case, and is found to be exactly the same, i.e.,

$$I_{\Gamma_R} = i a_1 = \frac{2E - \hbar\omega}{2\omega} \ . \tag{3.12}$$

We now substitute the values of I_{γ_1} and I_{Γ_R} from (3.11) and (3.12) in (3.8). The quantization rule $J(E) = n\hbar$, when inverted for E, gives the energy eigenvalue equation;

$$E = \left((2n+1) + \frac{1}{2}\right)\hbar\omega \ , \tag{3.13}$$

$$= \left(l + \frac{1}{2}\right)\hbar\omega \ , \tag{3.14}$$

where $l = 2n + 1 = 1, 3, 5, \cdots$ and thus only odd energy eigenstates **are** present.

3.2 Morse oscillator

For the Morse oscillator potential (see Fig. 3.3),

$$V(x) = V_0(e^{-2\alpha x} - 2e^{-\alpha x}) \ . \qquad (\alpha;\ V_0 > 0)$$

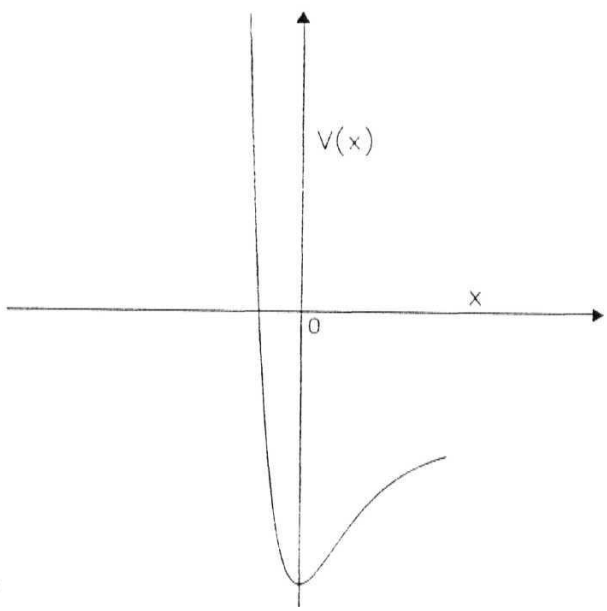

Figure 3.3: The Morse oscillator potential.

the QHJ equation is.

$$p^2 + \frac{\hbar}{i}\frac{\partial p(x,E)}{\partial x} = 2m\left(E - V_0(e^{-2\alpha x} - 2e^{-\alpha x})\right) = p_c^2 \ . \tag{3.15}$$

The turning points are gotten by solving $p = 0$ for x, and the quantization condition is given by,

$$J(E) = \frac{1}{2\pi}\oint_C p(x,E)dx = n\hbar \ , \tag{3.16}$$

where C is the contour enclosing the moving poles between these turning points. Writing $y = \exp(ax)$, we have the QHJ equation in y as,

$$\tilde{p}^2(y,E) + \frac{\alpha y\hbar}{i}\frac{\partial \tilde{p}(y)}{\partial y} = 2m\left(E - V_0\left(\frac{1}{y^2} - 2\frac{1}{y}\right)\right) = \tilde{p}_c^2 \ , \tag{3.17}$$

where $\tilde{p}(y, E) = p(x, E)$.

The corresponding quantization condition in y is therefore.

$$J(E) = \frac{1}{2\pi} \oint_{C'} \frac{\tilde{p}(y)dy}{\alpha y} = n\hbar \quad , \tag{3.18}$$

where C' is the contour enclosing the turning points in the complex y plane. Now $\tilde{p}(y, E)$ has the following singularities,

(i) Fixed pole of the integrand at $y = 0$ and

(ii) Moving poles between the turning points enclosed by the contour C'.

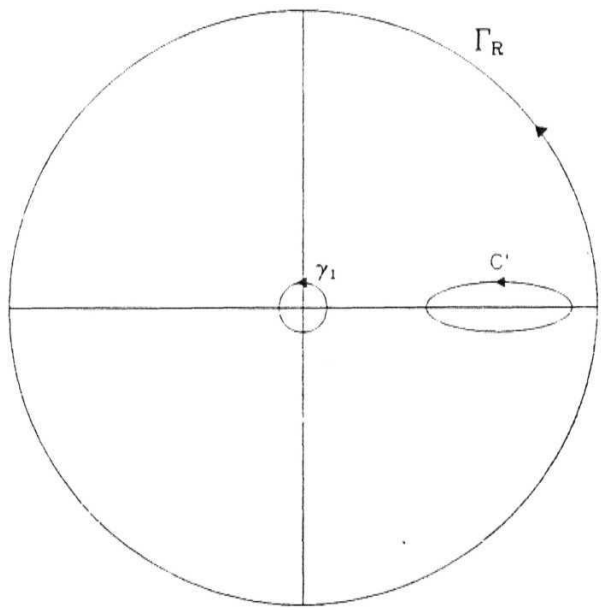

Figure 3.4: Contours for the Morse oscillator potential in the complex y plane.

To evaluate $J(E)$, we once again consider a circular contour Γ_R of radius R, such

that it encloses all the singularities of $\tilde{p}(y, E)$. We then have (see Fig. 3.4),

$$I_{\Gamma_R} = J(E) + I_{\gamma_1} \quad , \tag{3.19}$$

where I_{γ_1} is the contour integral for the contour γ_1 enclosing the pole at $y = 0$: given by

$$I_{\gamma_1} = \frac{1}{2\pi} \oint_{\gamma_1} \frac{\tilde{p}(y)dy}{\alpha y} \quad , \tag{3.20}$$

and

$$I_{\Gamma_R} \equiv \frac{1}{2\pi} \oint_{\Gamma_R} \frac{\tilde{p}(y, E)dy}{\alpha y} \quad , \tag{3.21}$$

is the contour integral for the circular contour Γ_R, which is large enough to enclose the above mentioned singularities of $\tilde{p}(y, E)$.

In order to evaluate these contour integrals, relevant Laurent and Taylor series expansions for p are substituted in the QHJ equation. For the calculation of the contour integral I_{γ_1}, one can easily note that only the constant (a_0) term in the Laurent expansion in $\tilde{p}(y)$ contributes to the calculation of the contour integral I_{γ_0} for the fixed pole at $y = 0$. The minimum term that exits in the expansion of $p(y)$ is b_1/y. We thus have $\tilde{p}(y, E) \sim a_0 + b_1/y$, and substitute the same in the QMF equation (3.17). Equating the different powers of y we have,

$$b_1 = \pm i\sqrt{2mV_0} \quad , \tag{3.22}$$

$$a_0 = \frac{4mV_0 - i\alpha\hbar b_1}{2b_1} \quad . \tag{3.23}$$

We will now fix the correct sign of b_1, so that a_0 can be fixed and I_{γ_1} can be evaluated. We define $\tilde{p}_c(y, E) = p_c(x, E)$, when $y = \exp(\alpha x)$. The value of $p_c(x)$ **is** taken to be positive just below the cut in the complex x plane as one approaches

the real axis from the lower half plane. Under the mapping $y = \exp(\alpha x)$, **this** point gets mapped just below the cut of $\tilde{p}_c(y) = p_c(x)$in the complex y plane and the direction of the contour too remains unchanged. Given this initial condition, the value of $\tilde{p}_c(y)$ can be found out uniquely by analytical continuation using complex analysis [5]. The value of $\tilde{p}_c(y)$, is given as.

$$\tilde{p}_c^2 = \pm\frac{1}{y}\sqrt{2m(Ey^2 - V_0 + 2V_0 y)} \ . \tag{3.24}$$

We now fix the correct value of $\tilde{p}_c(y)$ in the complex y plane. Given $x_1 > x_2 > 0$, are the two classical turning points in the complex x plane, let y_1 and y_2 be the images of x_1 and x_2 in the complex y plane. We can then rewrite,

$$\tilde{p}_c(y) = \pm i\lambda\frac{\sqrt{(y-y_1)(y-y_2)}}{y} \ , \tag{3.25}$$

where A = $(|2mE|)^{1/2}$as $E < 0$ for this potential. Introducing the variables r_1, r_2, θ_1, and θ_2 (see Fig 3.5), we write,

$$y - y_1 = r_1 \exp(i\theta_1) \qquad (0 < \theta_1 < 2\pi) \ , \tag{3.26}$$

$$y - y_2 = r_2 \exp(i\theta_2) \qquad (0 < \theta_2 < 2\pi) \ ; \ r_1, r_2 > 0 \ . \tag{3.27}$$

also $r_1 + r_2 > y_2 - y_1$, must be satisfied. When written in terms of these variables, $\tilde{p}_c(y, E)$ becomes,

$$\tilde{p}_c = \pm\frac{i\lambda}{y}(r_1 r_2)^{\frac{1}{2}} \exp\frac{i(\theta_1 + \theta_2)}{2} \ . \tag{3.28}$$

For the point just below the cut we have $\tilde{p}_c(y)$ as positive: have $\theta_1 \approx \pi$ and $\theta_2 \approx 2\pi$ (see Fig. 3.5). We are thus required to choose

$$\tilde{p}_c(y) = i\frac{\lambda}{y}(r_1 r_2)^{\frac{1}{2}} \exp i\frac{(\theta_1 + \theta_2)}{2} \ . \tag{3.29}$$

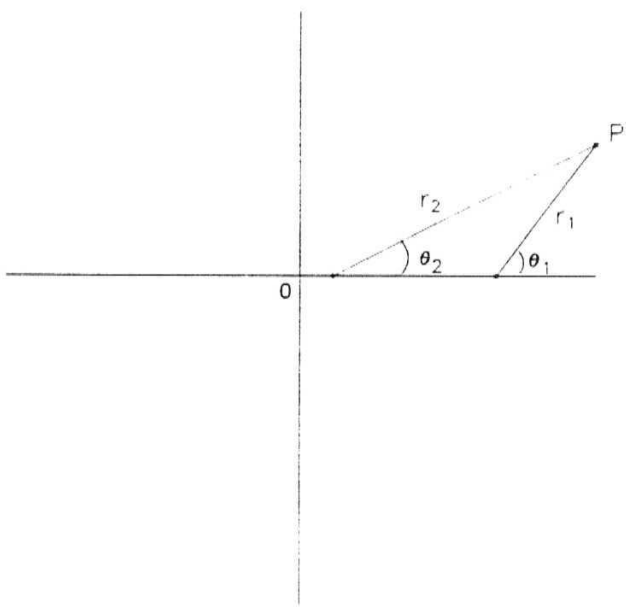

Figure 3.5: Fixing signs of $\tilde{p}_c(y,E)$ in the complex y plane.

The correct branch of the function $\tilde{p}_c(y)$ is thus selected. This completes the definition of $\tilde{p}_c(y,E)$ in the entire complex plane, except the branch cut.

For $y = \infty$, $\theta_1 = \theta_2 = 0$; we have $\tilde{p}_c(y) = i|W_c|$, so we are then able to fix the value of p_c at $y = \infty$ as $i|W_c|$. Similarly at $y = 0$ we have, $\theta_1 = \theta_2 = \pi$; therefore $\tilde{p}_c(y) = -i|W_c|/y$. Here, $|W_c|$ is a Dositive and real auantitv. So at $v = 0$ for Vn > 0. we are to choose $\tilde{p}_c = b_1/y = -i\sqrt{V_0}$. We then have,

$$a_0 = -\left(\frac{4mV_0 - \alpha\hbar\sqrt{2mV_0}}{2i\sqrt{2mV_0}}\right)$$

Therefore,

$$I_{\gamma_1} = -\frac{4mV_0 - \alpha\hbar\sqrt{2mV_0}}{2\alpha\sqrt{2mV_0}} \quad . \tag{3.30}$$

For the evaluation of the contour integral I_{Γ_R}, we substitute $y = 1/z$, and the QMF equation in z is obtained as,

$$\overset{\approx}{p}^2(z) - \frac{\alpha z\hbar}{i}\frac{\partial}{\partial z}\overset{\approx}{p}^2(z) = 2m\left(E - V_0(z^2 - 2z)\right) = \overset{\approx}{p}_c^2(z) \ ,$$

where $\overset{\approx}{p}(z, E) = \tilde{p}(1/y, E)$. So in terms of the new variable z, the contour integral I_{Γ_R} becomes,

$$\begin{aligned} I_{\Gamma_R} &= (1/2\pi)\oint_{\gamma_0} \frac{\overset{\approx}{p}(z, E)dz}{\alpha z} \ , \\ &\equiv I_{\gamma_0} \ . \end{aligned} \tag{3.31}$$

Here, γ_0 is a small circular contour that encloses the singular point at $z = 0$ (as the singularity at $y = \infty$ gets mapped to $z = 0$). Therefore (3.19) can be rewritten as,

$$I_{\gamma_0} = J(E) + I_{\gamma_1} \quad . \tag{3.32}$$

From (3.31), it is seen that one needs to calculate the constant term a_0 in the expansion of $\overset{\approx}{p}$ for the evaluation of the I_{γ_0}. Substituting $\overset{\approx}{p}(z) = a_0$ in the QMF equation for z and solving for a_0, we have $a_0 = +\sqrt{2mE}$, from the boundary conditions considered above. Therefore,

$$I_{\gamma_0} = \frac{i\sqrt{2mE}}{\alpha} \ .$$

On substituting the values of I_{γ_1} and I_{γ_0} from (3.30) and (3.31), and solving for E we arrive at

$$E = -V_0\left(1 - (n + 1/2)\frac{\alpha\hbar}{\sqrt{2mV_0}}\right)^2 \ .$$

3.3 The infinite well

The infinite well potential of width L is the simplest example of one-dimensional motion where a particle of mass m experiences a potential,

$$\begin{aligned} V(x) &= 0 \quad \text{for } 0 < x < L \quad , \\ &= \infty \quad \text{for } x < 0 \text{ and } x > L \quad . \end{aligned} \tag{3.33}$$

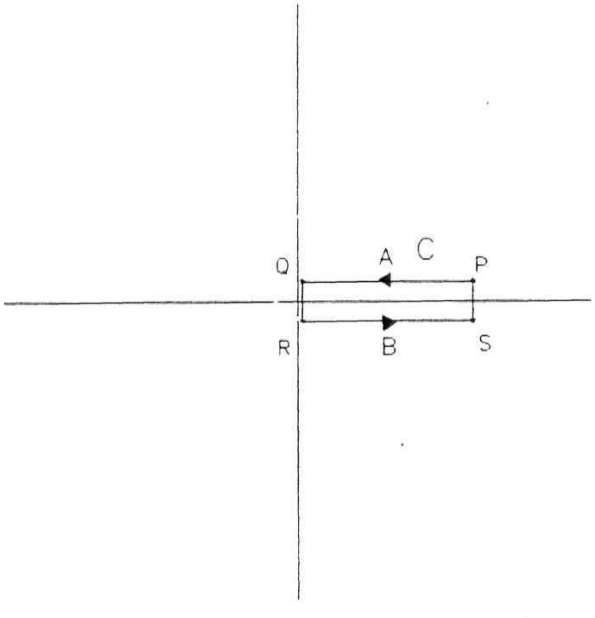

Figure 3.6: Contour for the infinite well potential problem, in the x plane.

The nodes of the eigeiifunctions and hence the moving poles of $p(x, E)$ are located between $x = 0$ and L. Let C be a rectangular contour enclosing all the moving poles (see Fig. 3.6). Then the quantization condition is given by

$$J(E) = \frac{1}{2\pi} \oint_C p(x, E) dx = n\hbar \quad , \tag{3.34}$$

where the QMF obeys the QHJ equation,

$$p^2(x, E) - i\hbar \frac{\partial p(x, E)}{\partial x} = 2mE \quad . \tag{3.35}$$

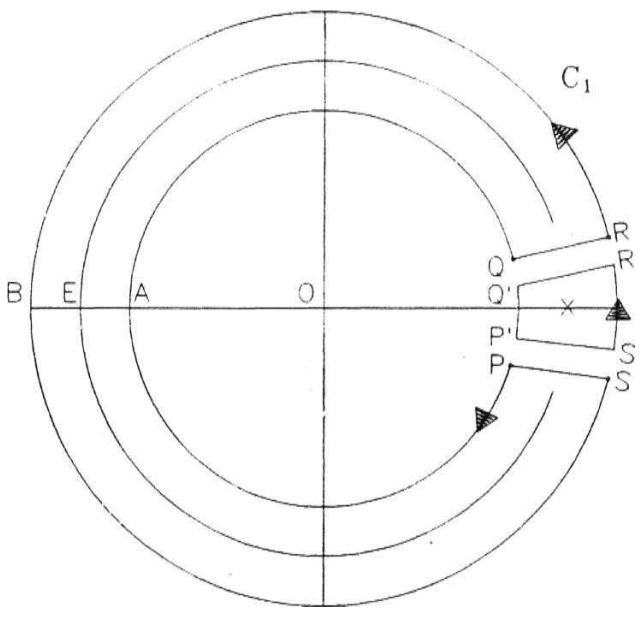

Figure 3.7: Contours for the infinite well potential problem in the complex z plane.

We now use a mapping $z = \exp((2\pi i x)/L)$; the contour C in the x plane (see Fig. 3.6) is mapped into the contour *PAQRBSP* in the $z-$plane. The moving

poles get mapped on the middle arc of unit radius (see Fig. 3.7). The quantization condition **is** now given **as**

$$J(E) = \frac{L}{4i\pi^2} \oint_{C_1} \frac{\tilde{p}(z,E)dz}{z} = n\hbar \tag{3.36}$$

where $C_1$is the contour *PAQRBSP* of Fig.3.7. The QHJ equation written in terms of the new variable z is,

$$\tilde{p}^2(z.E) + \frac{2\pi\hbar z}{L}\frac{\partial\tilde{p}(z,E)}{\partial z} = 2mE \quad , \tag{3.37}$$

where $\tilde{p}(z,E) = p(x,E)$. The boundary condition that, the wave function vanishes at $x = 0$ and $x = L$ gives rise to a pole in $\tilde{p}(z,E)$ at $z = 1$. Let γ and Γ be the inner and outer *full* circles of radii OA and OB respectively, both taken in the anti-clockwise direction. The integral in (3.36) can be written in terms of integrals over Γ, 7 and the contour *P'S'R'Q'P'* enclosing the pole at $z = 1$. Thus, we get

$$J(E) = \frac{L}{4i\pi^2}\left(\oint_\Gamma \frac{\tilde{p}(z,E)dz}{z} - \oint_\gamma \frac{\tilde{p}(z,E)dz}{z} - \oint_{P'S'R'Q'P'} \frac{\tilde{p}(z,E)dz}{z}\right) \tag{3.38}$$

The first integral is computed by changing variables from z to $y = 1/z$,as was done earlier for Γ_R. The last two integrals in the above expressions are calculated as usual by doing the Laurent expansion of $\tilde{p}(z,E)$ in powers of z and z — 1 respectively and we have,

$$\oint_\Gamma \frac{\tilde{p}(z,E)dz}{z} = -2\pi i\sqrt{2mE} \tag{3.39}$$

$$\oint_{\gamma} \frac{\tilde{p}(z,E)dz}{z} = 2\pi i\sqrt{2mE} \tag{3.40}$$

$$\oint_{P'S'R'Q'P'} \frac{\tilde{p}(z,E)dz}{z} = \frac{4\pi^2 i\hbar}{L} \ . \tag{3.41}$$

Substituting the above in (3.38), and solving for E we get,

$$E = \left(\frac{\pi^2\hbar^2}{2mL^2}\right)(n+1)^2 \ , \quad n = 0, 1, 2, \cdots \tag{3.42}$$

3.4 Three Dimensional case

We now apply the QHJ formalism to a three dimensional case, and show how it works for exactly solvable potential problems. The general **QHJ** equation in **three** dimensions given by,

$$-i\hbar\vec{\nabla}.(\vec{\nabla}W) + (\vec{\nabla}W).(\vec{\nabla}W) = E - V(r) \ ,$$

is variable separable.

Let us consider this for the r, θ, ϕ co-ordinate system. For spherically symmetric potentials, we can separate the three dimensional case into three separate one dimensional equations, as the potential that we assume here is dependent only on r. We then have the three QHJ equations given as

$$\frac{\hbar}{i}\frac{\partial p_\phi}{\partial \phi} + p_\phi^2 = D \ , \tag{3.43}$$

$$\frac{\hbar}{i}\frac{\partial(\sin\theta\ p_\theta)}{\partial r} + p_\theta^2 = \lambda - \frac{D}{Sin^2\theta} \ , \tag{3.44}$$

$$\frac{\hbar}{i}\frac{1}{r^2}\frac{\partial(r^2\ p_r)}{\partial r} + p_r^2 = E - V(r) - \frac{\lambda}{r^2} \ . \tag{3.45}$$

Calculations for the angular part

The solution of p_ϕ from (3.43) is similar to **the** evaluation **of the** free **particle case** and the eigenvalues are thus given by,

$$\sqrt{D} \equiv J_\phi(E) = n_\phi \hbar \quad \text{, where } n_\phi = 0, \pm 1, \pm 2, \cdots$$

The above is used in (3.44) to evaluate $J_\theta(E)$.

The QHJ equation for J_θ given by (3.44), has the quantization condition,

$$J_\theta(E) = \frac{1}{2\pi} \oint_C d\theta \, p_\theta(\theta, \lambda, J_\phi) = n_\theta \hbar$$

writing $y = -\cot\theta$, the QHJ equation in y is given by

$$\begin{aligned} \frac{\hbar}{i}\left(-y\tilde{p}_\theta + (1+y^2)\frac{\partial \tilde{p}_\theta}{\partial y}\right) + \tilde{p}_\theta^2 &= \lambda - D(1+y^2) \\ &\equiv \tilde{p}_c \ , \end{aligned} \tag{3.46}$$

where $\tilde{p}_\theta(y, E) = p_\theta(\theta, E)$, and we have the corresponding quantization condition as,

$$I_{C'} \equiv J_\theta(E) = -\frac{1}{2\pi} \oint \frac{dy \, \tilde{p}_\theta}{(y+i)(y-i)} = n_\theta \hbar \ . \tag{3.47}$$

Note that the contour changes direction under the above mapping, and this accounts for the minus sign before the above contour integral. The singularities of $\tilde{p}_\theta(y, E)$ are,

(i) The fixed poles of the integrand at $y = \pm i$

(ii) The moving poles between the turning points enclosed by the contour C'. Therefore,

$$I_{\Gamma_R} = I_{\gamma_1} + I_{\gamma_2} + I_{C'} \quad , \tag{3.48}$$

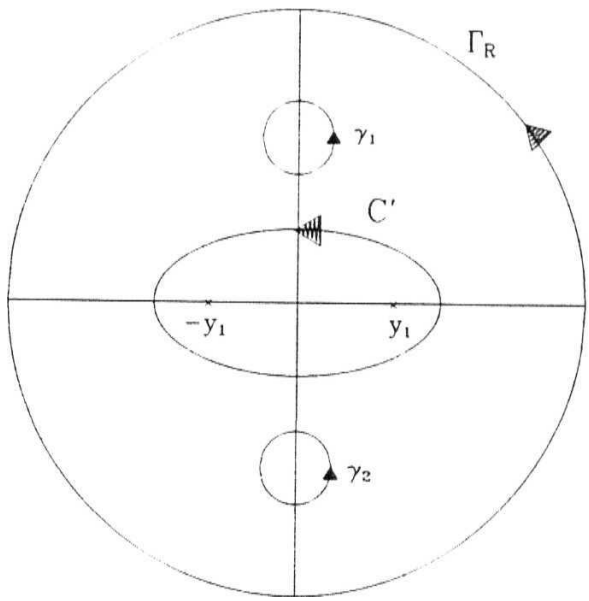

Figure 3.8: Contours for calculation of $J_\theta(E)$ in the complex y plane.

where I_{γ_1} and I_{γ_2} are the contour integrals for the contours γ_1 and γ_2 enclosing the poles at $y = +i$ and $y = -i$ (see Fig. 3.8), and are given by,

$$I_{\gamma_1} = -\frac{1}{2\pi}\oint_{\gamma_1} \frac{dy\tilde{p}_\theta}{(y+i)(y-i)} , \tag{3.49}$$

$$I_{\gamma_2} = -\frac{1}{2\pi}\oint_{\gamma_2} \frac{dy\tilde{p}_\theta}{(y+i)(y-i)} , \tag{3.50}$$

and I_{Γ_R}, the contour integral for the contour Γ_R, which encloses all the above mentioned singularities of $\tilde{p}(y, E)$ is,

$$I_{\Gamma_R} = \oint_{\Gamma_R} \frac{dy\tilde{p}_\theta}{y^2+1} . \tag{3.51}$$

In order to evaluate the residue for the fixed pole at y = i, we substitute, $p(y) = a_0$ in (3.46) and arrive at,

$$\hbar a_0 + a_0^2 = X \quad , \tag{3.52}$$

whose solutions are,

$$a_0 = -\frac{\hbar}{2} \pm \sqrt{\left(\frac{\hbar}{2}\right)^2 + \lambda} \ . \tag{3.53}$$

a_0 is also the residue of the contour integral (3.49). Therefore,

$$I_{\gamma_1} = -\frac{a_0}{2} \ . \tag{3.54}$$

Similarly for the pole $y = -i$, we substitute $\tilde{p}(y) = a_0'$ in (3.46) and get,

$$a_0'^2 + \hbar a_0' = \lambda \ , \tag{3.55}$$

whose solutions are,

$$a_0' = -\frac{\hbar}{2} \pm \sqrt{\left(\frac{\hbar}{2}\right)^2 + \lambda} \ . \tag{3.56}$$

Thus from (3.50),

$$I_{\gamma_2} = \frac{a_0'}{2} \ . \tag{3.57}$$

To evaluate the contour integral I_{Γ_R}, we substitute $y = \frac{1}{z}$; so, as $y \to \infty$, $z \to 0$ and the pole at $y = \infty$ is mapped to $z = 0$. The QHJ in z is given as

$$\frac{\hbar}{i}\left(-\frac{\approx{p}_\theta(z)}{z} - (1+z^2)\frac{\partial \approx{p}_\theta(z)}{\partial z}\right) + \approx{p}_\theta^2 = \lambda - D\frac{(1+z^2)}{z^2} \ . \tag{3.58}$$

Here p_θ (z, E) = $\tilde{p}_\theta(1/z, E)$ and we have,

$$I_{\Gamma_R} \equiv I_{\gamma_0} = -\frac{1}{2\pi}\oint_{\gamma_0} \frac{dz\, \tilde{\tilde{p}}_\theta(z)}{1+z^2} \quad , \tag{3.59}$$

where γ_0 is the contour enclosing the pole at $z = 0$. On considering a similar Laurent expansion in p_θ [z) in z, it is seen that only the b_1/z term in the expansion contributes to the evaluation of the contour integral (3.59). On substituting $p_\theta = b_1/z$ in (3.58), and equating the coefficients of $1/z^2$ term we have,

$$b_1 = \pm i\sqrt{D} \quad , \tag{3.60}$$

which is the residue of the contour integral (3.59); we thus have

$$I_{\Gamma_R} \equiv I_{\gamma_0} = -ib_1 \quad . \tag{3.61}$$

Therefore (3.48) can be written in terms of a_0, a_0', and b_1 as

$$\frac{a_0 - a_0'}{2} - ib_1 = n\hbar \equiv J_\theta(E) \quad . \tag{3.62}$$

We are now required to pick the correct signs of the residues a_0, a_0', and b_1. $p_c(\theta)$ is taken to be positive just below the branch cut joining the classical turning points of the complex θ plane, as one approaches the real axis from the lower half plane. Under the mapping $y = -\cot\theta$; this point gets mapped to a point just above the corresponding branch cut in the complex y plane. Thus $\tilde{p}_c(y)$, which is to be taken as positive for this point, can be fixed in the entire complex plane by analytical continuation, except for the branch cut. We have

$$\tilde{p}_c(y) = \sqrt{\lambda - D(1+y^2)} \quad . \tag{3.63}$$

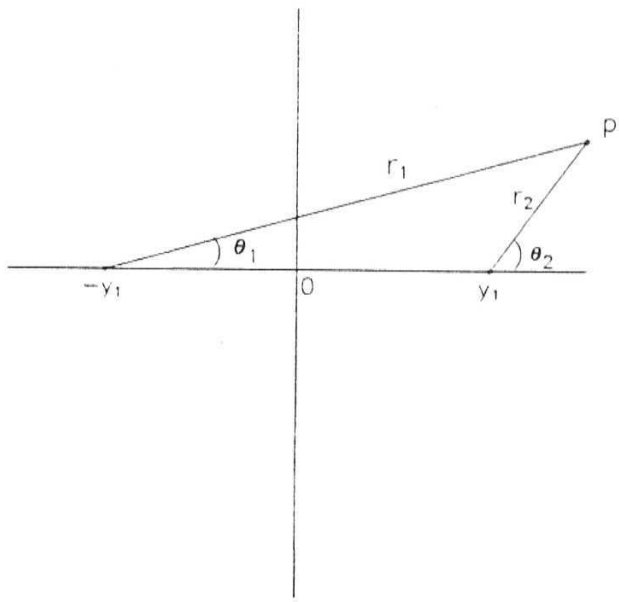

Figure 3.9: Fixing signs $of\,\tilde{p}_c(y)$ in the complex y plane.

Let $\theta_b > \theta_a > 0$, be the two turning points in the classical θ region and let and $-y_1$ be the images of θ_a and θ_b; we can then write,

$$\tilde{p}_c(y) = \pm\xi\sqrt{(y-y_1)(y+y_1)} \tag{3.64}$$

where $\xi = (|D|)^{\frac{1}{2}}$. Introducing the variables, r_1, r_2, θ_1, and θ_2 (see Fig. 3.9), we have,

$$y - y_1 = r_1 \exp(i\theta_1) \qquad (0 \le \theta_1 \le 2\pi)\ , \tag{3.65}$$

$$y - y_2 = r_2 \exp(i\theta_2) \qquad (0 \le \theta_2 \le 2\pi)\ ;\ r_1, r_2 > 0\ , \tag{3.66}$$

and in terms of these new variables, we arrive at,

$$\tilde{p}_c(y) = \pm i\xi(r_1 r_2)^{\frac{1}{2}} \exp i\frac{(\theta_1 + \theta_2)}{2} \quad . \tag{3.67}$$

For a point just above the rut we have $\tilde{p}_c(y)$ as positive; $\theta_1 \approx \pi$ and $\theta_2 \approx 0$ (see Fig. 3.9). We are thus required to choose,

$$\tilde{p}_c(y) = -i\xi(r_1 r_2)^{\frac{1}{2}} \exp i\frac{(\theta_1 + \theta_2)}{2} \quad . \tag{3.68}$$

This completes the definition of $\tilde{p}_c(y)$ in the entire complex plane, except for the **branch** cuts. For $y = \infty$, we have $\theta_1 = \theta_2 = 0$; therefore $p_c = -i|V_c|$, and we are able to fix the value of p_c at $y = \infty$. Here $|V_c|$ is a positive and real quantity. So at $y = 0$ for $D > 0$, we are to choose $b_1 = -i\sqrt{D}$ and we arrive at,

$$I_{\gamma_0} = +\sqrt{D} \quad , \tag{3.69}$$

We are now required to fix the value of *p(y)* at $y = \pm i$. At $y = +i$, we have $\theta_1 = \alpha$ and $\theta_2 = \pi - \alpha$ (see Fig. 3.10), therefore, substituting in (3.68), $\tilde{p}_c(y) = +|V_c|$ and we choose

$$a_0 = \frac{\hbar}{2} - \sqrt{\left(\frac{\hbar}{2}\right)^2 + \lambda} \quad . \tag{3.70}$$

Similarly at $y = -i$, $\theta_1 = 2\pi - \alpha$; $\theta_2 = \pi + \alpha$, (see **Fig. 3.10) thus,** $\tilde{p}_c(y) = -|V_c|$ **and we have,**

$$a_0' = \frac{\hbar}{2} + \sqrt{\left(\frac{\hbar}{2}\right)^2 + \lambda} \quad . \tag{3.71}$$

Substituting these values of a_0, a_0', **and** b_1 **in** (3.62), we **arrive at,**

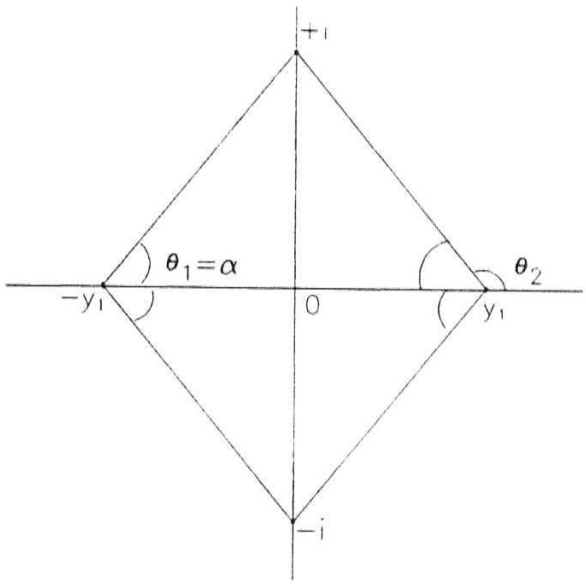

Figure 3.10: Fixing signs of $\tilde{p}_c(y)$ in the complex y plane at y — i and y = —i.

$$J_\theta(E) \equiv n_\theta \hbar = \left[\left(\frac{\hbar}{2}\right)^2 + \lambda\right]^{1/2} - \frac{\hbar}{2} - \sqrt{D} \ . \tag{3.72}$$

Given $J_\phi^2 = D$, one gets

$$\lambda = (n_\theta + n'_\phi)(n_\theta + n'_\phi + 1)\,\hbar^2 \ . \tag{3.73}$$

In the above, n'_ϕ is the positive square root of n_ϕ.

Calculations for the radial part

For the evaluation of $J_r(E)$ we shall consider the potential $V(r) = -g/r$ where

g is a positive, real constant. The corresponding QHJ equation is gotten by substituting this value of *V(r)* in (3.45) as,

$$\frac{\hbar}{i}\frac{2}{r}p_r + \frac{\hbar}{i}\frac{\partial p_r}{\partial r} + p_r^2 = E + \frac{g}{r} - \frac{\lambda}{r^2} \quad , (r \geq 0) \tag{3.74}$$

$$\equiv p_c(r) \quad , \tag{3.75}$$

$J_r(E)$ **is given by,**

$$I_C \equiv J_r(E) = \frac{1}{2\pi}\oint_C dr\, p_r(r, E, \lambda) = n_r\hbar \quad , \tag{3.76}$$

where C is the contour enclosing the moving poles between the classical turning points in the complex r plane. $p_r(r,E)$ has the following singularities:

(i) Fixed poles at $r = 0$.

(ii) Moving poles between the turning points enclosed in the complex r plane.

In order to calculate the contour integral $J_r(E)$, we once again consider a circular contour Γ_R of radius R, such that it encloses the above mentioned singularities of $p_r(r, E)$.We then have (see Fig. 3.11),

$$I_{\gamma_0} = +\sqrt{D} \quad , \tag{3.77}$$

$$I_{\Gamma_R} = I_{\gamma_1} + I_C \quad , \tag{3.78}$$

where I_{γ_1} is the contour integral evaluated for the pole at r = 0 and is given by,

$$I_{\gamma_1} = \frac{1}{2\pi}\oint_{\gamma_1} dr\, p_r(r, E, \lambda) \tag{3.79}$$

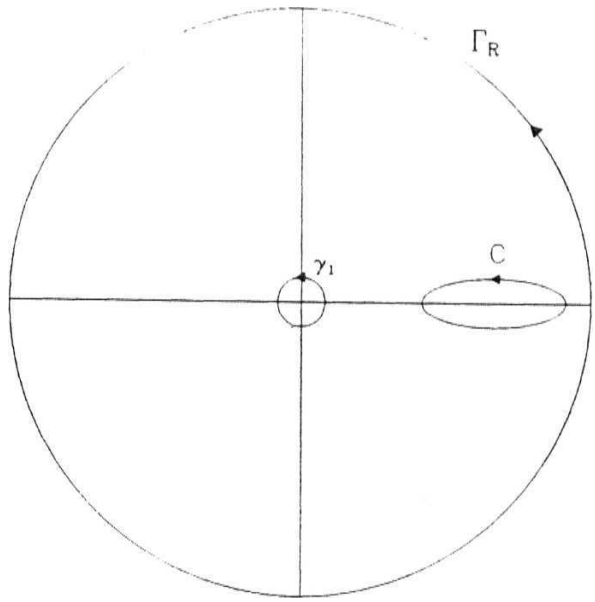

Figure 3.11: Contours for the evaluation of $J_r(E)$integral

I_{Γ_R} is the contour integral for the circular contour Γ_R, that encloses all the above mentioned contour integrals containing the moving and the fixed poles of $p_r(\theta,E)$. We once again seek relevant Taylor and Laurent series expansion in p_r for the above mentioned poles. For the computation of I_{γ_1}, one needs to evaluate the residue of $p_r(r,E)$ at $r = 0$, for which $p_r(r,E)$ is expanded in a Laurent series,

$$p(r, E) = \frac{b_1}{r} + \sum_{n=0}^{\infty} a_n r^n \quad . \tag{3.80}$$

Only the b_1 term in this expansion, contributes as the residue of I_{γ_1}, in the evaluation of (3,79). I_{γ_1} in terms of b_1 is thus given as,

So we are required to substitute $p_r = b_1/r$ in (3.74). Equating the coefficients of $1/r^2$ terms, we have,

$$b_1^2 - i\hbar = -X \quad . \tag{3.81}$$

On solving (3.81), we get,

$$b_1 = \frac{+i\hbar \pm \sqrt{\hbar^2 + 4\lambda}}{2} \quad . \tag{3.82}$$

Now, for the evaluation of I_{Γ_R}, we write r = $\frac{1}{}$. As $r \longrightarrow \infty, z \longrightarrow 0$. The QHJ equation in z is given as,

$$\frac{2z\hbar}{i}\tilde{p}_z - \frac{z^2\hbar}{i}\frac{\partial \tilde{p}_z}{\partial z} + \tilde{p}_z^2 = E + gz - \lambda z^2 \quad . \tag{3.83}$$

$$\equiv \tilde{p}_c(z) \quad . \tag{3.84}$$

The corresponding contour integral that has to be calculated is

$$I_{\Gamma_R} \equiv I_{\gamma_0} = \frac{1}{2\pi}\oint_{\gamma_0} \frac{dz\, \tilde{p}_z}{z^2} \quad , \tag{3.85}$$

where $\tilde{p}_z(z,E) = p(r,E)$, and γ_0 is the contour enclosing the pole at $z = 0$. In the evaluation of the above integral, a Taylor series expansion in z is done, for $\tilde{p}(z,E)$, which is given by,

$$\tilde{p}(z,E) = \sum_{n=0}^{\infty} a_n z^n \quad .$$

It is seen that only the a_1 term in the expansion for p_z contributes as the residue of I_{γ_0}, in the evaluation of the contour integral I_{γ_0} and is thus given **by**

$$I_{\gamma_0} = ia_1 \ .$$

Equation (3.78) in terms of a_1 and b_1 is given as

$$I_{\gamma_0} = i(a_1 - b_1) = n_r\hbar \ . \tag{3.86}$$

The minimum power that exists in the expansion of p_z is a_0. So we substitute $p_z = a_0 + a_1 z$ in (3.84) and equate the powers of z and solve for a_1. We then arrive at the following equations,

$$a_0 = \pm i(|E|)^{\frac{1}{2}} \ , \qquad (\text{as} E < 0) \tag{3.87}$$

$$a_1 = \frac{g}{2a_0} + i\hbar \ . \tag{3.88}$$

$$I_{\gamma_0} = +\sqrt{D} \ , \tag{3.89}$$

We are now required to fix the signs for b_1, a_0, and a_1, for which we have to fix the sign of $p_c(r)$ in the various regions of interest in the complex r plane. $p_c(r)$ is taken to be positive just below the branch cut joining the classical turning points in the complex r plane, as one approaches the real axis from the negative lower half plane. The value of $p_c(r)$ can then be fixed in the entire complex r plane, except **for** the branch cut. From (3.74), we have,

$$p_c(r) \equiv \sqrt{E + \frac{g}{r} - \frac{\lambda}{r^2}} \ .$$

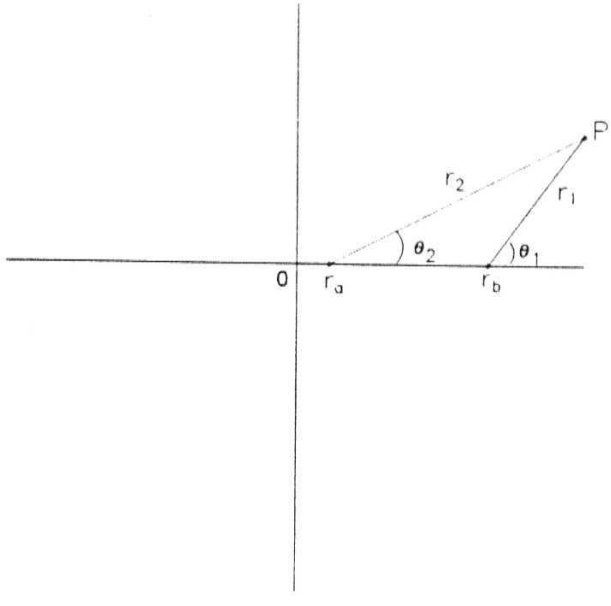

Figure 3.12: Fixing signs of $\tilde{p}_c(r, E, \mathrm{A})$ in the complex r plane.

Given r_a and r_b are the turning points,

$$p_c = \pm i\chi \frac{\sqrt{(r - r_a)(r - r_b)}}{r} \quad , \tag{3.90}$$

where, χ — $(|E|)^{\frac{1}{2}}$. Introducing variables, r_1, r_2, θ_1, and θ_2 (see Fig. 3.12), we have

$$r - r_a = r_1 \exp(i\theta_1) \quad , \tag{3.91}$$

$$r - r_b = r_2 \exp(i\theta_2) \quad , \tag{3.92}$$

where, $r_2 + r_1 > r_b - r_a$. Therefore,

$$p_c(r) = \pm i\chi(r_1 r_2)^{\frac{1}{2}} \exp i\frac{(\theta_1 + \theta_2)}{2} \tag{3.93}$$

For the point just below the branch cut (see Fig. 3.12) we have $\theta_1 = 2\pi$, and $\theta_2 = 7r$: SO we are to choose.

$$p_c(r) = +i\chi(r_1 r_2)^{\frac{1}{2}} \exp i\frac{(\theta_1 + \theta_2)}{2} \quad . \tag{3.94}$$

For $r = 0$, we have $\theta_1 = \theta_2 = \pi$; we then have $p_c(r) = -i\frac{|W_c|}{r}$ which implies b_1 is pure imaginary and negative; and for r = oo, $p_c(r) = +i|W_c|$ (here W_c is real), which implies that a_0 is to be taken as positive. Therefore,

$$a_1 = \frac{g}{2i|E|^{\frac{1}{2}}} + i\hbar \ , \tag{3.95}$$

$$b_1 = \frac{i\hbar - i\sqrt{\hbar^2 + 4\lambda}}{2} \quad . \tag{3.96}$$

Substituting the above values of a_1 and b_1 in (3.86), and writing the answer in terms of $/ = n_\theta + n_\phi$ (given A $= /(/ + 1)\hbar^2$), we arrive at,

$$n_r\hbar = \frac{g}{2\sqrt{-E}} - l\hbar - \hbar \ , \tag{3.97}$$

which when inverted for E, gives the exact energy eigenvalues,

$$E = -\frac{g^2}{4\hbar^2}\frac{1}{(n_r + l + 1)^2} \quad . \tag{3.98}$$

References

[1] Leacock R A and Padgett M J Phys. Rev. Lett. 50 3 (1983).
Leacock R A and Padgett M J Phys. Rev. **D28** 2491 (1983).

[2] R. Dutt, A. Khare, and U.P. Sukhatme, Am. J. Phys. 56, 163-168 (1988).

[3] For treatment of some of these well-known potentials, see Morse P and Feshbach H *Methods of Theoretical Physics* (McGraw-Hill, New York, 1953).

[4] Landau L D and Lifshitz E M *Quantum Mechanics Non Relativistic Theory* (Pergamon Press, New York 1958).

[5] Churchill R V, J W Brown, and R F Verhey *Complex Variables and Applications* (McGraw-Hill Book company Inc., New York 1972).

Chapter 4

Supersymmetry in quantum mechanics

Supersymmetry (SUSY) has played a significant role in throwing new light on many aspects of well-studied quantum mechanical problems [1]. In non-relativistic quantum mechanics, the solution of the harmonic oscillator potential via the raising and lowering operator method is well-known [2]. SUSY quantum mechanics provides a generalization of this operator method [3, 4] to many well-known potential problems; when combined with a discrete reparametrization invariance of these potentials, called *shape invariance*, a property which will be discussed in detail in the following section. This was first noticed by Gendenshtein [3]. For a potential $V_-(x)$, with the help of SUSY, one can construct a partner potential called $V_+(x)$, with the same energy eigenvalues except for the ground-state.

In this chapter, after briefly discussing the operator method for the harmonic oscillator in ordinary quantum mechanics, an introduction to the operator method based on SUSY algebra is given in section 4.1, for the purpose of comparison of the two methods. We then apply this formalism to a simple example in section 4.2, to demonstrate its working. In section 4.3, we discuss different phases of SUSY, **and** about the Gozzi index in this context which helps to distinguish between the unbroken and broken phases of SUSY.

4.1 Operator method for the harmonic oscillator and SUSY algebra

The one dimensional harmonic oscillator Hamiltonian is given by,

$$H = -\frac{\hbar^2}{2m}\frac{d^2}{dx^2} + \frac{1}{2}m\omega^2 x^2 \ . \tag{4.1}$$

which in terms of the lowering and raising operators a and $a^\dagger$,

$$\begin{aligned} a &= \left(\frac{\hbar}{2m\omega}\right)^{\frac{1}{2}}\frac{d}{dx} + \frac{1}{2}\left(\frac{2m\omega}{\hbar}\right)^{\frac{1}{2}} x \ , \\ a^\dagger &= -\left(\frac{\hbar}{2m\omega}\right)^{\frac{1}{2}}\frac{d}{dx} + \frac{1}{2}\left(\frac{2m\omega}{\hbar}\right)^{\frac{1}{2}} x \ , \end{aligned} \tag{4.2}$$

can be written as

$$H = (a^\dagger a + \frac{1}{2})\hbar\omega \ . \tag{4.3}$$

From the above equations, the commutation relations

$$[a, a^\dagger] = 1, \quad [a, H] = a\hbar\omega, \quad [a^\dagger, H] = -a^\dagger\hbar\omega, \tag{4.4}$$

are easily seen to be satisfied. The operators $a, a^\dagger$ are useful in generating new eigenstates starting from any given state. Given ψ_n is an eigenstate of H, with , eigenvalue $E_n, a\psi_n$ and $a^\dagger\psi_n$ are also eigenfunctions of // with eigenvalues $E_n - \hbar\omega$ and $E_n + \hbar\omega$ respectively. Since the operator $a^\dagger a$ in (4.3) is positive semi-definite, all eigenvalues satisfy $E_n > \frac{1}{2}\hbar\omega$. The successive lowering of eigenstates of the operator a is therefore stalled at the ground-state wavefunction ψ_0, which satisfies,

$$a\psi_0 = 0 \ . \tag{4.5}$$

Therefore,

$$\hbar\omega a^\dagger a\psi_0(x) = (H - \frac{1}{2}\hbar\omega)\psi_0(x) = 0 \ , \tag{4.6}$$

which yields $E_0 = \frac{1}{2}\hbar\omega$. From (4.2) and (4.5) one arrives at the normalized ground-state wavefunction:

$$\psi_0(x) = (m\omega/\pi\hbar)^{\frac{1}{4}} \exp[-(m\omega/2\hbar)x^2] \ . \tag{4.7}$$

The higher eigenstates are arrived at, by repeated application of the raising operator $a^\dagger$ on $\psi_0(x)$. The energy eigenvalues

$$E_n = (n + \frac{1}{2})\hbar\omega \ , \quad n = 0, 1, 2, \cdots \ , \tag{4.8}$$

and the corresponding normalized eigenfunctions,

$$\psi_n(x) = \frac{(a^\dagger)^n}{\sqrt{n!}}\psi_0(x) \ , \tag{4.9}$$

are arrived at straightforwardly, without having to solve the second order Schrödinger differential equation in terms of the Hermite polynomials.

The SUSY algebra, relevant for the non-relativistic quantum mechanical problems, can be written as,

$$[Q_i, H] = 0 \ , \{Q_i, Q_j\} = H\delta_{ij} \ . \tag{4.10}$$

Here, Q_i's $(i = 1, 2, \cdots, N)$ are the self-adjoint supercharge operators and H is the supersymmetric Hamiltonian. For the case $N = 2$, to be considered here, the above algebra can be presented in terms of $Q = (Q_1 + iQ_2)/\sqrt{2}$ and its adjoint $Q^\dagger = (Q_1 - iQ_2)/\sqrt{2}$, as,

$$H = \{Q, Q^\dagger\} \ , \ \ Q^2 = (Q^\dagger)^2 = 0 \ , \tag{4.11}$$

and

$$[Q, H] = [Q^\dagger, H] = 0 \ . \tag{4.12}$$

A convenient matrix realization of the supercharges can be given by,

$$Q = \begin{pmatrix} 0 & 0 \\ A & 0 \end{pmatrix} \quad , \quad Q^\dagger = \begin{pmatrix} 0 & A^\dagger \\ 0 & 0 \end{pmatrix} \quad . \tag{4.13}$$

Here, A is a linear operator and $A^\dagger$ is its adjoint:

$$A = \hbar \frac{d}{dx} + \omega(x) \quad , \tag{4.14}$$

$$A^\dagger = -\hbar \frac{d}{dx} + \omega(x) \quad , \tag{4.15}$$

where $\omega(x)$ is called the superpotential. A straightforward calculation yields,

$$H = \begin{pmatrix} H_- & 0 \\ 0 & H_+ \end{pmatrix} \quad , \tag{4.16}$$

where,

$$H_- = A^\dagger A \quad , \tag{4.17}$$

$$H_+ = A A^\dagger \quad , \tag{4.18}$$

are the partner Hamiltonians. Making use of (4.14) and (4.15) one gets ($2m = 1$),

$$H_\pm = -\hbar^2 \frac{\partial^2}{\partial x^2} + V_\pm(x) \quad ,$$

where,

$$V_\pm = \omega^2(x) \pm \hbar \frac{\partial \omega(x)}{\partial x} \quad , \tag{4.19}$$

are the partner potentials. The superpotential $\omega(x)$ is related to the ground-state eigenfunction $\psi_0^{(-)}(x)$ of H_- as,

$$\omega(x) = -\frac{\hbar}{\sqrt{2m}} \frac{\psi_0^{(-)\prime}}{\psi_0^{(-)}} \quad . \tag{4.20}$$

This happens because of the following reasons: Assuming that one has a potential $V_-(x)$, whose ground-state wavefunction $\psi_0^{(-)}(x)$ is known, and whose ground-state energy has been adjusted so that $E_0^{(-)} = 0$, one gets $(2m = 1)$,

$$H_-\psi_0^{(-)}(x) = \left(-\hbar^2\frac{d^2}{dx^2} + V_-(x)\right)\psi_0^{(-)}(x) = 0 \ . \tag{4.21}$$

Using the form of $V_-(x)$, one easily gets (4.20). This also implies,

$$\psi_0^{(-)} = \exp\left(\frac{\sqrt{2m}}{\hbar}\int^x \omega(x)\right) \ , \tag{4.22}$$

which has been assumed to be normalizable. It can be seen that $V_-(x)$ and $V_+(x)$ have the same energy spectra, except that the ground-state, of $V_-(x)$ with energy $E_0^{(-)}$ has no corresponding level for V_+.

If $\psi_n^{(-)}$ is an eigenfunction of H_-, with eigenvalue $E_n^{(-)}$, then $A\psi_n^{(-)}$ is an eigenfunction of H_+ with the same eigenvalue. Similarly, if $\psi_n^{(+)}$ is an eigenfunction of H_+ with eigenvalue $E_n^{(+)}$, then $A^\dagger\psi_n^{(+)}$ is an eigenfunction of H_- with the same eigenvalue. This is so because,

$$H_+(A\psi_n^{(-)}) = AA^\dagger(A\psi_n^{(-)}) = AH_-\psi_n^{(-)} = E_n^{(-)}(A\psi_n^{(-)}) \ , \tag{4.23}$$

$$H_-(A^\dagger\psi_n^{(+)}) = A^\dagger A(A^\dagger\psi_n^{(+)}) = A^\dagger H_+\psi_n^{(+)} = E_n^{(+)}(A^\dagger\psi_n^{(+)}) \ . \tag{4.24}$$

From the above equations it is clear that the eigenvalues and the normalized eigenstates of H_+ and H_- are related as

$$E_n^{(+)} = E_{n+1}^{(-)} \ , \tag{4.25}$$

$$\psi_n^{(+)} = (E_{n+1}^{(-)})^{-\frac{1}{2}}A\psi_{n+1}^{(-)} \ , \tag{4.26}$$

and

$$\psi_{n+1}^{(-)} = (E_n^{(-)})^{-\frac{1}{2}}A^\dagger\psi_n^{(+)} \ , \ . \tag{4.27}$$

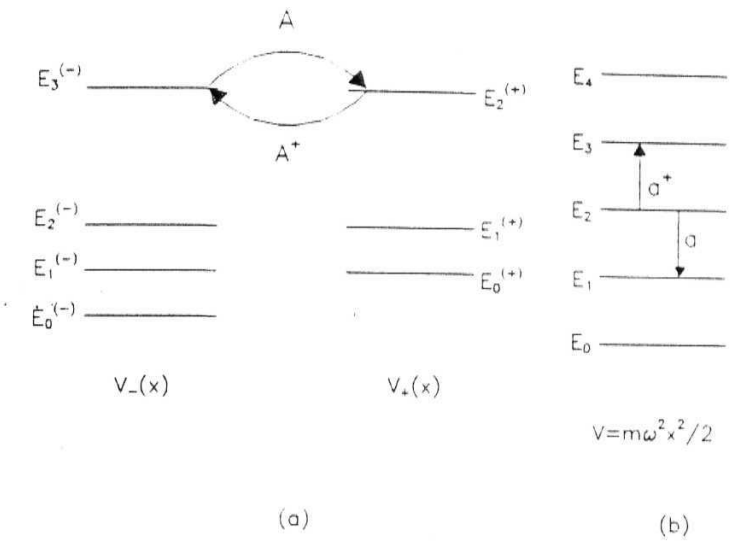

Figure 4.1: (a) Shows the energy spectra of partner potential V_- and V_+ and the action of operators A and $A^\dagger$ and (b) shows the action of raising and lowering operators a and $a^\dagger$.

Here $n = 0, 1, 2, \cdots$, is the number of nodes of the wavefunction. Clearly, for the zero energy ground-state, $A\psi_0^- = 0$, (4.23)'is not valid and hence ψ_0^- is unpaired. Fig 4.1 shows the energy spectra of the two supersymmetric partner Hamiltonians and the roles played by the operators A and $A^\dagger$; this is also contrasted with the conventional harmonic oscillator case. It may be noted that when the energy levels for the partner potentials match exactly, except for the zero energy ground-state, SUSY is unbroken. When the spectra of the partner Hamiltonians match identically with a ground-state having non-zero energy, SUSY is said to be broken spontaneously .

In the following section, we apply this method **of** arriving **at the** energy **eigenvalues, to a potential problem for illustration.**

4.2 Eigenvalues of shape invariant potentials

The known analytically solvable potentials in non-relativistic quantum mechanics e.g., the Coulomb, harmonic oscillator, Morse, Eckart, and Pöschl-Teller potentials [6] can be cast into a supersymmetric form by suitably adjusting the ground-state energies. It was noticed by Gendenshtein [3] that apart from this, origin of their solvability lies in a discrete reparameterization invariance called shape invariance.

The supersymmetric partner potentials $V_{\pm}(x)$ defined by (4.19), are said to be *shape invariant*, if these potentials have the same shape but differ only in the parameters that appear in the potentials. In other words if $V_-(x, a_0)$ and $V_+(x, a_1)$ are the partner potentials,

$$V_+(x, a_0) = V_-(x, a_1) + R(a_1) \ , \tag{4.28}$$

and $R(a_1)$ is independent of x and a_0 and a_1's are parameters of the Hamiltonians. Given

$$H^{(s)} = -\frac{\hbar^2}{2m}\frac{d^2}{dx^2} + V_-(x, a_s) + \sum_{k=1}^{s} R(a_k) \ , \tag{4.29}$$

where $a_s = f^s(a_0)$ i.e., the function f applied s times; we then have,

$$\begin{aligned} H^{(s+1)} &= -\frac{\hbar^2}{2m}\frac{d^2}{dx^2} + V_-(x, a_s + 1) + \sum_{k=1}^{s+1} R(a_k) \ , \\ &= -\frac{\hbar^2}{2m}\frac{d^2}{dx^2} + V_+(x, a_s) + \sum_{k=1}^{s} R(a_k) \ . \end{aligned} \tag{4.30}$$

Comparing (4.29) and (4.30) we see that these two are supersymmetric partner Hamiltonians and have identical bound-state spectra except for the lowest level of $H^{(s)}$ whose energy is given by

$$E_0^{(s)} = \sum_{k=1}^{s} R(a_k) \ . \tag{4.31}$$

On going back from $H^{(s)}$ to $H^{(s-1)}$, one would eventually arrive at $H^{(1)}$ and $H^{(0)}$. Hence, the complete energy spectrum of H_- is obtained as

$$E_n^{(-)} = \sum_{k=1}^{n} R(a_k), \quad E_0^{(-)} = 0 \ . \tag{4.32}$$

We now illustrate this procedure via an example by arriving at the energy eigenvalues for the potential,

$$V(x) = -V_0 \mathrm{sech}^2 \beta x \ , \tag{4.33}$$

whose superpotential is given as

$$\omega(x) = A \tanh \beta x \ , A > 0 \ . \tag{4.34}$$

The supersymmetric partner potentials are thus,

$$\begin{aligned} V_-(x, A) &= A^2 - A(A + \frac{\beta\hbar}{\sqrt{2m}})\mathrm{sech}^2 \beta x \ , \\ V_+(x, A) &= A^2 - A(A - \frac{\beta\hbar}{\sqrt{2m}})\mathrm{sech}^2 \beta x \ , \end{aligned} \tag{4.35}$$

One can thus write

$$V_+(x, A) = V_-(x, A - \frac{\beta\hbar}{\sqrt{2m}}) + A^2 - (A - \frac{\beta\hbar}{\sqrt{2m}})^2 \ , \tag{4.36}$$

On comparison of the above equation with (4.28) we get,

$$a_0 = A; a_1 = f(a_0) = A - \frac{\beta\hbar}{\sqrt{2m}}; R(a_1) = a_0^2 - a_1^2 \ . \tag{4.37}$$

Applying this procedure successively, we see that the successive Hamiltonians in the sequence $H^{(s)}$, $(s = 0, 1, 2, \cdots)$, have parameters $a_s = f^s(a_0) = A - \frac{s\beta\hbar}{\sqrt{2m}}$. We thus arrive at the bound-state energies of the potentials $V_-(x, A) \equiv V_-(x, a_0)$ and these are given by,

$$\begin{aligned} E_n^{(-)} &= \sum_{k=1}^{n} R(a_k) = \sum_{k=1}^{n} (a_{k-1}^2 - a_k^2) \ , \\ &= a_0^2 - a_n^2 = A^2 - \left(A - \frac{n\hbar\beta}{\sqrt{2m}}\right)^2 \ . \end{aligned} \tag{4.38}$$

In the next section we discuss the two phases of SUSY and the Gozzi index which helps differentiate them.

4.3 Broken and unbroken SUSY and Gozzi Index

In the previous section, we discussed the procedure for arriving at the energy eigenvalues for partner SUSY potentials, when SUSY is unbroken i.e, $E_{n+1}^{(-)} = E_n^{(+)}$ For spontaneously broken SUSY, apriori, this algebraic method is not applicable. In this section we discuss how to differentiate different phases (unbroken or spontaneously broken) of SUSY, by looking at the energy eigenstates.

The eigenstates of H, apart from the ground-state for the unbroken case, are doublets, given by

$$\psi_n(x) = \begin{pmatrix} \psi_{n+1}^{(-)} \\ \psi_n^{(+)} \end{pmatrix} \ , \tag{4.39}$$

where n represents the number of nodes of the wave function. In this case, using the intertwining relations $AH_- = H_+A$ and $A^\dagger H_+ = H_- A^\dagger$, it has been shown in the previous section that $E_{n+1}^{(-)} = E_n^{(+)}$ $n \neq 0$. Here $E_{n+1}^{(-)}$ and $E_n^{(+)}$ are the energy

eigenvalues for H_- and H_+ respectively. For the spontaneously broken SUSY [1], all states of H_- and H_+ are paired.

When SUSY is unbroken, the ground-state $|0>$ satisfies,

$$Q^\dagger|0>=0 \text{ or } Q|0>=0 \ . \tag{4.40}$$

In terms of the wave function this gives,

$$A^\dagger\psi_0^{(+)}=0 \quad \text{or} \quad A\psi_0^{(-)}=0 \ . \tag{4.41}$$

Whenever the function $\exp\left(-\int^x \omega(y)dy\right)$ is square integrable, it represents the ground-state wavefunction $\psi_0^{(-)}$ of H_- with zero eigenvalue. It can be seen from $A\psi_0^{(-)}=0$ that,

$$\omega(x)=-\hbar\frac{1}{\psi_0^{(-)}}\frac{\partial\psi_0^{(-)}}{\partial x} \ . \tag{4.42}$$

If $\psi_0^{(-)}$ is not normalizable, then, $\frac{1}{\psi_0^{(-)}}$, which satisfies $A^\dagger\frac{1}{\psi_0^{(-)}}=A^\dagger\psi_0^{(+)}=0$ is the unpaired zero energy ground-state of H_+. In this case, the role of H_- and H_+ are interchanged.

For the spontaneously broken case, the ground-state, having non-zero energy, is no longer annihilated by either of the supercharges and for this case neither $\psi_0^{(-)}$ nor $1/\psi_0^{(-)}$ is normalizable. In this case, it is well known that the eigenvalues of H_- and H_+ coincide i.e., $E_n^{(-)}=E_n^{(+)}$, with a non-vanishing ground-state energy.

Given $\psi_n^{(-)}$ and $\psi_m^{(+)}$ are the wave functions of H^- and H^+, with eigenvalues $E_n^{(-)}$ and $E_m^{(+)}$ respectively, Gozzi [7] noticed that by examining the wavefunctions for any given state, where the eigenvalues matched, one could determine whether

SUSY is intact or spontaneously broken. This could be done with the help of the wave functions $\psi_E^{(-)}$ and $\psi_E^{(+)}$, by defining the quantities,

$$p^{(-)}(E) \equiv \frac{\hbar}{i}\frac{\partial\psi_E^{(-)}}{\partial x}\frac{1}{\psi_E^{(-)}} \quad ,$$

$$p^{(+)}(E) \equiv \frac{\hbar}{i}\frac{\partial\psi_E^{(+)}}{\partial x}\frac{1}{\psi_E^{(+)}} \quad .$$

Gozzi index is given by

$$\delta \equiv \oint p^{(-)}(E)dx - \oint p^{(+)}(E)dx \quad , \tag{4.43}$$

where the integral is taken around a contour in the complex x plane enclosing part of the real axis, between the turning points. It can easily be verified that $p^{(\pm)}(E)$ has a pole at each node of $\psi_E^{(\pm)}$. Near a node x_0, $\psi_E \approx K(x - x_0)$ gives,

$$p^{(\pm)}(E) = \frac{\hbar}{i}\frac{1}{x - x_0} \quad .$$

Thus, a contour integral enclosing $p(E)$ between the turning points counts the number of nodes (n) and thus gives,

$$\oint p^{(\pm)}(E)dx = n\hbar \quad .$$

Therefore depending upon phases of spontaneously broken and unbroken SUSY (setting $\hbar = 1$), S can take values 0 and ± 1 respectively. The relationship between the QHJ formalism and the Gozzi index will be discussed in a later chapter VI where we would be using the QHJ formalism to distinguish these two phases of SUSY.

References

[1] E. Witten. Nucl. Phys. **B185,** 513, (1981); F. Cooper and B. freedman, Ann. Phys. (NY) **146.** 262 (1983); F. Cooper, .]. Ginocchio, and A. Khare. Phys. Rev. **D36.** 2458 (1987); For a recent review of the application of SUSY to quantum mechanics, see F. Cooper. A. Khare and *V.* Sukhatme, *Phys. Rep.* **251,** 267 (1995); and for a quick introduction, see R. Dutt, A. Khare. and U.P. Sukhatme, Am. J. Phys. **56,** (1988).

[2] See for example, L. Schiff, *Quantum Mechanics* (McGraw-Hill, New York, 1968); L. Landau and Lifshitz, *Principles of Quantum Mechanics* (Pergamon, New York, 1977).

[3] L. Gendenshtein JETP Lett. **38,** 356 (1983).

[4] R. Dutt, A. Khare, and U. Sukhatme, Phys. Lett. **B181,** 295 (1986).

[5] A. Inomata and G. Junker, in *Proc. Adriatic Research Conf. on path-integration and its applications, ICTP, Italy, 3-6 Sept.* (1991)

[6] P.M. Morse, Phys. Rev. 34, 57 (1927); C. Eckart, Phys. Rev. 35, 1303 (1930); G. Pöschl and E. Teller, Z. Phys. 83, 143 (1933); N. Rosen and P. Morse, Phys. Rev. 42, 210 (1932).

[7] E. Gozzi, *Phys. Rev.* **D33,** 3665 (1986).

Chapter 5

Examples from SUSY quantum mechanics

In this chapter, the quantum Hamilton-Jacobi (QHJ) formalism [1, 2], is used to obtain exact energy eigenvalues for potentials which exhibit supersymmetry (SUSY) and shape invariance (SI) [3]. It is well known that for potentials having the above two properties, one can find out the eigenvalues algebraically. Our motivation in carrying out this explicit computation has been (a) to gain a better understanding of the working of the QHJ formalism and (b) to see what kind of singularities are possible for the quantum momentum function (QMF), which play a significant role, as will be seen later, in determining the eigenvalues. It is seen that the singularity structure of QMF will enable us to analyze exactness or nonexactness of the well-known SUSY WKB [3, 4, 5] and the broken SUSY WKB formulae [6, 7].

We apply this formalism to a whole set of hyperbolic and trigonometric potentials that exhibit the above properties of SUSY and SI, discussed in chapter IV. As discussed in the previous chapter, the non-linear nature of the QHJ equation, gives two possible values for residues. We had made use of the boundary conditions as suggested by Leacock and Padgett [1], to choose the correct residues. In this chapter we make use of an alternate procedure to arrive at the correct value of residues. We noticed in the context of SUSY quantum mechanics discussed in the previous

chapter, that, for the unbroken cases [3], the **QMF** $p(x, E)|_{E=0} = i\omega(x)$. **We are thus** able to choose the correct residues making use of this condition, and therefore **arrive** at the exact energy eigenvalues for cases where SUSY is unbroken. We also retain the constraints on the parameters of these potentials in order that SUSY remains exact. This also helps us compare our answers with energy eigenvalues obtained from unbroken SUSY algebra.

As seen in chapter III, mapping plays a key role in both, simplifying as well as ascertaining the singularity structure of the QMF. To demonstrate this, we first consider the Eckart potential using the mapping $y = \coth \alpha x$. We then unify this approach of mappings by using $y = \exp(\alpha x)$ for the hyperbolic cases and $y = \exp(i\alpha x)$for the trigonometric cases and tabulate our results. These results are presented in two tables for clarity. We conclude this chapter with some comments and discussions on future directions of work to be carried out in chapters VI and VII.

5.1 Eckart Potential

In case of SI potentials both V_+ and V_- are of the same functional form, albeit with different values of the parameter. In the following, we will consider only V_- and apply the QHJ formalism to obtain the corresponding eigenvalues. In this section we shall obtain the energy eigenvalues for bound states of the Eckart potential given by,

$$V(x) = A^2 + \frac{B^2}{A^2} + A(A - \alpha\hbar)\text{cosech}^2\alpha x - 2B\coth \alpha x \quad . \qquad (x \geq 0) \tag{5.1}$$

Here, A and B, $\{B > A^2)$ are constants. The corresponding superpotential is given by

$$\omega(x) = -A\coth\alpha x + \frac{B}{A}, \tag{5.2}$$

where A and B are constants and the quantum Hamilton-Jacobi equation is given by

$$p^2(x,E) - i\hbar\frac{\partial p(x,E)}{\partial x} = E - A^2 - \frac{B^2}{A^2} - A(A-\alpha\hbar)\mathrm{cosech}^2\alpha x + 2B\coth\alpha x \ . \tag{5.3}$$

A simple way to obtain the eigenvalues of Eckart Hamiltonian is to make use of the transformation

$$y = \coth\alpha x. \tag{5.4}$$

Under this mapping, $p(x,E)$ becomes a function of y when x is expressed in terms of y. Thus $\tilde{p}(y,E)$ is nothing but the QMF $p(x,E)$, expressed in terms of the variable y. *This will be understood for all change of variables to be considered below.*

The quantization condition $J(E) = n\hbar$ then becomes

$$I_{C_1} \equiv \frac{1}{2\pi\alpha}\oint_{C_1}\frac{\tilde{p}(y,E)dy}{1-y^2} = n\hbar \ , \tag{5.5}$$

where, C_1 is the image of the contour C of $J(E)$, enclosing the turning points, under the mapping $x \to y = \coth\alpha x$. The QHJ equation written in terms of y is given as

$$\tilde{p}^2 - i\hbar\alpha\frac{d\tilde{p}}{dy}(1+y)(1-y) = E - A^2 - \frac{B^2}{A^2} - A(A-\alpha\hbar)(y+1)(y-1) + 2By \ . \tag{5.6}$$

Note that the above mapping $y = \coth\alpha x$ introduces additional singularities in the integrand at $y = \pm 1$. The contour integral I_{C_1} is calculated by deforming

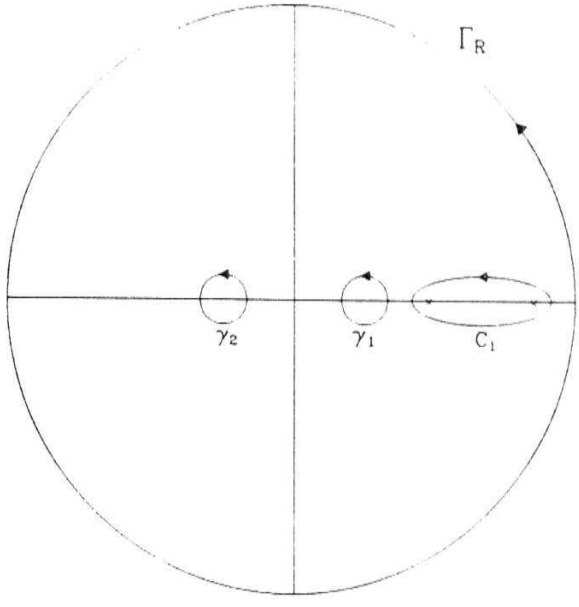

Figure 5.1: Contours for the Eckart potential problem, using the mapping $y = \coth ax$.

the contour, (see Fig 5.1) so as to enclose all the singular points of the integrand. The poles of QMF can be located using available results [8] on complex zeroes of solutions of linear differential equations. They are easily found by inspection for all the problems of interest in this chapter. For evaluation of the integral (5.5) consider the contour integral I_{Γ_R} for a circle Γ_R of radius R which is taken to be large enough so that outside Γ_R, $p(y)$ has no singularities. $p(y)$ has the following singularities:

a) the singular points of the integrand are the poles at $y = \pm 1$ and

b) the moving poles enclosed inside C_1.

Therefore, we have

$$\frac{1}{2\pi\alpha}\oint_{\Gamma_R}\frac{pdy}{1-y^2}=\frac{1}{2\pi\alpha}\left(\oint_{C_1}\frac{pdy}{1-y^2}+\oint_{\gamma_1}\frac{pdy}{1-y^2}+\oint_{\gamma_2}\frac{pdy}{1-y^2}\right) . \tag{5.7}$$

Denoting the integrals in (5.7) as I_{Γ_R}, I_{C_1}, I_{γ_1} and I_{γ_2} (Fig. 5.1), we rewrite (5.7) as

$$I_{\Gamma_R}=I_{C_1}+I_{\gamma_1}+I_{\gamma_2} . \tag{5.8}$$

The contour integral I_{Γ_R} is calculated by one more change of variable to $z=1/y$. In terms of the variable z the integral I_{Γ_R} becomes

$$\begin{aligned} I_{\Gamma_R} &= \oint_{\Gamma_R}\frac{pdy}{1-y^2} && (5.9)\\ &= \oint_{\gamma_0}\frac{pdz}{z^2-1} && (5.10)\\ &\equiv I_{\gamma_0} && (5.11)\end{aligned}$$

where γ_0 is a small circle in the complex z plane enclosing only one singular point located at $z=0$. It is worth reminding that both the contours are in the counter-clockwise direction and the singularity at $y\to\infty$ is mapped to the singularity at $z=0$.

Therefore (5.5), (5.8) and (5.11) give

$$n\alpha\hbar=\frac{1}{2\pi}\oint_{C_1}\frac{pdy}{1-y^2}=\frac{1}{2\pi}\left(\oint_{\gamma_0}\frac{pdz}{z^2-1}-\oint_{\gamma_1}\frac{pdy}{1-y^2}-\oint_{\gamma_2}\frac{pdy}{1-y^2}\right). \tag{5.12}$$

The calculation of various integrals requires behaviour of the momentum function near the singular points. In particular, we need the value of the function at $y=\pm 1$ and its residue at $z=0$. These are calculated by substituting appropriate Taylor or Laurent series expansions of p in the QHJ equation and solving for the first few coefficients in the series expansion as done in the previous chapters. For example,

for calculation of the contour integral around $y = \pm 1$, the series expansion of $p(y, E)$ around $y = \pm 1$ is used. The integrand suggests that we need to calculate only the coefficient of the constant term. We illustrate this for computing the integrals I_{γ_1}: for this purpose we at first expand $\tilde{p}(y, E)$ as

$$\tilde{p}(y, E) = \alpha_0 + \alpha_1(y-1) + \alpha_2(y-1)^2 + \cdots\cdots ,$$

and substitute the above expansion in (5.6). Comparing the terms independent of y on both sides gives

$$\alpha_0^2 = E - A^2 - \frac{B^2}{A^2} + 2B \ . \tag{5.13}$$

Let β_0 be the constant term in the expansion of $\tilde{p}(y, E)$ in powers of $(y+1)$. Then β_0 is similarly determined and is given by

$$\beta_0^2 = E - A^2 - \frac{B^2}{A^2} - 2B \ . \tag{5.14}$$

Note that, there are two roots for α_0 and β_0, corresponding to the two signs of the square of the right hand side in (5.13) and (5.14). Similarly for obtaining the integral I_{γ_0}, we need to compute the residue of $p(z, E)$ at $z = 0$. We expand $p(z, E)$ as

$$p(z, E) = b_1/z + a_0 + a_1 z + \cdots \ , \tag{5.15}$$

and substitute (5.15) in the QHJ equation written in terms of the variable z

$$p^2 - i\alpha\hbar\left(\frac{1-z^2}{z^2}\right)\frac{dp}{dz} = E - A^2 - \frac{B^2}{A^2} - A(A - \alpha\hbar)\left(\frac{1-z^2}{z^2}\right) + \frac{2B}{z} . \tag{5.16}$$

Comparing the coefficients of $1/z^2$ on the two sides gives,

$$b_1 = \frac{-i\alpha\hbar \pm i(\alpha\hbar - 2A)}{2} \tag{5.17}$$

We select the correct roots for α_0, β_0 and b_1 from (5.17), (5.13) and (5.14) by comparing them with the answer **for E = 0. It is straightforward to obtain the value of** b_1, α_0 and β_0 for $E = 0$. by recalling that for zero energy the QMF is related to the superpotential by $p\{x. E = 0) = i\omega(x)$. Writing the superpotential $\omega(x)$ in terms of z, we get

$$\omega(z) = -\frac{A}{z} + \frac{B}{A} \ . \tag{5.1S}$$

The residue of $\omega(z)$ at $z = 0$ is $-A$. Comparing this answer with value of b_1, we see that the correct choice of b_1 is given by $b_1 = -iA$ for all E. Similarly one looks for the coefficient of expansion of ω in powers of $y \pm 1$ and this is compared with the values of α_0 and β_0 respectively for $E = 0$ and are given by.

$$\alpha_0 = i\left|\sqrt{E - A^2 - \frac{B^2}{A^2} + 2B}\right| , \tag{5.19}$$

$$\beta_0 = i\left|\sqrt{E - A^2 - \frac{B^2}{A^2} - 2B}\right| . \tag{5.20}$$

It may be noted that the correct sign of the residues calculated can also be fixed by taking % $\rightarrow$ 0 and looking at the behavior of p_c near the point of interest. This procedure, as originally suggested by Leacock and Padgett, is a bit complicated. For SUSY potentials under consideration in this section we have found it useful to follow the alternate procedure as explained above. However in context of later chapters we will follow the alternate procedure and show how we can arrive at cases of unbroken and spontaneously broken SUSY for these examples, for different values of parameters appearing in the superpotential.

The contour integrals I_{γ_0}, I_{γ_1} and I_{γ_2} are, therefore, computed to be

$$I_{\gamma_1} = -\frac{i\alpha_0}{2\alpha}, \qquad I_{\gamma_2} = \frac{i\beta_0}{2\alpha}, \qquad \text{and} \qquad I_{\gamma_0} = -\frac{A}{\alpha}.$$

Thus the energy eigenvalues are obtained from

$$I_{C_1} = n\hbar = -\frac{A}{\alpha} - \frac{i\beta_0}{2\alpha} + \frac{i\alpha_0}{2\alpha} \ , \tag{5.21}$$

which on further simplification gives

$$E_n = A^2 + \frac{B^2}{A^2} - \frac{B^2}{(n\alpha\hbar + A)^2} - (n\alpha\hbar + A)^2 \ . \tag{5.22}$$

One can arrive at the above energy eigenvalues using other mappings. Use of **a** different mapping will be considered in the next section **and we** shall then show **how** to obtain the bound state eigenvalues for other SUSY potentials.

5.2 Other SUSY potentials

In this section, we will show how the QHJ method could be used for other SUSY potentials. We will use $y = \exp(i\alpha x)$mapping for the SUSY potentials involving trigonometric functions. The remaining potentials involving hyperbolic functions, $y = exp(ax)$ will be used. The treatment of each of these cases runs parallel to the treatment given to the Eckart potential in the previous section except for a new point which requires special attention. The use of the mapping $y = \exp(\alpha x)$ gives rise to extra energy dependent poles in $p(x, E)$ in the non-classical region. Computation of the exact energy eigenvalues requires the knowledge of an integral along a contour enclosing these energy dependent poles. In ail the cases investigated in this chapter this integral can be related to the integral around the contour which encloses poles in the classical region on the real axis.

In this section, at first we shall work out the eigenvalues for the Eckart potential again, using the mapping $y = \exp(\alpha x)$, but concentrating only on the new points as

compared to the treatment in the previous section.

The corresponding superpotential for the Eckart potential written in terms of the variable $y = \exp(\alpha x)$ is

$$\omega(y) = -A\left(\frac{y^2+1}{y^2-1}\right) + \frac{B}{A} \ , \tag{5.23}$$

and the QHJ equation is

$$p^2 - i\hbar\alpha y\frac{dp}{dy} = E - A^2 - \frac{B^2}{A^2} - \frac{4A(A-\alpha\hbar)y^2}{(y^2-1)^2} + \frac{2B(y^2+1)}{(y^2-1)} \ . \tag{5.24}$$

Now the equation

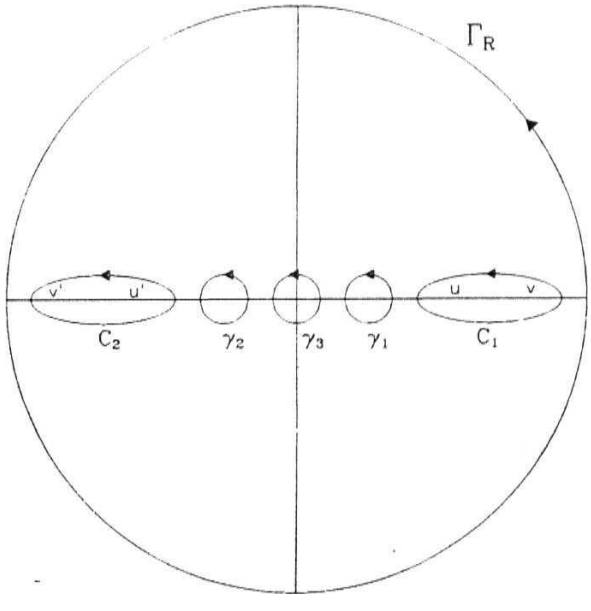

Figure 5.2: Contours for the Eckart potential problem, using the mapping $y = \exp \alpha x$.

$$E - A^2 - \frac{B^2}{A^2} - \frac{4A(A-\alpha\hbar)y^2}{(y^2-1)^2} + \frac{2B(y^2+1)}{(y^2-1)} = 0 \ , \tag{5.25}$$

has four solutions for the turning points. These are shown as U, V, U' V **(see Fig.** 5.2). The moving poles of p are (i) on the real axis and between U and V and (ii) on the real axis between V and V. It should however be noted, that two of these turning points U' and V are in the non-classical region. We note that the symmetry $y \to -y$ in (5.25) interchanges U with V and V with V. This symmetry implies

$$I_{C_1} = I_{C_2} \ , \tag{5.26}$$

where C_1 and C_2 are contours enclosing U, V, and U', V respectively as shown in Fig. 5.2. Next note that now $y = 0$ is a pole of the integrand in the action integral (see (5.28) below). Also $\tilde{p}(y)$ has poles at $y = 1$ and $y = -1$ because the right hand side of QHJ is singular at $y = 1$ and $y = -1$. Introducing I_{Γ_R} for the large circle Γ_R enclosing all the singular points we arrive at

$$I_{\Gamma_R} = I_{C_1} + I_{C_2} + I\gamma_1 + I_{\gamma_2} + I_{\gamma_3} \ . \tag{5.27}$$

Here, $I_{\gamma_1}, I_{\gamma_2}, and I_{\gamma_3}$ are integrals along contours $\gamma_1, \gamma_2, and \gamma_3$ which enclose the singular points $y = 1, y = -1$ and $y = 0$ respectively. Therefore, using (5.26), the quantization condition

$$I_{C_1} \equiv \frac{1}{2\pi\alpha} \oint_{C_1} \frac{dy}{y} \tilde{p}(y, E) = n\hbar \ . \tag{5.28}$$

becomes

$$I_{\Gamma_R} - \sum_p I_{\gamma_p} = 2n\hbar \ . \tag{5.29}$$

The rest of the calculation is same as in Sec. 5.2. and one easily arrives at

$$E_n = A^2 + \frac{B^2}{A^2} - \frac{B^2}{(n\alpha\hbar + A)^2} - (n\alpha\hbar + A)^2 \ . \tag{5.30}$$

The calculation of eigenvalues for the Scarf I (trigonometric), Rosen-Morse I (trigonometric), Scarf II (hyperbolic), Rosen-Morse II (hyperbolic) and the generalized

P5schl-Teller potentials proceeds in a similar fashion. The results obtained using the QHJ formalism matches exactly with those obtained earlier by other methods, and are summarized in Table 5.1 and Table 5.2. To facilitate the comparison, we have taken the same parameters in our potentials as is given in [9]. The range of the variable x is $-\infty < x <$ oo, unless indicated otherwise. The expressions listed in the column four are α times the value of the integral I_{γ_p} for the contour γ_p enclosing only the singular point indicated in the third column of the table. The value of I_{γ_p} for the pole at oo represents the value of I_{Γ_R}. For the fixed poles at $y = 0$ and oo, the square roots in the residues are found to have relatively opposite sign, on comparison with the coefficients of corresponding terms in the expansion of $\omega(x)$, for $E = 0$. The eigenvalues listed in the last column are obtained using (5.29), and solving for E_n.

In this chapter we have explicitly worked out the eigenvalues for the SUSY potentials using the QHJ method. Apart from checking the correctness of the formalism, this exercise provides insight into solvability of these potentials.

The main effort involved in use of this scheme lies in selecting the correct root for the residues needed. This problem was solved here by comparing the answers obtained from the QHJ for $E = 0$ with that obtained from the superpotential. In general the choice of the correct root for the residue can be made by using the boundary condition on QMF, viz., $p \to p_c$ in the limit $\hbar \to 0$ and where the branch of p_c is selected in such a way that it corresponds to the positive sign just below the cut on the real axis joining the physical turning points. We will come back to this pornt in the next chapter.

Table 5.1 : Trigonometric Potentials.

For all the potentials listed in this table the mapping $y = \exp(i\alpha x)$ is used.

Name of potential	Potential	Location of fixed poles	$\alpha f_{\gamma p}$	Eigen value
Scarf I (Trigonometric)	$-A^2 + (A^2 + B^2 + A\alpha\hbar)\times \sec^2 \alpha x - B(2A + \alpha\hbar)\times \sec \alpha x \tan \alpha x$ $(-\pi/2 \leq \alpha x \leq \pi/2)$	0	$\sqrt{E + A^2}$	
		1	$-A + B$	$(A + n\alpha\hbar)^2 - A^2$
		-1	$-(A + B)$	
		∞	$-\sqrt{E + A^2}$	
Rosen-Morse-I (trigonometric)	$A(A - \alpha\hbar)\mathrm{cosec}^2 \alpha x - A^2 + B^2/A^2 + 2B \cot \alpha x$ $(0 \leq \alpha x \leq \pi)$	0	$-\sqrt{E + A^2 - B^2/A^2 + 2iB}$	
		1	A	$+B^2/A^2$
		-1	A	$A^2 - (A + n\alpha\hbar)^2 - B^2/(A + n\alpha\hbar)^2$
		∞	$\sqrt{E + A^2 - B^2/A^2 - 2iB}$	

Table 5.2 : Hyperbolic Potentials.

For all the potentials listed in this table the mapping $y = \exp(\alpha x)$ is used.

Name of potential	Potential	Location of fixed poles	$\alpha l_{\gamma p}$	Eigen value
Scarf II (hyperbolic)	$A^2 + (B^2 - A^2 - A\alpha\hbar) \times \operatorname{sech}^2 \alpha x + B(2A + \alpha\hbar) \times \operatorname{sech} \alpha x \tanh \alpha x$	0	$-i\sqrt{E - A^2}$	$A^2 - (A - n\alpha\hbar)^2$
		i	$iB - A$	
		$-i$	$-iB - A$	
		∞	$i\sqrt{E - A^2}$	
Rosen - Morse II (hyperbolic)	$A^2 + B^2/A^2 - A(A + \alpha\hbar) \operatorname{sech}^2 \alpha x + 2B \tanh \alpha x$	0	$-i\sqrt{E - A^2 - B^2/A^2 + 2B}$	$A^2 + B^2/A^2 - (A - n\alpha\hbar)^2 - B^2/(A - n\alpha\hbar)^2$
		i	$-A$	
		$-i$	$-A$	
		∞	$i\sqrt{E - A^2 - B^2/A^2 - 2B}$	
Eckart (hyperbolic)	$A^2 + B^2/A^2 + A(A - \alpha\hbar) \operatorname{cosech}^2 \alpha x - 2B \coth \alpha x$ $(x \geq 0)$	0	$i\sqrt{E - A^2 - B^2/A^2 - 2B}$	$A^2 + B^2/A^2 - (A + n\alpha\hbar)^2 - B^2/(A + n\alpha\hbar)^2$
		1	A	
		-1	A	
		∞	$-i\sqrt{E - A^2 - B^2/A^2 + 2B}$	
Generalized Pöschl-Teller	$A^2 + (B^2 + A^2 + A\alpha\hbar) \times \operatorname{cosech}^2 \alpha x - B(2A + \alpha\hbar) \times \coth \alpha x \operatorname{cosech} \alpha x$ $(x \geq 0)$	0	$-i\sqrt{E - A^2}$	$A^2 - (A - n\alpha\hbar)^2$
		1	$-A + B$	
		-1	$-(A + B)$	
		∞	$i\sqrt{E - A^2}$	

References

[1] R.A. Leacock and M.J. Padgett. Phys. Rev. D28. 2491 (1983): R.A. Leacock and M.J. Padgett, Phys. Rev. Lett. 50. 3 (1983).

[2] R.S. Bhalla, A.K. Kapoor and P.K. Panigrahi, *Quantum Hamilton-Jacobi formalism and the bound state spectra* (quant-ph/950018), to appear in Am. Jour. of Phys. (1997).

[3] F. Cooper, A. Khare and U. Sukhatme, Phys. Rep. **251,** 267 (1995), and references therein.

[4] A. Comtet, A. Bandrauk and D.K. Campbell, Phys. Lett. **B150,** 159 (1985); A. Khare Phys. Lett. **B161,** 131 (1985).

[5] R.S. Bhalla, A.K. Kapoor and P.K. Panigrahi, *Exactness of the supersymmetric WKB approximation scheme* (quant-ph/950019), to appear in Phys. Rev. A (1996).

[6] R. Dutt, A. Gangopadhya, A. Khare, A Pagnamenta and U. Sukhatme. Phys. Rev **A48,** 1845 (1993).

[7] R.S. Bhalla, A.K. Kapoor and P.K. Panigrahi *Quantum Hamilton-Jacobi analysis of phases of supersymmetry in quantum mechanics*. preprint MRI-PHYS/96-17, May (1996).

[8] E.L. Ince *Ordinary Differential Equations* (Dover Publications, New York (1956).

[9] See Table 4.1, page 296-297 of ref. 4.

Chapter 6

Analyses of phases of supersymmetry in quantum mechanics

In earlier chapters of this thesis, use has been made of the quantum Hamilton-Jacobi (QHJ) formalism [1] for solving the bound state problems [2, 3]. In chapter V we have calculated the exact energy eigenvalues for the examples from supersymmetric (SUSY) quantum mechanics; which were solved for particular ranges of parameters where in SUSY was unbroken. In this context, we had made use of an alternate boundary condition on the quantum momentum function, $p(x, E = 0) = i\omega(x)$. This helped us choose the correct signs of the residues evaluated, for arriving at the energy eigenvalues of these potentials, but only for the particular range where SUSY was unbroken.

Study of different phases of SUSY has generated a lot of interest in recent years [4]. It has been found that for appropriate ranges of the parameters appearing in some of these potentials, a given Hamiltonian can exhibit either broken or unbroken phases of SUSY. In this chapter, we show as to how, within the framework of QHJ formalism, both the unbroken and spontaneously broken phases of SUSY in quantum mechanics can arise in a natural manner, for appropriate ranges of the parameters appearing in the potential. The origin of the restrictions, on the parameters of the Hamiltonians in these two phases, is studied in detail. It is found that,

the boundary condition in this method, plays a crucial **role in naturally** differentiating **the two** phases of SUSY, for different ranges **of the parameters appearing in the potentials.**

In sections 6.1 and 6.2, we apply the QHJ method to the generalized Poschl-Teller and Scarf I potentials respectively, which show both spontaneously broken **and** unbroken phases of SUSY for suitable values of the parameters of the Hamiltonians. The results are summarized in a tabulated form. The Gozzi index [5], is computed for each of these examples, and is shown to differentiate between the two phases of SUSY for all the examples considered in the text. An alternate approach of evaluation of the Gozzi index, is also given. We investigate other potentials of SUSY in section 6.3, and find that they exhibit unbroken SUSY for the complete ranges of the parameters of the Hamiltonians. We then present our conclusions.

6.1 Generalized Poschl-Teller potential

Quantum action integral

For the generalized Poschl-Teller potential, the superpotential is given by

$$\omega(x) = A\coth\alpha x - B\,\mathrm{cosech}\,\alpha x \qquad (x \geq 0)\ . \tag{6.1}$$

The partner potentials are

$$V_{\pm}(x) = A^2 + (A^2 + B^2 \mp A\alpha\hbar)\mathrm{cosech}^2\alpha x - B(2A \mp \alpha\hbar)\coth\alpha x\ \mathrm{cosech}\,\alpha x \tag{6.2}$$

and the corresponding QHJ equations are given by,

$$p_{\pm}^2(x,E) - i\hbar\frac{\partial p_{\pm}}{\partial x} = E - A^2 - (a^2 + b^2 \mp A\alpha\hbar)\mathrm{cosech}^2\alpha x$$

$$+ \quad B(2A \text{ qp } ah) \coth \alpha x \operatorname{cosech} \alpha x \quad . \tag{6.3}$$

We shall present the calculations **for** only one **of** the partner Hamiltonians (H_-) as the calculational details for the other is similar. For the convenience of calculation. we introduce the variable *y:*

$$\coth \alpha x + \operatorname{cosech} \alpha x = y \quad , \tag{6.4}$$

$$\coth \alpha x - \operatorname{cosech} \alpha x = \frac{1}{y} \quad . \tag{6.5}$$

The corresponding QHJ equation in variable y is

$$\begin{aligned} \tilde{p}^2(y,E) \; &+ \; \frac{i\hbar\alpha}{2}\frac{\tilde{p}(y,E)}{\partial y}(1-y^2) \\ &= \; E - A^2 - (A^2 + B^2 + A\alpha\hbar)\frac{(y^2-1)^2}{4y^2} + B(2A+\alpha\hbar)\frac{(y^4-1)}{4y^2} \end{aligned} \tag{6.6}$$

and the quantization condition $J(E) = n\hbar$ is given by,

$$J(E) \equiv \frac{-1}{\pi}\oint_{C_1} \frac{\tilde{p}(y,E)}{\alpha(y^2-1)} = n\hbar \quad , \tag{6.7}$$

where $\tilde{p}(y) = p_-(x)$. The quantum action integral around contour $C\backslash$ enclosing the moving poles between the turning points in the classical region in the complex y plane., will be denoted by I_{C_1}.

The mappings given by (6.4) and (6.5) introduce singularities in the integrand of (6.7) at $y = \pm 1$. QMF has a fixed pole at $y = 0$ and in addition $\tilde{p}(y)$ has extra energy dependent poles in the region $y <$ — 1.

In order to calculate the quantum action integral I_{C_1}, we deform the contour C_1 (see Fig. 6.1), so as to enclose all the singular points of the integrand and the extra,

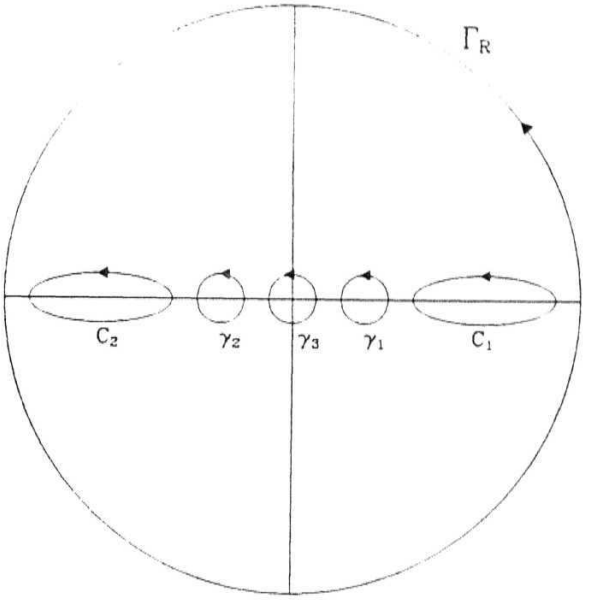

Figure 6.1: Contours for the generalized Pöschl-Teller potential.

energy dependent poles in the non-classical region.. The integral (6.7) is calculated, by considering a contour integral I_{Γ_R} for a circle Γ_R of radius R, which is large enough so as to enclose the above mentioned singularities in *p(y)* and is such that there is no other singularity outside Γ_R. We thus have

$$I_{\Gamma_R} = I_{C_1} + I_{C_2} + I_{\gamma_1} + I_{\gamma_2} + I_{\gamma_3} \quad , \tag{6.8}$$

where I_{C_2} represents the integral around the contour C_2 enclosing the moving poles between the turning points in the non-classical region of the complex y plane; γ_1, γ_2, and 73 represent the contours around the poles at y = 1, -1 and 0 respectively (see

Fig. 6.1) and we have

$$I_{\Gamma_R} = \frac{-1}{\pi}\oint_{\Gamma_R}\frac{\tilde{p}(y)dy}{\alpha(y^2-1)} , \tag{6.9}$$

$$I_{\gamma_1} = \frac{-1}{\pi}\oint_{\gamma_1}\frac{\tilde{p}(y)dy}{\alpha(y^2-1)} , \tag{6.10}$$

$$I_{\gamma_2} = \frac{-1}{\pi}\oint_{\gamma_2}\frac{\tilde{p}(y)dy}{\alpha(y^2-1)} , \tag{6.11}$$

$$I_{\gamma_3} = \frac{-1}{\pi}\oint_{\gamma_3}\frac{\tilde{p}(y)dy}{\alpha(y^2-1)} . \tag{6.12}$$

It is worth pointing out that the symmetry $y \rightarrow -y$ in $\tilde{p}_c(y)$ interchanges **the** turning points in the classical region of the complex y plane with those in the non-classical region. Therefore I_{C_1} and I_{C_2} contribute equally in (6.8). Thus

$$I_{C_2} = I_{C_1} = -\frac{1}{\pi}\oint_{C_1}\frac{\tilde{p}(y)dy}{\alpha(y^2-1)} = n\hbar , \tag{6.13}$$

The contour integral I_{Γ_R} is calculated by one more change of variable: $z = 1/y$. So in terms of the new variable z, the integral I_{Γ_R} becomes,

$$I_{\Gamma_R} = -\frac{1}{\pi}\oint_{\gamma_0}\frac{\tilde{\tilde{p}}(z,E)}{\alpha(1-z^2)} \tag{6.14}$$

$$\equiv I_{\gamma_0} , \tag{6.15}$$

where γ_0 is a small circle in the complex z plane that encloses the singular point at $z = 0$ and $\tilde{\tilde{p}}(z,E) = \tilde{p}(1/z,E)$.

The QHJ equation in z is,

$$\tilde{\tilde{p}}^2(z,E) + \frac{i\hbar\alpha}{2}\frac{\partial\tilde{\tilde{p}}}{\partial z}(z^2-1) = E - A^2 - (A^2+B^2+A\alpha)\frac{(z^2-1)^2}{4z^2} + B(2A+\alpha\hbar)\frac{(1-z^4)}{4z^2} . \tag{6.16}$$

Therefore, (6.8) now can be written as,

$$n\hbar = (I_{\gamma_0} - I_{\gamma_1} - I_{\gamma_2} - I_{\gamma_3})/2 \tag{6.17}$$

Various **integrals in (6.17) can be evaluated in terms of four** constants $a_0, a_0', b_0,$ **and** b_0' **which are, respectively, the values of** ***p(y)*** **at** $y = +1, -1$, **the residue of** ***p(y)*** **at** $y = 0$ **and** the residue of p at $z = 0$. The **quantization condition then takes the** form

$$(a_0' - a_0) + 2(b_1 + b_1') = 2in\hbar\alpha \ . \tag{6.18}$$

Each of the four constants, introduced above, is determined by substituting the relevant Taylor or Laurent series expansions, around the appropriate point, into **QHJ** and comparing the coefficients of different powers of y or z on both sides. Because the QHJ is quadratic, this process leads, in general, to a quadratic equation for the constants to be determined. Thus QHJ, in general, leads to two answers for each of the four constants.

We shall now give the answers for the four constants as obtained from the QHJ. For evaluating the values a_0 and a_0' of $\tilde{p}(y)$ at $y = 1$ and $y = -1$, we set $y = \pm 1$ in the QHJ equation, and noting that *p(y)* is not singular at $y = \pm 1$ we get

$$a_0^2 = E - A^2 \ , \tag{6.19}$$

$$a_0'^2 = E - A^2 \ . \tag{6.20}$$

For the evaluation of b_1, the residue of $\tilde{p}(y)$ at $y = 0$, the expansion $\tilde{p}(y) = b_1/y + \alpha_0 + \alpha_1 y + \cdots$ is substituted in (6.6). We thus have

$$b_1 = i\frac{A+B}{2} \ , \qquad -i\frac{A+B+\alpha\hbar}{2} \ . \tag{6.21}$$

The residue of the pole at $z = 0$, b_1', is needed for the integral (6.15). It is evaluated by substituting $\tilde{\tilde{p}}(z) = b_1'/z + \beta_0 + \beta_1 z + \cdots$ in (6.16) and equating the coefficient of $1/z^2$ terms and this leads to

$$b_1' = i\frac{A-B}{2} \ , \qquad -i\frac{\alpha\hbar + A - B}{2} \ . \tag{6.22}$$

The correct choice for each of the four constants $a_0, a_0', b_0,$ **and** b_0' depends **on the actual values of the** parameters appearing in **the** superpotential. The choice **of the** correct answer can be made by implementing the boundary condition $p(x) \to p^{\circ}(x)$ and specifying the correct branch of $\tilde{p}_c(y, E)$ in the complex y plane. The energy eigenvalues are then determined by solving (6.18) for E.

Boundary conditions

The non-linear nature of the QHJ equation, gives rise to a quadratic equation **for** the residues, and one obtains two values for the residues needed for completing **the** computation of eigenvalues. The boundary condition mentioned above, plays an important role in the picking up of the correct residue. The boundary condition on $p(x)$ is that it becomes equal to $p_c(x)$ in the limit $\hbar \to 0$. The classical momentum function $p_c(x) = \sqrt{E - V(x)}$, as a function of complex variable x, is a multiple valued function and is to be denned carefully. It has a branch cut in the classically accessible region between the turning points. Depending on the potential it may also have branch cuts at other locations in the complex plane. The condition that will be used to define $p_c(x)$ is that, $p_c(x)$ is positive for Re x in the classical region as one approaches the real axis from the lower half plane. This condition is easily translated into a similar condition on p_c expressed in terms of the complex variable y or z. We shall at first define $\tilde{p}_c(y) = p_c(x)$ as a function of complex variable y in the cut plane. Next we shall compare values or residues of $p(y)$ and of $\tilde{p}_c(y)$ in the limit $\hbar \to 0$. This comparison will allow us to select the correct value, or **the** residue, of QMF.

The process outlined above will now be implemented for the case of generalized

Pöschl-Teller potential. The classical momentum function

$$p_c(x) = \sqrt{E - V(x)} \ ,$$

when written in terms of the variable y, becomes

$$\tilde{p}_c(y) = \pm\frac{1}{2y}\sqrt{-(A-B)^2y^4 + y^2(4E + 2B^2 - 2A^2) - (A+B)^2} \tag{6.23}$$

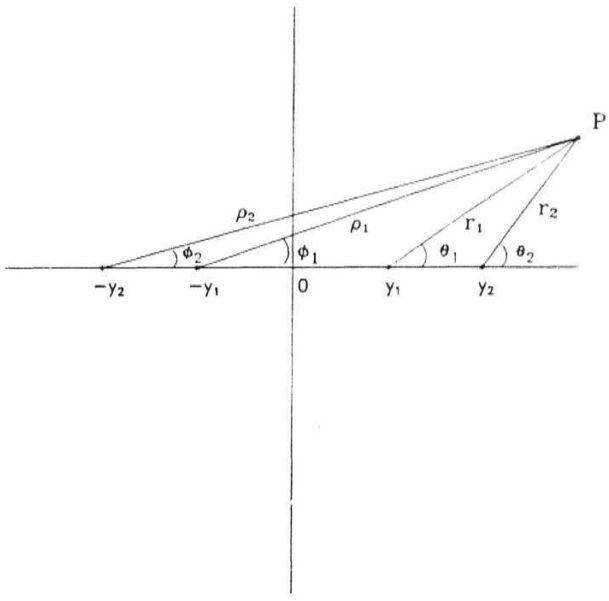

Figure 6.2: Definitions of angles $\theta_1, \theta_2, \phi_1, \phi_2$ and distances r_1, r_2, ρ_1, ρ_2 used in text.

Let $x_2 > x_1 > 0$, be the two turning points in the classical region. The other two zeros of the momentum function $p_c(x)$ are $-x_1$ and $-x_2$. Let y_1, y_2 be the images of x_1, x_2. Then we can write (6.23) as,

$$\tilde{p}_c(y) = \pm\frac{i\lambda}{2y}\sqrt{(y-y_1)(y-y_2)(y+y_1)(y+y_2)} \ , \tag{6.24}$$

where

$$\lambda = |A - B| \ .$$

We introduce the variables $r_1, r_2, \rho_1, \rho_2, \theta_1, \theta_2, \phi_1$, and ϕ_2, as shown in Fig. 6.2, where

$$y - y_1 = r_1 \exp(i\theta_1) \ , \tag{6.25}$$

$$y - y_2 = r_2 \exp(i\theta_2) \ , \tag{6.26}$$

$$y + y_1 = \rho_1 \exp(i\phi_1) \ , \tag{6.27}$$

$$y + y_2 = \rho_2 \exp(i\phi_2) \ . \tag{6.28}$$

and write $\tilde{p}_c$ as

$$\tilde{p}_c(y) = \pm\frac{i\lambda}{2y}(r_1 r_2 \rho_1 \rho_2)^{1/2} \exp\left[\frac{i(\theta_1 + \theta_2 + \phi_1 + \phi_2)}{2}\right] \ . \tag{6.29}$$

All the four angles, $\theta_1, \theta_2, \phi_1, \phi_2$, are chosen to lie between 0 and 2π. Also $r_1 + r_2 > y_2 - y_1$, and $\rho_1 + \rho_2 > y_2 - y_1$must be satisfied. It must be emphasized that we still have to fix the sign in (6.29) which will decide the branch of the function $\tilde{p}_c(y)$ to be selected.

Now we have to choose the correct sign in (6.29). It is easy to check that a point *just below* the real axis in the complex x plane and lying between x_1 and x_2 is mapped to a point *just above the cut* between y_1 and y_2 in the complex y plane. Such a point corresponds to

$$\theta_1 = 0, \theta_2 = \pi, \phi_1 = 0, \phi_2 = 0 \ ,$$

and for these values of angles, $\tilde{p}_c(y)$ must be positive if Re y is between y_1 and y_2. This together with (6.25) to (6.29) fixes the sign in (6.29) to be negative and completes the definition of $\tilde{p}_c(y)$ in the entire complex plane except the two branch cuts, the first one lying between y_1 and y_2 and the other one between $-y_2$ and $-y_1$.

We are now ready to implement the boundary condition that in the limit ft $\to 0$ the QMF p goes to p_c. The values **at points $y = \pm 1$, and the residues at $y = 0$ and** ∞ of the QMF and the classical momentum function can now be compared. Note that all the four parameters are purely imaginary. Also it is easy to see that we get the following constraints on the imaginary parts of the four constants a_0, a_0', b_1, and b_1'.

1. $\mathrm{Im}\, a_0$ is positive.
2. $\mathrm{Im}\, a_0'$ is negative.
3. $\mathrm{Im}\, b_1$ is positive.
4. $\mathrm{Im}\, b_1'$ is negative.

As already indicated the parameters a_0, a_0', b_1, and b_1' are determined by substituting appropriate Taylor or Laurent expansions of QMF in QH J in terms of variable y. This leads to two values of the parameters a_0, a_0', b_1, and b_1'. For different ranges of the parameters A and B appearing in the potential, only one of the two roots for a_0, a_0', b_1, and b_1' satisfies the restrictions listed above, leading to unique values for the constants. The imaginary parts of the four constants are listed in the Table 6.1 for different ranges of the parameters A and B appearing in the potential. The values of QMF and its residues listed in Table 6.1 can be utilized to compute the energy eigenvalues using (6.18).

A similar treatment can be given for the partner potential H_+. We do not list the residues and the values of QMF for the partner potential, however, the final energy eigenvalues for H_- and H_+ are listed in Table 6.2. This table also gives the

Gozzi index, which is the difference between the quantum action integral for the partner Hamiltonians H_+ and H_- (taking $\hbar = 1$), and is evaluated for each of these set of ranges. The evaluation of Gozzi index ran be done making use of the values and residues of the QMF already found for the two potentials V_+ and V_-. A close look at these energy eigenvalues reveals that SUSY is intact for a set of ranges of .4 and *B*, where as for another range of values of these parameters SUSY is broken. It should also be noted that for yet another set of values of parameters *A* and *B*, the roles of H_+ and H_- are interchanged in the sense that the E — 0 is the ground state of H_+, instead of H_-. It can be seen from the Table 6.2 that for the broken phases, as expected, Gozzi index is 0 and for the unbroken case it is ± 1.

An alternate way of computing the Gozzi index, requires knowledge of the spectrum of H_- and H_+. Let E_m^- and E_n^+ be the energy eigenvalues for the mth and n^{th} excited states where m and n represent the number of nodes of the respective eigenfunctions. Notice that the number of nodes coincides with the value of the action integral, and is given by,

$$J_m(E) = m\hbar \quad .$$

Therefore Gozzi index is easily seen to be equal to $m - n\ (\hbar - 1)$, where m and n are such that the corresponding energy eigenvalues E_m^- and E_n^+ are equal. Taking this discussion into account, the Gozzi index can be easily found from the energy eigenvalues, H_- and H_+, already tabulated in Table 6.2. It must be remarked that the boundary condition of QMF automatically leads to the correct energy eigenvalues and our analysis exhausts the entire range of parameters *A* and *B*.

Table 6.1 : Correct values and residues of the QMF for different sets of values of A and B for generalized Pöschl-Teller potential ($V_-(y)$). The four constants a_0, a_0', b_1, and b_1', are pure imaginary.

S.No.	Parameter ranges	$\mathrm{Im}\, a_0$	$\mathrm{Im}\, a_0'$	$\mathrm{Im}\, b_1$	$\mathrm{Im}\, b_1'$
1.	$A+B>0$ and $A-B<0$	$\sqrt{\lvert E-A^2\rvert}$	$-\sqrt{\lvert E-A^2\rvert}$	$\frac{1}{2}(A+B)$	$\frac{1}{2}(A-B)$
2.	$A+B>0$ and $A-B>0$	$\sqrt{\lvert E-A^2\rvert}$	$-\sqrt{\lvert E-A^2\rvert}$	$\frac{1}{2}(A+B)$	$\frac{1}{2}(B-A-\alpha\hbar)$
3.	$A+B<0$ and $A-B>0$	$\sqrt{\lvert E-A^2\rvert}$	$-\sqrt{\lvert E-A^2\rvert}$	$-\frac{1}{2}(A+B+\alpha\hbar)$	$\frac{1}{2}(B-A-\alpha\hbar)$
4.	$A-B<0$ and $A+B<0$	$\sqrt{\lvert E-A^2\rvert}$	$-\sqrt{\lvert E-A^2\rvert}$	$-\frac{1}{2}(A+B+\alpha\hbar)$	$\frac{1}{2}(A-B)$

Table 6.2: Different phases of SUSY for generalized Pöschl-Teller potential ($V_-(y)$), for ranges of A and B

Parameter ranges	$E_n^{(-)}$	$E_n^{(+)}$	Gozzi index δ	Remarks
Set I	$A^2-(A-n\hbar\alpha)^2$	$A^2-(A-(n+1)\hbar\alpha)^2$	1	SUSY is unbroken
Set II	$A^2-(B-(n+\frac{1}{2})\hbar\alpha)^2$	$A^2-(B-(n+\frac{1}{2})\hbar\alpha)^2$	0	SUSY is broken
Set III	$A^2-(A+(n+1)\hbar\alpha)^2$	$A^2-(A+n\hbar\alpha)^2$	-1	Roles of $H^{(-)}$ & $H^{(+)}$ interchanged
Set IV	$A^2-(B+(n+\frac{1}{2})\hbar\alpha)^2$	$A^2-(B+(n+\frac{1}{2})\hbar\alpha)^2$	0	SUSY is broken

For all the cases listed above, n takes integer values ≥ 0.

6.2 Scarf I (trigonometric) potential

Quantum action integral

We next investigate different phases of SUSY for the Scarf I potential. Although the previous example has been investigated earlier in the literature using a different technique by Dutt *et. al.* [6] The analysis of the Scarf I potential for broken phases of SUSY is new [7]. The superpotential for this case is given by,

$$\omega(x) = -A\tan\alpha x + B\sec\alpha x \qquad (-\pi/2 \leq \alpha x \leq \pi/2) \quad . \tag{6.30}$$

The partner potentials are,

$$V_+(x) = (A^2 + B^2 - \alpha\hbar A)\sec^2\alpha x - A^2 - B(2A - \alpha\hbar)\tan\alpha x\sec\alpha x \quad , \tag{6.31}$$

$$V_-(x) = (A^2 + B^2 + \alpha\hbar A)\sec^2\alpha x - A^2 - B(2A + \alpha\hbar)\tan\alpha x\sec\alpha x \quad . \tag{6.32}$$

We shall once again present analysis only for H_-: the results for H_+ will be stated at the end. The QHJ equation for V_- is given by,

$$p^2(x,E) - i\hbar\frac{\partial p}{\partial x} = E + A^2 - (A^2 + B^2 + A\alpha\hbar)\sec^2\alpha x + B(2A + \alpha\hbar)\tan\alpha x\sec\alpha x \quad . \tag{6.33}$$

Using the transformation

$$y = \sec\alpha x + \tan\alpha x \quad , \tag{6.34}$$

$$1/y = \sec\alpha x - \tan\alpha x \quad , \tag{6.35}$$

the QHJ equation in terms of the variable y is

$$\tilde{p}^2(y,E) - \frac{i\hbar\alpha}{2}(y^2+1)\frac{\partial\tilde{p}(y,E)}{\partial y} =$$
$$E + A^2 - (A^2 + B^2 + A\alpha\hbar)\frac{(y^2+1)}{4y^2} + B(2A+\alpha\hbar)\frac{(y^4-1)}{4y^2} \quad . \qquad (6.36)$$

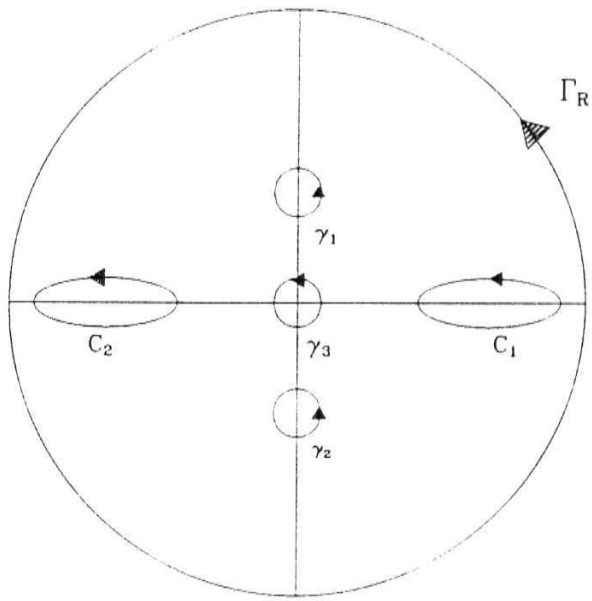

Figure 6.3: Contours for the Scarf I potential.

The quantization condition $J(E) = n\hbar$ as in (6.7) becomes,

$$\frac{1}{\pi\alpha}\oint_{C_1}\frac{\tilde{p}(y,E)dy}{(y^2+1)} = n\hbar \quad . \qquad (6.37)$$

Here $\tilde{p}(y,E) = p(x,E)$ and $C\backslash$ is the contour enclosing the moving poles in the complex y plane. The integral in the above equation will be denoted by I_{C_1}. The mapping from x to y gives rise to singularities in the integrand at $y = \pm i$. In addition the QMF $\tilde{p}(y)$, has pole at $y = 0$ and extra energy dependent moving poles in the region $y < 0$.

We calculate the quantum action integral, I_{C_1}, in (6.37). As in the case of the generalized Poschl-Teller, we deform the contour (see Fig. 6.3), so as to enclose all the singular points of the integrand inside a large circle Γ_R of radius R. We thus have,

$$I_{\Gamma_R} = I_{C_1} + I_{C_2} + I_{\gamma_1} + I_{\gamma_2} + I_{\gamma_3} \quad . \tag{6.38}$$

where I_{Γ_R} is the contour integral for the circle Γ_R; I_{γ_1}, I_{γ_2}, and I_{γ_3} are the contour integrals evaluated along the contours γ_1, γ_2, and 73 enclosing the poles at $y = i, -i$ and 0 respectively, and I_{C_2} encloses the moving poles between the turning points in the non-classical region. These contour integrals are given by

$$I_{\Gamma_R} = \frac{1}{\pi} \oint_{\Gamma_R} \frac{\tilde{p}(y)dy}{\alpha(y^2+1)} \quad , \tag{6.39}$$

$$I_{C_2} = \frac{1}{\pi} \oint_{C_1} \frac{\tilde{p}(y)dy}{\alpha(y^2+1)} \quad , \tag{6.40}$$

$$I_{\gamma_1} = \frac{1}{\pi} \oint_{\gamma_1} \frac{\tilde{p}(y)dy}{\alpha(y^2+1)} \quad , \tag{6.41}$$

$$I_{\gamma_2} = \frac{1}{\pi} \oint_{\gamma_2} \frac{\tilde{p}(y)dy}{\alpha(y^2+1)} \quad , \tag{6.42}$$

$$I_{\gamma_3} = \frac{1}{\pi} \oint_{\gamma_3} \frac{\tilde{p}(y)dy}{\alpha(y^2+1)} \quad . \tag{6.43}$$

Under the symmetry, $y \to -y$ of the QHJ equation, the turning points on the real axis in the classical region, Re $y > 0$, are interchanged with those in Re $y < 0$ region, and we have that I_{C_1} and I_{C_2} are equal (see Fig. 6.3). Therefore,

$$I_{C_2} = I_{C_1} = n\hbar \quad . \tag{6.44}$$

The contour integral I_{Γ_R} is once again calculated by the change of variable $z \to 1/y$ as in (6.15). The QHJ equation in z is

$$\tilde{\tilde{p}}^2(z,E) + \frac{i\hbar\alpha}{2}(z^2+1)\frac{\partial\,\tilde{\tilde{p}}(z,E)}{\partial z} =$$
$$E + A^2 - (A^2 + B^2 + A\alpha\hbar)\frac{(z^2+1)}{4z^2} + B(2A - \alpha\hbar)\frac{(z^4-1)}{4z^2} \quad , \quad (6.45)$$

where $\tilde{\tilde{p}}(z,E) = \tilde{p}(1/z,E)$. In terms of the new variable z, we have,

$$I_{\Gamma_R} = \frac{1}{2\pi}\oint_{\gamma_0}\frac{\tilde{\tilde{p}}(z,E)}{\alpha(1+z^2)} \quad (6.46)$$
$$\equiv I_{\gamma_0} \quad . \quad (6.47)$$

Therefore (6.38) can be rewritten in terms of the above contour integrals as,

$$\oint_{\gamma_0}\frac{\tilde{\tilde{p}}(z)}{(1+z^2)} = 2n\hbar\alpha\pi + \oint_{\gamma_1}\frac{\tilde{p}(y)dy}{(y^2+1)} + \oint_{\gamma_2}\frac{\tilde{p}(y)dy}{(y^2+1)} + \oint_{\gamma_3}\frac{\tilde{p}(y)dy}{(y^2+1)} \quad . \quad (6.48)$$

Various integrals can be evaluated in terms of values and residues of the QMF at different points. As in the previous case, equations which are quadratic, and which determine the required values and residues of QMF, can be found using the QHJ equation. The choice of correct root is to be made by making use of the boundary condition on QMF in the limit $\hbar \to 0$. The QMF in this limit is equal to the classical momentum function which is multiple valued in the complex plane. Hence we must define classical momentum function properly before the boundary condition can be used. This program has been spelled out in detail for the generalized Poschl-Teller potential. We shall now give the main steps for the present case of Scarf I potential.

The integrals in (6.48) can be expressed in terms of four constants a_0, a_0', b_1, and b_1' which are, respectively, the values of *p(y)* at $y = +i, -i$, the residue of *p(y)* at $y = 0$ and the residue of $\tilde{p}$ *(z)* at $z = 0$. The quantization condition then takes the form

$$(a_0' - a_0) + 2i(b_1' - b_1) = 2n\hbar\alpha \ . \tag{6.49}$$

As in the previous case the four constants, introduced above, are computed by substituting the relevant Taylor or Laurent series expansions, around the appropriate point, into the QHJ equation and comparing the coefficients of different powers of y or z on both sides. Because the QHJ equation is quadratic, this process leads, in general, to a quadratic equation for the constant to be determined. Thus QHJ, leads to two roots for each of the four constants. We shall now give the answers for the four constants as obtained from the QHJ.

$$a_0^2 = E + A^2 \ , \tag{6.50}$$

$$a_0'^2 = E + A^2 \ , \tag{6.51}$$

$$b_1 = i\frac{A+B}{2} \ , \quad -i\frac{A+B+\alpha\hbar}{2} \ , \tag{6.52}$$

$$b_1' = i\frac{B-A}{2} \ , \quad i\frac{\alpha\hbar + A - B}{2} \ . \tag{6.53}$$

Boundary Condition

We now define the classical momentum function as function of the complex variable y. The classical momentum function

$$p_c(x) = \sqrt{E - V(x)} \ ,$$

when written in terms of the variable y, becomes

$$\tilde{p}_c(y) = \pm\frac{1}{2y}\sqrt{-(A-B)^2y^4 + y^2(4E + 2A^2 - 2B^2) - (A+B)^2} \quad . \tag{6.54}$$

Let $x_2 > x_1 > 0$ be the two turning points in the classical region. The other two zeros of the momentum function $p_c(x)$ are $-x_1$ and $-x_2$. Let y_1, y_2 be the images of x_1, x_2 . Then we can write

$$\tilde{p}_c(y) = \pm\frac{i\lambda}{2y}\sqrt{(y-y_1)(y-y_2)(y+y_1)(y+y_2)} \quad , \tag{6.55}$$

where y_1, y_2 are the positive zeros of $\tilde{p}_c(x)$, and

$$\lambda = |A - B| \quad .$$

The sign in (6.55) is yet to be fixed .

As in the previous case, we introduce the variables $r_1, r_2, p\backslash, \rho_2, \theta_1, \theta_2, \phi_1$, and ϕ_2, as shown in Fig. 6.2, where

$$y - y_1 = r_1 \exp(i\theta_1) \quad , \tag{6.56}$$

$$y - y_2 = r_2 \exp(i\theta_2) \quad , \tag{6.57}$$

$$y + y_1 = \rho_1 \exp(i\phi_1) \quad , \tag{6.58}$$

$$y + y_2 = \rho_2 \exp(i\phi_2) \quad , \tag{6.59}$$

and write p_c as

$$\tilde{p}_c(y) = \pm\frac{i\lambda}{2y}(r_1 r_2 \rho_1 \rho_2)^{1/2} \exp\left[\frac{i(\theta_1 + \theta_2 + \phi_1 + \phi_2)}{2}\right] \quad . \tag{6.60}$$

All the four angles, $\theta_1, \theta_2, \phi_1, \phi_2$, are chosen to lie between 0 and 2π. It must be emphasized that we still have to fix the sign in (6.60) which will fix the branch of the function $\tilde{p}_c(y)$ to be selected.

Now we come to the choice of the correct sign in (6.60). It is easy to check that a point just below the real axis in the complex x plane and lying between x_1 and x_2 is mapped to a point just below the cut between y_1 and y_2 in the complex y plane. Such a point corresponds to

$$\theta_1 = 2\pi, \ \theta_2 = \pi, \ \phi_1 = 0, \ \phi_2 = 0 \ ,$$

and for these values, $\tilde{p}_c(y)$ must be positive if Re y is between y_1 and y_2. This result fixes the sign in (6.60) to be positive. This completes the definition of $\tilde{p}_c(y)$ in the entire complex plane except the two branch cuts, the first one lying between y_1 and y_2 and the other one between $-y_2$ and $-y_1$.

We are now ready to implement the boundary condition that in the limit $ft \to 0$ the QMF $p(y)$ goes to $\tilde{p}_c(y)$. The values at points $y = \pm i$, and the residue at $y = 0$ and ∞ ($z = 0$) of the quantum momentum function and the classical momentum function can now be compared.

It is easy to see that we get the following constraints on the **four constants**

1. a_0 is real and negative.
2. a_0' is real and positive.
3. b_1 is pure imaginary and $\mathrm{Im}\, b_1$ is negative.
4. b_1' is pure imaginary and $\mathrm{Im}\, b_1'$ is positive.

The correct choice for each of the four constants is made by demanding that the above conditions hold in the limit ft $\rightarrow$ 0. The expression selected for a_0, a_0', b_0, and b_0' depend on the actual values of the parameters appearing in the superpotential. The different possible ranges of the parameters A and B and the corresponding choices of the four constants are given in Table 6.3. Having fixed the expressions to be used for the four constants, computing the energy eigenvalues is straightforward. This same procedure can be followed for H_+. The energy eigenvalues for both H_- and H_+ and the Gozzi index *6* as evaluated in the previous section are listed in Table 6.4. We once again find that for some sets of parameter values, the supersymmetry is spontaneously broken.

6.3 Other potentials with supersymmetry

We have used the QHJ formalism to analyze the generalized Pöschl-Teller and Scarf I potentials, and have been able to arrive at the phases of broken and unbroken SUSY within the framework of this formalism. Our results **are** summarized in Table 6.2 and Table 6.4, classifying cases of unbroken and broken SUSY.

In addition to the two cases reported in detail, we have also investigated the Scarf II, Eckart, Rosen Morse II potentials (all hyperbolic) and Rosen Morse I (trigonometric) potential making use of the mapping $y = \exp(2\alpha x)$ for the hyperbolic potentials and $y = \exp(2i\alpha x)$ for the trigonometric potentials. For these potentials we find that no cases of spontaneously broken SUSY arise and infact SUSY remains unbroken for the entire range of parameters.

For the cases where SUSY is unbroken, the energy spectra can be found rather easily making use of an additional discrete reparameterization invariance of these potentials. However, in the broken phase the same algebraic procedure does not work. From the point of view of the QHJ method, both of these phases can be treated on an equal footing, since the locations of the singularities of the QMF remains unchanged. The only difference between the two phases is the contribution of an additional $\hbar$ dependent term from the residue of the integrand evaluated, in the broken phase. The boundary condition $p(x, E) \overset{\hookrightarrow}{\rightarrow} p_c$ clearly differentiates the broken and unbroken phases.

Finally, we remark that in addition to being a simple scheme for arriving at energy eigenvalues, this approach does not require any information about exact or broken nature of supersymmetry.

Table 6.3: The residues and values of the QMF for different sets of values of A and B in the Scarf I (trigonometric) potential ($V_-(y)$). The constants a_0, a_0' are real and b_1, b_1' are pure imaginary

S. No	Parameter ranges	a_0	a_0'	$\mathrm{Im}\, b_1$	$\mathrm{Im}\, b_1'$
1	$A - B > 0$ and $A + B > 0$	$-\sqrt{E + A^2}$	$\sqrt{E + A^2}$	$-\frac{1}{2}(A + B + \alpha h)$	$\frac{1}{2}(A - B + \alpha h)$
2.	$A - B < 0$ and $A + B > 0$	$-\sqrt{E + A^2}$	$\sqrt{E + A^2}$	$-\frac{1}{2}(A + B + \alpha h)$	$\frac{1}{2}(B - A)$
3.	$A + B < 0$ and $A - B < 0$	$-\sqrt{E + A^2}$	$\sqrt{E + A^2}$	$\frac{1}{2}(A + B)$	$\frac{1}{2}(B - A)$
4.	$A + B < 0$ and $A - B > 0$	$-\sqrt{E + A^2}$	$\sqrt{E + A^2}$	$\frac{1}{2}(A + B)$	$\frac{1}{2}(A - B + \alpha h)$

Table 6.4: Different Phases of SUSY for Scarf I (trigonometric) potential ($V_-(y)$)

Parameter ranges	$E_n^{(-)}$	$E_n^{(+)}$	Witten index Δ	Remarks
Set I	$(A+n\hbar\alpha)^2 - A^2$	$(A+(n+1)\hbar\alpha)^2 - A^2$	1	SUSY is unbroken
Set II	$(B+(n+\frac{1}{2})\hbar\alpha)^2 - A^2$	$(B+(n+\frac{1}{2})\hbar\alpha)^2 - A^2$	0	SUSY is broken
Set III	$(A-(n+1)\hbar\alpha)^2 - A^2$	$(A-n\hbar\alpha)^2 - A^2$	1	Roles of $H^{(-)}$ & $H^{(+)}$ interchanged
Set IV	$(B-(n+\frac{1}{2})\hbar\alpha)^2 - A^2$	$(B-(n+\frac{1}{2})\hbar\alpha)^2 - A^2$	0	SUSY is broken

The constants a_0, a_0' are real and b_1, b_1' are pure imaginary.

References

[1] R.A. Leacock and M.J. Padgett. *Phys. Rev. Lett.* **50**, 3 (1983); R.A. Leacork and M.J. Padgett, *Phys. Rev.* **D28.** 2491 (1983).

[2] R.S. Bhalla, A.K. Kapoor and P.K. Panigrahi, preprint, quant-ph/9512018, accepted for publication in Am. Jour. Phys.

[3] R.S. Bhalla, A.K. Kapoor and P.K. Pauigrahi, preprint, hep-th/9507154.

[4] E. Witten, *Nucl. Phys.* **B188,** 513 (1981); A. Jevicki and J.P. Rodrigues, *Phys. Lett.* **B146,** 55 (1984); T. Imbo and U.P. Sukhatme, *Phys. Rev.* **D33,** 3147 (1986); P.K. Panigrahi and U.P. Sukhatme, *Phys. Lett.* **A178,** 251 (1993); C.X. Chuan, *Jour. of Phys.* **A23,** L659 (1992); Y. Ralchenko and V. Semenov, *Jour. of Phys.* **A24,** L1305 (1992); R. Dutt, A. Gangopadhyaya, A. Khare. A. Pagnamenta and U.P. Sukhatme, *Phys. Rev.* **A48,** 1845 (1993).

[5] E. Gozzi. *Phys. Rev.* **D33.** 3665 (1986); R.S. Bhalla, A.K. Kapoor and P.K. Panigrahi, preprint quant-ph/9512019, accepted for publication in Phys. Rev. A.

[6] A. Inomata and G. Junker, in *Proc. Adriatic Research Conf. on path-integration and its applications, ICTP, Italy, 3-6 Sept.* (1991); R. Dutt, A. Gangopadhyaya, A. Khare. A. Pagnamenta and U.P. Sukhatme, *Phys. Lett.* **A174,** 363 (1993).

[7] R.S. Bhalla, A.K. Kapoor and P.K. Pauigrahi, preprint MRI-PHYS/96-17.

Chapter 7

Exactness Of The SWKB Formula

Exactness of the lowest-order supersymmetric WKB (SWKB) approximation scheme for a class of potentials has been the subject of wide discussions in the literature [1]. It has been found in context of SUSY quantum mechanics, that the lowest order SWKB approximation scheme gives exact answers for cases where SUSY is unbroken [1]. Explicit calculations, akin to that of the celebrated harmonic oscillator case [2], first revealed the absence of $O(\hbar^2)$ to $O(\hbar^6)$ corrections to the lowest order result [3]. Subsequently, for one of the above potentials, it was shown **that** all higher-order corrections vanish identically [4]. A discrete reparameterization symmetry, the so-called shape invariance, of these potentials, has been thought to be responsible for this exactness [5]. Recently, a class of shape invariant potentials have been found for which the exactness of SWKB quantization does not hold true [6].

For the broken SUSY [7] cases, SWKB failed to give exact answers. However gave better answers than that of the ordinary WKB. It was later shown that a change in **the** quantization condition, termed as the broken SUSY quantization condition in literature, mysteriously gave the correct answers [8, 9, 10].

In chapter VI, we had seen how the boundary conditions naturally differentiated cases of broken and unbroken SUSY in quantum mechanics and we were able to

arrive at the exact energy eigenvalues for these cases using the **QHJ** formalism. We are **now** in a position to compare the QHJ approach **with that of the SWKB method** of evaluation of energy eigenvalues and are able to elucidate the **reasons for** the exactness of these semi-classical quantization scheme. Considering the importance of this quantization scheme in the potential problems, a deeper analysis of the origin of this exactness is of utmost significance.

In section 6.1 and 6.2 we had discussed two examples of generalized Poschl-Teller and Scarf I potentials that exhibit both these phases of symmetries but for different ranges of parameters, A and B, that appear in the potential. We arrived at the energy eigenvalues using the quantization condition, $<f_c p(x,E)dx = n\hbar$, from the QHJ formalism.

In this chapter, we use the QHJ approach to investigate the reasons for this exactness. In section 7.1, we discuss the same two examples, but, making use of complex integration technique on the lowest order supersymmetric **WKB** (SWKB) quantization condition

$$\int_{x_1}^{x_2} \sqrt{E - \omega^2(x)}dx = 2n\hbar\pi \quad , \tag{7.1}$$

to facilitate the comparision of these two approaches. We first compare the singularity structure of these two approaches, and see how they match. We then evaluate the corresponding residues and contour integrals, and compare our results.

Comparison of the above scheme with the *exact* quantization condition,

$$\oint_c p(x, E)dx = 2\pi n\hbar \quad , \tag{7.2}$$

originating from the quantum Hamilton-Jacobi formalism reveals that, for the range of parameters that appear in the potential, where SUSY is unbroken, the locations

and residues of poles **that** contribute **to the evaluation of these integrals match identically.** As these poles completely determine the eigenvalues in these **two cases,** the exactness of the SVVKB for these potentials is accounted for. However for the range where SUSY is broken, even though the location of the poles that contribute to the evaluation of two integrals match identically, on evaluation of residues, it is seen that the contribution to the contour integrals differ by ft/2. It was noticed that **a** new quantization condition given by broken SUSY WKB (BSVVKB) quantization formula,

$$\frac{1}{2\pi}\int_{x_1}^{x_2}\sqrt{E-\omega^2(x)}dx = (n+\frac{1}{2})\hbar \ , \tag{7.3}$$

reproduces the energy spectra for known cases of broken SUSY. The locations and the residues of the poles that contribute to these integrals match identically, for both these cases. This accounts for the exactness of the broken SVVKB quantization condition [11]. In section 7.2, potentials of the type $V(x) = \omega + \beta\frac{\partial\omega}{\partial x}$ are analysed and their eigenvalues are arrived at making use of the QHJ formalism. This unifies the method of arriving at the energy eigenvalues of V_+ and V_- potentials in addition to giving a deeper understanding of why the SWKB and BSVVKB quantization condition gives exact answers. We then analyse SUSY potentials, for which SWKB and BSWKB quantization condition fail to give exact answers three cases where SUSY non-exact cases in section 7.3; the origin of this non-exactness is shown to be due the presence of additional singularities in $\sqrt{E-\omega^2(x)}$, like branch cuts in the x-plane.

7.1 Comparison of J_{SWKB} and $J(E)$

The integral J_{SWKB}, also called here as the approximate action integral, will be evaluated using the techniques of complex integration. The answer will then be compared with the exact answer for the action integral, $J(E)$, in QHJ. We will at first take up the Pöschl-Teller potential whose superpotential is given by,

$$\omega(x) = A\coth\alpha x - B\,\mathrm{cosech}\,\alpha x \qquad x \geq 0 \ , \tag{7.4}$$

and its partner potentials $V_{\pm}(x)$ are,

$$V_{\pm}(x) = A^2 + (A^2 + B^2 \mp A\alpha\hbar)\mathrm{cosech}^2\,\alpha x - B(2A \mp \alpha\hbar)\coth\alpha x\ \mathrm{cosech}\,\alpha x \ . \tag{7.5}$$

Using the mapping

$$\coth\alpha x + \mathrm{cosech}\,\alpha x = y \ , \tag{7.6}$$

the approximate action integral (see (7.3)), in terms of the variable y is given by,

$$J_{\mathrm{SWKB}} = -\frac{1}{\pi}\oint_{C_1} \frac{\sqrt{E - \tilde{\omega}^2(y)}}{\alpha(y^2 - 1)} \ . \tag{7.7}$$

where

$$\tilde{\omega}(y) = \frac{A(y^2+1)}{2y} - \frac{B(y^2-1)}{2y} \ , \tag{7.8}$$

and $\tilde{\omega}(y)$ equals $\omega(x)$ expressed in terms of y. Here C_1 is the contour in the complex y plane, enclosing the classical branch points. These are defined as the roots of the equation $E - \tilde{\omega}^2(y) = 0$ lying in the classical region. There are two other roots present in the nonclassical ($y < 0$) region of the complex y plane. The above contour integral can be evaluated in terms of the other singularities of $\sqrt{E - \omega^2(y)}$, in the

complex y plane.

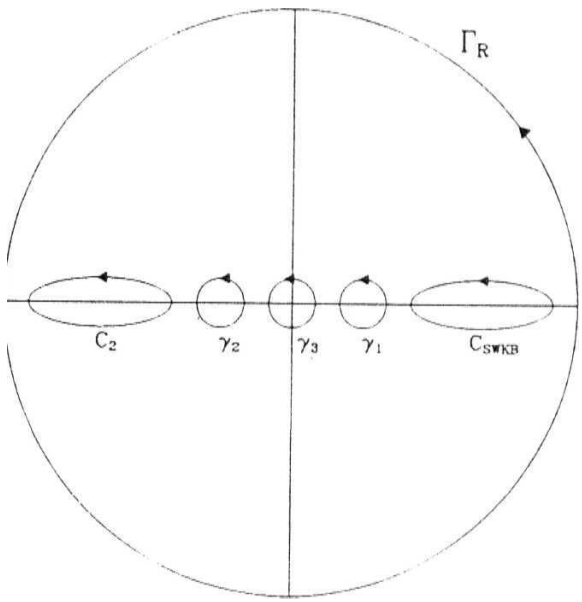

Figure 7.1: Contours for the generalized Poschl-Teller potential.

We now evaluate this contour integral for the range $A + B > 0$ and $A - B < 0$; $A + B < 0$ and $A - B > 0$ for which SUSY is known to be unbroken and also for the range $A - B < 0$ and $A + B > 0$; $A + B < 0$ and $A - B > 0$ for which SUSY is broken [12], on lines of chapter 6, but making use of the quantization conditions (7.1) and (7.3) respectively. It is clear from (7.7) that the integrand has singularities, at $y = 0$ and $y = \pm 1$. To evaluate the above integral, we consider a counterclockwise contour integral J_{Γ_R} for a circle Γ_R of radius R, such that this circle encloses all the singular

points of the above integrand (see Fig. 7.1). Then,

$$J_{\Gamma_R} = J_{\text{SWKB}} + J_{C_2} + J_{\gamma_1} + J_{\gamma_2} + J_{\gamma_3} \quad . \tag{7.9}$$

Here, J_{C_2} is the integral along the counterclockwise contour C_2 enclosing the branch cut in the real $y < 0$ region. $J_{\gamma_1}, J_{\gamma_2}$ and J_{γ_3} are the integrals along contours γ_1, γ_2 and γ_3 enclosing the singular points at $y = 1$, $y = -1$ and 0 respectively. The integral J_{Γ_R} is given by,

$$J_{\Gamma_R} = \frac{-1}{\pi} \oint_{\Gamma_R} \frac{\sqrt{E - \tilde{\omega}^2(y)}dy}{\alpha(y^2 - 1)} \quad . \tag{7.10}$$

The integrals $J_{\gamma_1}, J_{\gamma_2}$, and J_{γ_3} are similarly defined. It may be noticed that the symmetry $y \to -y$ of $E - \omega^2(y)$ implies,

$$J_{\text{SWKB}} = J_{C_2} \quad . \tag{7.11}$$

Now for the calculation of J_{Γ_R} one more change of variable $z = 1/y$ is sought; the singularity at $y \to \infty$ is then mapped to the singularity at $z = 0$. The contour integral for the pole at $z = 0$ is,

$$J_{\Gamma_R} = \frac{-1}{\pi} \oint_{\gamma_0} \frac{\sqrt{E - \tilde{\tilde{\omega}}^2(z)}dz}{\alpha(1 - z^2)} \tag{7.12}$$

$$\equiv J_{\gamma_0} \quad , \tag{7.13}$$

where γ_0 is a small circle in the complex z plane that encloses the singular point at $z = 0$, and $\tilde{\tilde{\omega}}(z)$ is equal to $\omega(x)$ expressed in terms of z. This, together with (7.9) gives

$$J_{SWKB} = \frac{1}{2}(J_{\gamma_0} - J_{\gamma_1} - J_{\gamma_2} - J_{\gamma_3}) \quad . \tag{7.14}$$

It is straightforward to compute the contour integrals appearing in (7.14) except that $\sqrt{E - \omega^2(x)}$, as a function of complex variable x, is a multiple valued function

and therefore this square root function is to be defined carefully. It has a branch cut in the classically accessible region between the turning points and another one on the negative real axis. We demand that $\sqrt{E-\omega^2(x)}$ be positive for real x in the classical region as one approaches the real axis from the lower half plane, to fix its values uniquely. In terms of the variable y, we have $\sqrt{E-\tilde{\omega}^2(y)}$ given by,

$$\tilde{p}_o(y) \equiv \sqrt{E-\omega^2(y)} = \frac{i\xi\sqrt{(y-y_1)(y-y_2)(y+y_1)(y+y_2)}}{2y} , \tag{7.15}$$

where y_1 and y_2 are the images of x_1 and x_2, given x_1 and x_2 are the two turning points in the classical region, of the complex x plane and $\xi = \pm|A-B|$. It is easy to check that a point lying just below the real axis between x_1 and x_2 in the complex x plane, is mapped to a point just above the cut between y_1 and y_2 in the complex y plane. We thus choose the negative sign of ξ and this enables us to fix the sign of $\tilde{p}_o(y)$ in the cut complex y plane. Various integrals J_{γ_k} on the right hand side of (7.14) are now evaluated and tabulated in the column four of Table 7,1.

We now compare the above computation with similar procedure applied to the action integral $J(E)$ of (7.2), where $p(x)$ is the quantum momentum function satisfying the QHJ equation.

$$p^2 - i\hbar\frac{dp(x)}{dx} = E - V(x) \tag{7.16}$$

The exact action integral has been computed within the QHJ formalism in section 6.1 in the previous chapter [12]. We find that locations of singularities of $\sqrt{E-\omega^2}$, other than the branch cuts, match exactly with that of the fixed poles of QMF $p(x,E)$. The value of the exact action integral $J(E)$ is again given by contour

integrals as in (7.14):

$$J(E) = \frac{1}{2}\left(I_{\gamma_0} - I_{\gamma_1} - I_{\gamma_2} - I_{\gamma_3}\right) \quad , \tag{7.17}$$

except that the integrals $I_{\gamma_0}, I_{\gamma_1}, I_{\gamma_2}$, and I_{γ_3} are now given by expressions of the form

$$I_{\gamma_k} = -\frac{1}{\pi}\oint_{\gamma_k} \frac{\tilde{p}(y)dy}{\alpha(y^2-1)} \quad , \tag{7.18}$$

and the contours are same as appearing in Fig. 7.1. The values of the integrals I_{γ_k} are given in Table 7.1.

It is seen that the value of the action integral in the SWKB approximation match exactly with that of $J(E)$ evaluated for the unbroken range, but differ from the exact value by $\hbar/2$, for the broken case. This explains appearance of the $(n+\frac{1}{2})\hbar$ in the quantization condition in the SWKB approximation for the broken SWKB quantization condition.

We repeat the above investigation for the Scarf I (trigonometric) case and we will highlight only the new points here. The superpotential in this case is given by

$$\omega(x) = -A\tan\alpha x + B\sec\alpha x \qquad (-\pi/2 \le \alpha x \le \pi/2) \quad . \tag{7.19}$$

Using the transformation

$$y = \sec\alpha x + \tan\alpha x \quad , \tag{7.20}$$

the quantization condition in the SWKB approximation is given by

$$J_{\text{SWKB}} = \frac{1}{2\pi\alpha}\oint_{C_1} \frac{\sqrt{E-\tilde{\omega}^2(y)}dy}{(y^2+1)} = (n+1/2)\hbar \quad . \tag{7.21}$$

The mapping from x to y gives rise to singularities in the integrand at $y = \pm i$ and at $y = 0$ and in order to calculate J_{SWKB} we once again deform the contour so as to

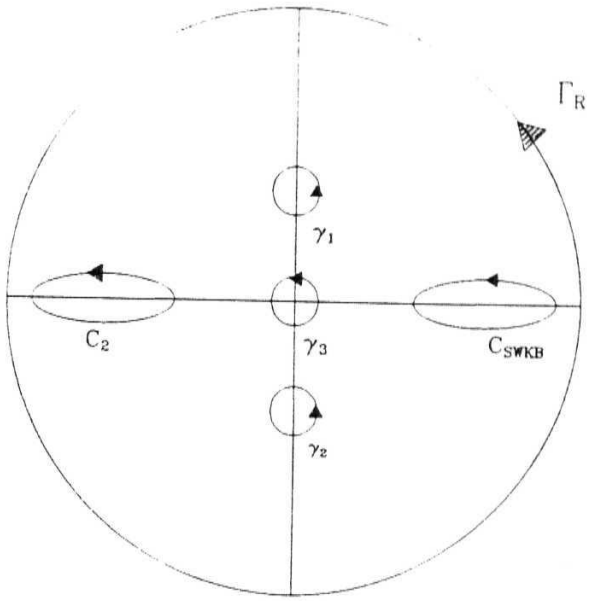

Figure 7.2: Contours for the Scarf I potential.

enclose all the singularities inside a large circle Γ_R of radius R (see Fig. 7.2). We thus have

$$J_{\Gamma_R} = J_{\text{SWKB}} + J_{C_2} + J_{\gamma_1} + J_{\gamma_2} + J_{\gamma_3} \quad , \tag{7.22}$$

where J_{Γ_R} is the contour integral for the circle Γ_R; J_{γ_1}, J_{γ_2} and J_{γ_3} are the contour integrals evaluated along the contours γ_1, γ_2 and γ_3 enclosing the poles at $y = i, -i$ and 0 respectively, and J_{C_2} is the integral along the counterclockwise contour C_2 enclosing the branch cut in the real $y < 0$ region. These contour integrals are given by

$$J_{\Gamma_R} = \frac{1}{\pi} \oint_{\Gamma_R} \frac{\sqrt{E - \tilde{\omega}^2(y)}dy}{\alpha(y^2+1)} \quad , \tag{7.23}$$

and similar equations for the other ones.

The contour integral J_{Γ_R} is once again calculated by the change **of variable** $z \to 1/y$and **we** have,

$$J_{\Gamma_R} = \frac{1}{\pi}\oint_{\gamma_0} \frac{\sqrt{E-\tilde{\tilde{\omega}}^2(z)}dz}{\alpha(1+z^2)} \tag{7.24}$$

$$\equiv J_{\gamma_0} \quad . \tag{7.25}$$

In this case also, due to the symmetry under $y \to -y$ of the QHJ equation, the turning points on the real axis in the classical region, $y > 0$, are interchanged with those in $y < 0$ region, and we have that J_{SWKB} and J_{C_2} are equal (see Fig. 7.2). Therefore,

$$J_{\text{SWKB}} = \frac{1}{2}\left(J_{\gamma_0} - J_{\gamma_1} - J_{\gamma_2} - J_{\gamma_3}\right) \quad . \tag{7.26}$$

The various integrals appearing on the right hand side of the above equation can be computed in a straightforward fashion except that once again care is needed to define the multiple valued function $\sqrt{E-\tilde{\omega}^2(y)}$. This is done following a procedure similar to that used for the generalized Pöschl-Teller potential . The values of the integrals obtained are also listed in the Table 7.1. The exact action integral for the Scarf-I potential has been evaluated using the QHJ formalism in the previous chapter VI [12] and is given by an expression similar to (7.26):

$$J(E) = \frac{1}{2}\left(I_{\gamma_0} - I_{\gamma_1} - I_{\gamma_2} - I_{\gamma_3}\right) \quad . \tag{7.27}$$

where, in the above equation, the integrals are to be taken as

$$I_{\gamma_k} = -\frac{1}{\pi}\oint_{\gamma_k} \frac{\tilde{p}(y)dy}{\alpha(1+y^2)} \quad . \tag{7.28}$$

The values of these integrals were computed in [12] and are given in the Table 7.1. It is now clear that, for the two potentials under study, we have the relation

$$J_{\text{SWKB}} = J(E) \quad , \tag{7.29}$$

for the unbroken case. For the broken case we have.

$$J_{\rm SWKB} = J(E) + \frac{\hbar}{2} \tag{7.30}$$

and the exact quantization condition $J(E) = n\hbar$. valid for all potentials, becomes $J_{\rm SWKB} - n\hbar$ when SUSY is unbroken, and $J_{\rm SWKB} = (n + \frac{1}{2})\hbar$ for these two potentials when the supersymmetry is broken. Similar analysis have been carried out for the Eckart, Rosen-Morse II, Scarf II (all hyperbolic); and the Rosen-Morse I superpotentials which are known to have cases of unbroken SUSY for entire range of parameters. A and B and we see that SWKB is exact for these cases for the same reason.

7.2 Analysis of potentials of the type $V(x) = \omega^2(x) + \hbar\beta\omega'(x)$

We have applied the QHJ method to study a general one parameter dependent Hamiltonian

$$H = p^2 + \omega^2(x) + \hbar\beta\omega'(x),$$

which reproduces the partner Hamiltonians H_+ and H_- for specific values of this parameter 0. It may be noted that β is not a scaling factor. The poles and the corresponding residues of the QMF are evaluated after taking into account the boundary condition.

We briefly highlight the analysis for generalized Pöschl-Teller superpotential given by,

$$\omega(x) = A\coth\alpha x - B\,{\rm cosech}\,\alpha x\ . \tag{7.31}$$

We thus have

$$\begin{aligned} V(x) &= \omega^2(x) + \beta\omega'(x) \ , \\ &= A^2 + (A^2 + B^2 - \beta A\alpha\hbar)\mathrm{cosech}^2\alpha x \\ &\quad - B(2A - \beta\alpha\hbar)\coth\alpha x\,\mathrm{cosech}\,\alpha x \ . \end{aligned} \tag{7.32}$$

making use of the transformation (7.6) as done earlier, the QHJ equation is given by

$$\tilde{p}^2 - \frac{i\hbar\alpha}{2}\frac{\partial\tilde{p}}{\partial y}(1-y^2) =$$
$$E - A^2 - B^2/A^2 - (A^2 + B^2 - A\alpha\beta\hbar)\frac{(y^2-1)^2}{4y^2} + B(2A - \alpha\hbar\beta)\frac{(y^4-1)}{4y^2} \tag{7.33}$$

The quantization condition remains the same as in the case of generalized Pöschl-Teller case as solved in chapter VI. [12]. With the inclusion of β in the potential, the singularity structure of QMF, $\tilde{p}(y, E)$ as well as $p_c(x,E)$ remains unchanged and the integral $J(E)$ is evaluated by,

$$J(E) = \frac{1}{2}(I_{\gamma_0} - I_{\gamma_1} - I_{\gamma_2} - I_{\gamma_3}) \ . \tag{7.34}$$

The contours for the integrals appearing in the above equation are given in Fig. 7.1. Given a_0, a_0' b_1 and b_1' are the residues for the contour integrals I_{γ_1}, I_{γ_2}, I_{γ_3}, and I_{γ_0} respectively, the residues at different poles are determined by substituting Laurent expansion in the QHJ equation. The QHJ equation, being non-linear gives quadratic equations for the residues which are required to compute various contour integrals I_{γ_k}. The procedure for picking the correct root for the residues remains exactly the same as carried out in chapter VI [12]. We thus have the values for these residues as,

$$a_0 = i\sqrt{|E - A^2|} \ , \tag{7.35}$$

$$a_0' = -i\sqrt{|E - A^2|} \ , \tag{7.36}$$

$$b_1 = -i\frac{1}{2}\left(\alpha\hbar - |\sqrt{(2A + 2B - \alpha\hbar)^2 + 4(\beta + 1)\alpha\hbar(A + B)}|\right) \ , \tag{7.37}$$

$$b_1' = i\frac{1}{2}\left(\alpha\hbar - |\sqrt{(2A - 2B + \alpha\hbar)^2 + 4(\beta + 1)\alpha\hbar(B - A)}|\right) \tag{7.38}$$

for the range $A + B > 0$, $A - B > 0$, and $\beta \approx -1$ and tabulate the results for other ranges in Table 7.2. The energy eigenvalues for general β in terms of these residues is given by,

$$E_n = A^2 + (n\hbar\alpha + i(b_1 - b_1'))^2 \ ,$$

The various contour integrals appearing in (7.26) are computed as

$$\alpha I_{\gamma_1} = -\sqrt{|E - A^2|} \ , \tag{7.39}$$

$$\alpha I_{\gamma_2} = -\sqrt{|E - A^2|} \ , \tag{7.40}$$

$$\alpha I_{\gamma_3} = \frac{1}{2}\left(\alpha\hbar - |\sqrt{(2A + 2B - \alpha\hbar)^2 + 4(\beta + 1)\alpha\hbar(A + B)}|\right) \ , \tag{7.41}$$

$$\alpha I_{\gamma_0} = \frac{1}{2}\left(\alpha\hbar - |\sqrt{(2A - 2B + \alpha\hbar)^2 + 4(\beta + 1)\alpha\hbar(B - A)}|\right) \tag{7.42}$$

so that one can compare the results with the QHJ for $\beta = \pm 1$. The quantization condition $J(E) = n\hbar$ gives the energy eigenvalues. It is seen that the difference between the exact action integral, $J(E)$,and the approximate action integral,J_{SWKB}, cannot be expressed as a simple function of β. Except for the values $\beta = 0, \pm 1$, no simple modification of SUSY WKB quantization condition can give exact eigenvalues for all β. In addition to the generalized Poschl-Teller potential, we have also carried out calculations for the Eckart, Rosen-Morse II, Scarf II (all hyperbolic); and the Rosen-Morse I and Scarf I potential (trigonometric) superpotentials using the QHJ formalism for the entire range of parameters, A and B. Conclusions similar to those for generalized Poschl-Teller potential are found to be true for these other potentials modified by including the parameter β.

7.3 Analysis of non-exact SWKB approximation cases

We next consider the cases where lowest-order SWKB fail to give exact answer. We at first look at the potential [5, 13].

$$V(x) = \frac{1}{4}(x^2 + \frac{3}{4x^2}) - 2 + \frac{(3x^2 + x^4)}{(1 + x^4)} \quad . \tag{7.43}$$

with

$$\omega(x) = \frac{2x^6 + 3x^4 - x^2 - 6}{2x(x^2 + 1)(x^2 + 2)} \quad . \tag{7.44}$$

The SWKB quantization condition reads

$$J_{\text{SWKB}} = \frac{1}{2\pi} \oint_C \sqrt{E - \omega^2(x)} dx = n\hbar \quad , \tag{7.45}$$

It is noticed that the above integrand becomes zero at twelve points in the complex x plane, giving rise to six branch cuts. One of these branch cuts is included in the contour C. The integral around a branch cut on the negative axis is equal to the above integral due to the symmetry $x \to -x$.

The integrals around the other four branch cuts cannot be related to the integral J_C. We use J_{OBC} to denote the sum of the integrals along contours enclosing the four remaining branch cuts.

We now proceed with the evaluation of these integrals, in parallel to the examples considered earlier. Let J_{Γ_R} be a circular contour with the center at the origin and radius large enough to enclose all the singular points of the integrand. Note that the integrand has poles at $y = 0$; $y = \pm i$, and $y = \pm\sqrt{2}i$. The contour integral J_{Γ_R} is given by

$$J_{\Gamma_R} = 2n\hbar + J_{\text{OBC}} + J_{\gamma_1} + J_{\gamma_2} + J_{\gamma_3} + J_{\gamma_4} + J_{\gamma_5} \quad , \tag{7.46}$$

or

$$J_{\Gamma_R} - \sum_{p=1}^{5} J_{\gamma_p} = 2n\hbar - J_{\mathrm{OBC}} \quad , \tag{7.47}$$

where J_{γ_1}, J_{γ_2}, J_{γ_3}, J_{γ_4}, and J_{γ_5} are the corresponding contour integrals for the contours γ_1, γ_2, γ_3, γ_4, and γ_5, around $y = 0, +i, -i, +\sqrt{2}i$, and $-\sqrt{2}i$

Various contour integrals have been evaluated as before, and we get $J_{\gamma_1} = 3/2$, $J_{\gamma_2} = -1$, $J_{\gamma_3} = -1$, $J_{\gamma_4} = 1$, and $J_{\gamma_5} = 1$. The signs of the residues needed, have been fixed, making use of the boundary condition $p(x, E = 0) = i\omega(x)$,as discussed in chapter V. J_{Γ_R} is again calculated making the mapping $y \to 1/z$and looking for the residue of the pole at $z \to 0$. The corresponding contour integral is found to be

$$J_{\Gamma_R} = 2E + 3/2 \quad . \tag{7.48}$$

The SWKB quantization condition is equivalent to Eq. (7.47) and this condition involves the unknown integral J_{OBC}. Therefore, the complex variables approach cannot be used to complete the calculation of energy eigenvalues in SWKB approximation for the potential (7.43). However, it is easily checked that if we substitute the values of J_{Γ_R},J_{γ_1},J_{γ_2}, J_{γ_3}, $J_{\gamma_4}$and J_{γ_5} in

$$J_{\Gamma_R} - \sum_{p=1}^{5} J_{\gamma_p} = 2n\hbar \quad , \tag{7.49}$$

we obtain the exact eigenvalues.

Therefore, it is clear that if the sum of the contributions coming from other branch cuts is nonzero, the SWKB approximation will not be exact.

A similar analysis can be repeated for some of the other potentials. **It is known that** [5, **13] for**

$$V(x) = -1/x + \frac{x(x+2)}{(1+x+x^2/2)^2} + 1/16 \tag{7.50}$$

and

$$V(x) = (1-y^2)\left[-\lambda^2\nu(\nu+1) + \frac{1}{4}(1-\lambda^2)[2-(7-\lambda^2)y^2 + 5(1-\lambda^2)y^4]\right] . \tag{7.51}$$

with superpotentials,

$$\omega(x) = \frac{x^6 - 16x^4 - 56x^3 - 108x^2 - 240x - 192}{4x(x^2+2x+2)(x^3+6x^2+16x+24)} , \tag{7.52}$$

and

$$\omega(x) = \frac{1}{2}(1-\lambda^2)y(y^2-1)\mu_0\lambda^2 y , \tag{7.53}$$

SWKB does not give exact answers. We once again see that SWKB is not exact because of the contributions from the other branch cuts that are present in both these cases.

7.4 Conclusions

In conclusion, we have studied a class of Hamiltonians which exhibit both broken and unbroken SUSY for suitable values of the parameters appearing in the potentials. It is found that, both for the broken and unbroken phases of SUSY, the poles of the QMF match identically with that of the integrand $\sqrt{E-\omega^2(x)}$ appearing in the approximate quantization formula. However, for the broken case, there is a difference in the residues of the QMF and $\sqrt{E-\omega^2(x)}$ in the complex plane which gives rise

to the modified BSWKB quantization condition. Since these poles **determine the** eigenvalues completely the exactness of the semi-classical schemes is accounted **for.**

The finding that the residues of $\sqrt{E-\omega^2(x)}$ and QMF match for the unbroken SUSY, and do not match in the broken SUSY example, suggests that it is the quantum effect that breaks SUSY. It is interesting to note that the difference in residues for the above two cases is precisely $\hbar\pi$. Analysis of a general one parameter dependent Hamiltonian revealed that only for the unbroken and spontaneously broken cases of SUSY, the appropriate semi-classical quantization formulae can reproduce the exact spectra for the examples considered in the text.

We have shown using the complex contour technique, for several solvable potentials in one dimension, that SWKB gives exact results. We then compared it with the answers gotten using the quantum H-J method, from the *exact* quantization condition. This has provided some useful insight: It is the similarity of the singularity structure of $p(x, E)$ and $\sqrt{2m(E-\omega^2)}$ in the non-classical regions of the $x-$plane, namely the matching of the poles and the contributions from the residues evaluated, that is responsible for this exactness. Table 7.1 summarizes our results.

For the non-exact potentials, it is the inability to deform the contour appropriately because of the presence of other poles and branch cuts in the complex $x-$plane that prevents an exact solution in SWKB approach.

There are potentials **for** which the singularity structure of $\sqrt{E-\omega^2(x)}$ and of QMF are very different. In these cases, no simple SWKB type approximation is known which may give exact answers [13]. The QHJ analyses of these potentials is still in progress and will he presented as future work in this direction [14].

Table 7.1 : Values of contour integrals contributing to J_{SWKB} and $J(E)$

Potential	Range of Parameters	Contour γ_k	$J_{\gamma_k} \times \alpha$ (SWKB)	$J_{\gamma_k} \times \alpha$ (QHJ)
Generalized	$A - B > 0$,	γ_1	$-\sqrt{\lvert E - A^2 \rvert}$	$-\sqrt{\lvert E - A^2 \rvert}$
Pöschl-	and	γ_2	$-\sqrt{\lvert E - A^2 \rvert}$	$-\sqrt{\lvert E - A^2 \rvert}$
Teller	$A + B > 0$	γ_3	$-(A + B)/2$	$-(A + B)/2$
		γ_0	$(B - A)/2$	$(B - A - \alpha\hbar)/2$
Generalized	$A - B < 0$;	γ_1	$-\sqrt{\lvert E - A^2 \rvert}$	$-\sqrt{\lvert E - A^2 \rvert}$
Pöschl-	and	γ_2	$-\sqrt{\lvert E - A^2 \rvert}$	$-\sqrt{\lvert E - A^2 \rvert}$
Teller	$A + B < 0$	γ_3	$(A + B)/2$	$(A + B + \alpha\hbar)/2$
		γ_0	$(A - B)/2$	$(A - B)/2$
Generalized	$A + B > 0$	γ_1	$-\sqrt{\lvert E - A^2 \rvert}$	$-\sqrt{\lvert E - A^2 \rvert}$
Pöschl-	and	γ_2	$-\sqrt{\lvert E - A^2 \rvert}$	$-\sqrt{\lvert E - A^2 \rvert}$
Teller	$A - B < 0$	γ_3	$-(A + B)/2$	$-(A + B)/2$
		γ_0	$(A - B)/2$	$(A - B)/2$
Generalized	$A + B < 0$,	γ_1	$-\sqrt{\lvert E - A^2 \rvert}$	$-\sqrt{\lvert E - A^2 \rvert}$
Pöschl-	and	γ_2	$-\sqrt{\lvert E - A^2 \rvert}$	$-\sqrt{\lvert E - A^2 \rvert}$
Teller	$A - B > 0$	γ_3	$(A + B)/2$	$(A + B)/2$
		γ_0	$(B - A)/2$	$(B - A - \alpha\hbar)/2$
Scarf I	$A - B < 0$	γ_1	$-\sqrt{E + A^2}$	$-\sqrt{E + A^2}$
(trigono-	and	γ_2	$-\sqrt{E + A^2}$	$-\sqrt{E + A^2}$
metric)	$A + B > 0$	γ_3	$(A + B)/2$	$(A + B + \alpha\hbar)/2$
		γ_0	$(A - B)/2$	$(A - B)/2$
Scarf I	$A - B > 0$	γ_1	$-\sqrt{E + A^2}$	$-\sqrt{E + A^2}$
(trigono-	and	γ_2	$-\sqrt{E + A^2}$	$-\sqrt{E + A^2}$
metric)	$A + B < 0$	γ_3	$-(A + B)/2$	$-(A + B)/2$
		γ_0	$-(A - B)/2$	$-(A - B + \alpha\hbar)/2$
Scarf I	$A - B > 0$	γ_1	$-\sqrt{E + A^2}$	$-\sqrt{E + A^2}$
(trigono-	and	γ_2	$-\sqrt{E + A^2}$	$-\sqrt{E + A^2}$
metric)	$A + B > 0$	γ_3	$(A + B)/2$	$(A + B + \alpha\hbar)/2$
		γ_0	$(A - B)/2$	$(A - B + \alpha\hbar)/2$
Scarf I	$B < A < 0$;	γ_3	$i(A + B)/2$	$i(A+B)/2$
(trigono-	$A > 0, B < 0$	γ_1	$-\sqrt{E + A^2}$	$-\sqrt{E + A^2}$
metric)	$A - B > 0$	γ_2	$-\sqrt{E + A^2}$	$-\sqrt{E + A^2}$
		γ_0	$(B - A)/2$	$(B - A)/2$

Table 7.2 : Values of residues and energy eigenvalues for potentials of the type $\omega'(x) + \beta\omega'$.

Potential	Range of Parameters	Pole at	Residue	Energy eigenvalues
		1	$a_0 = i\sqrt{\lvert E - A^2\rvert}$	$E_n =$
Generalized	$A + B > 0$	-1	$a_0' = -i\sqrt{\lvert E - A^2\rvert}$	$A^2 + (n\hbar\alpha +$
Pöschl-	and	0	$b_1 = -i\frac{\alpha\hbar - \lvert\sqrt{(\alpha\hbar+2(A+B))^2 - 4(A+B)(1+\beta)\alpha\hbar}\rvert}{4}$	$i(b_1 - b_1'))^2$
Teller	$A - B > 0$	∞	$b_1' = -i\frac{\alpha\hbar + \lvert\sqrt{(\alpha\hbar+2(A-B))^2 + 4(B-A)(\beta+1)\alpha\hbar}\rvert}{4}$	
		1	$a_0 = i\sqrt{\lvert E - A^2\rvert}$	$E_n =$
Generalized	$A + B < 0$	-1	$a_0' = -i\sqrt{\lvert E - A^2\rvert}$	$A^2 + (n\hbar\alpha +$
Pöschl-	and	0	$b_1 = -i\frac{\alpha\hbar + \lvert\sqrt{(\alpha\hbar+2(A+B))^2 - 4(A+B)(\beta+1)\alpha\hbar}\rvert}{4}$	$i(b_1 - b_1'))^2$
Teller	$A - B < 0$	∞	$b_1' = -i\frac{\alpha\hbar - \lvert\sqrt{(\alpha\hbar+2(A-B))^2 + 4(B-A)(\beta+1)\alpha\hbar}\rvert}{4}$	
		1	$a_0 = i\sqrt{\lvert E - A^2\rvert}$	$E_n =$
Generalized	$A + B > 0$	-1	$a_0' = -i\sqrt{\lvert E - A^2\rvert}$	$A^2 + (n\hbar\alpha +$
Pöschl-	and	0	$b_1 = -i\frac{\alpha\hbar - \lvert\sqrt{(\alpha\hbar+2(A+B))^2 - 4(A+B)(\beta+1)\alpha\hbar}\rvert}{4}$	$i(b_1 - b_1'))^2$
Teller	$A - B < 0$	∞	$b_1' = -i\frac{\alpha\hbar - \lvert\sqrt{(\alpha\hbar+2((A-B))^2 + 4(B-A)(\beta+1)\alpha\hbar}\rvert}{4}$	
		1	$a_0 = i\sqrt{\lvert E - A^2\rvert}$	$E_n =$
Generalized	$A + B < 0$	-1	$a_0' = -i\sqrt{\lvert E - A^2\rvert}$	$A^2 + (n\hbar\alpha +$
Pöschl-	and	0	$b_1 = -i\frac{\alpha\hbar + \lvert\sqrt{(\alpha\hbar+2(A+B))^2 - 4(A+B)(\beta+1)\alpha\hbar}\rvert}{4}$	$i(b_1 - b_1'))^2$
Teller	$A - B > 0$	∞	$b_1' = -i\frac{\alpha\hbar - \lvert\sqrt{(\alpha\hbar+2(A-B))^2 + 4(B-A)(\beta+1)\alpha\hbar}\rvert}{4}$	

Table 7.3 : Values of residues and energy eigenvalues for potentials of the type $\omega'(x) + \beta\omega'$.

Potential	Range of Parameters	Pole at	Residue	Energy eigenvalues
Scarf I (trigo-nometric)	$A+B>0$; and $A-B>0$	i	$a_0 = -\sqrt{E+A^2}$	$E_n =$
		$-i$	$a_0' = \sqrt{E+A^2}$	$-A^2 + (n\hbar$
		0	$b_1 = -i\frac{\alpha\hbar+\lvert\sqrt{(\alpha\hbar+2(A+B))^2-4(\beta+1)(A+B)\alpha\hbar}\rvert}{4}$	$i(b_1 - b_1'))^2$
		∞	$b_1' = i\frac{\alpha\hbar+\lvert\sqrt{(\alpha\hbar+2(A-B))^2+4(\beta+1)(B-A)\alpha\hbar}\rvert}{4}$	
Scarf I (trigo-nometric)	$A+B<0$; and $A-B<0$	i	$a_0 = -\sqrt{E+A^2}$	$E_n =$
		$-i$	$a_0' = \sqrt{E+A^2}$	$-A^2 + (n\hbar$
		0	$b_1 = -i\frac{\alpha\hbar-\lvert\sqrt{(\alpha\hbar+2(A+B))^2-4(\beta+1)(A+B)\alpha\hbar}\rvert}{4}$	$i(b_1 - b_1'))^2$
		∞	$b_1' = i\frac{\alpha\hbar-\lvert\sqrt{(\alpha\hbar+2(A-B))^2+4(\beta+1)(B-A)\alpha\hbar}\rvert}{4}$	
Scarf I (trigo-nometric)	$A+B>0$; and $A-B<0$	i	$a_0 = -\sqrt{E+A^2}$	$E_n =$
		$-i$	$a_0' = \sqrt{E+A^2}$	$-A^2 + (n\hbar$
		0	$b_1 = -i\frac{\alpha\hbar+\lvert\sqrt{(\alpha\hbar+2(A+B))^2-4(\beta+1)(A+B)\alpha\hbar}\rvert}{4}$	$i(b_1 - b_1'))^2$
		∞	$b_1' = i\frac{\alpha\hbar-\lvert\sqrt{(\alpha\hbar+2(A-B))^2+4(\beta+1)(B-A)\alpha\hbar}}{4}$	
Scarf I (trigo-nometric)	$A+B<0$; and $A-B>0$	i	$a_0 = -\sqrt{E+A^2}$	$E_n =$
		$-i$	$a_0' = \sqrt{E+A^2}$	$-A^2 + (n\hbar$
		0	$b_1 = -i\frac{\alpha\hbar-\lvert\sqrt{(\alpha\hbar+2(A+B))^2-4(\beta+1)(A+B)\alpha\hbar}\rvert}{4}$	$i(b_1 - b_1'))^2$
		∞	$b_1' = i\frac{\alpha\hbar+\lvert\sqrt{(\alpha\hbar+2(A+B))^2+4(\beta+1)(B-A)\alpha\hbar}}{4}$	

Table 7.4 : Values of residues and energy eigenvalues for potentials of the type $\omega'(x) + \beta\omega'$.

Potential	Range of Parameters	Pole at	Residue	Energy eigenvalues
		0	$a_0 = -i\sqrt{\lvert E - A^2 - B^2/A^2 - 2B\rvert}$	$E_n = A^2 + B^2/A^2 -$
	$A > 0$	∞	$a_0' = i\sqrt{\lvert E - A^2 - B^2/A^2 + 2B\rvert}$	$(\frac{ib_1}{2} + n\hbar\alpha)^2 -$
Eckart		1	$b_1 = -i(\alpha\hbar - \lvert\sqrt{(\alpha\hbar - 2A)^2 + 4(\beta+1)A\alpha\hbar}\rvert)$	$B^2/(\frac{ib_1}{2} + n\hbar\alpha)$
(Hyper-				
bolic)		0	$a_0 = -i\sqrt{\lvert E - A^2 - B^2/A^2 - 2B\rvert}$	$E_n = A^2 + B^2/A^2 -$
	$A > 0$	∞	$a_0' = i\sqrt{\lvert E - A^2 - B^2/A^2 + 2B\rvert}$	$(\frac{ib_1}{2} + n\hbar\alpha)^2 -$
		1	$b_1 = -i(\alpha\hbar + \lvert\sqrt{(\alpha\hbar - 2A)^2 + 4(\beta+1)A\alpha\hbar}\rvert)$	$B^2/(\frac{ib_1}{2} + n\hbar\alpha)$
		0	$a_0 = -i\sqrt{\lvert E - A^2 - B^2/A^2 - 2B\rvert}$	$E_n = A^2 + B^2/A^2 -$
	$A > 0$	∞	$a_0' = i\sqrt{\lvert E - A^2 - B^2/A^2 + 2B\rvert}$	$(-\frac{ib_1}{2} + n\hbar\alpha)^2 -$
Rosen		-1	$b_1 = i(\alpha\hbar - \lvert\sqrt{(\alpha\hbar - 2A)^2 + 4(\beta+1)A\alpha\hbar}\rvert)$	$B^2/(\frac{-ib_1}{2} + n\hbar\alpha)$
Morse II				
(Hyper-		0	$a_0 = -i\sqrt{\lvert E - A^2 - B^2/A^2 - 2B\rvert}$	$E_n = A^2 + B^2/A^2 -$
bolic)	$A < 0$	∞	$a_0' = i\sqrt{\lvert E - A^2 - B^2/A^2 + 2B\rvert}$	$(-\frac{ib_1}{2} + n\hbar\alpha)^2 -$
		-1	$b_1 = i(\alpha\hbar + \lvert\sqrt{(\alpha\hbar - 2A)^2 + 4(\beta+1)A\alpha\hbar}\rvert)$	$B^2/(-ib_1/2 + n\hbar\alpha)$

Table 7.5 : Values of residues and energy eigenvalues for potentials of the type $\omega(x) + \beta\omega'$.

Potential	Range of Parameters	Pole at	Residue	Energy eigenvalues
Rosen Morse II (Trigonometric)	$A > 0$	0	$a_0 = -\sqrt{E + A^2 - B^2/A^2 + 2iB}$	$E_n = A^2 + B^2/A^2 - -(-\frac{b_1}{2} + nh\alpha)^2 - B^2/(\frac{-b_1}{2} + nh\alpha)$
		∞	$a_0' = \sqrt{E + A^2 - B^2/A^2 - 2iB}$	
		-1	$b_1 = -(\alpha h - \lvert\sqrt{(\alpha h - 2A)^2 + 4(\beta + 1)A\alpha h}\rvert)$	
	$A < 0$	0	$a_0 = -\sqrt{\lvert E + A^2 - B^2/A^2 + 2iB\rvert}$	$E_n = -A^2 + B^2/A^2 + (-\frac{b_1}{2} + nh\alpha)^2 - B^2/(-\frac{b_1}{2} + nh\alpha)$
		∞	$a_0' = i\sqrt{E + A^2 - B^2/A^2 - 2iB}$	
		-1	$b_1 = -(\alpha h + \lvert\sqrt{(\alpha h - 2A)^2 + 4(\beta + 1)A\alpha h}\rvert)$	
Scarf II (Hyperbolic)	$A > 0$	0	$a_0 = -i\sqrt{\lvert E - A^2\rvert}$	$E_n = A^2 - (b_1 - b_1')/2 + n\alpha h)^2$
		∞	$a_0' = i\sqrt{\lvert E - A^2\rvert}$	
		i	$b_1 = \frac{\alpha h - \lvert\sqrt{(\alpha h - 2(A - iB))^2 - 4(\beta+1)(A - iB)\alpha h}\rvert}{2}$	
		$-i$	$b_1 = \frac{-\alpha h + \lvert\sqrt{(\alpha h + 2(A + iB))^2 - 4(\beta+1)(A + iB)\alpha h}\rvert}{2}$	
	$A < 0$	0	$a_0 = -i\sqrt{\lvert E - A^2\rvert}$	$E_n = A^2 - (b_1 - b_1')/2 + n\alpha h)^2$
		∞	$a_0' = \sqrt{\lvert E - A^2\rvert}$	
		i	$b_1 = \frac{\alpha h + \lvert\sqrt{(\alpha h)^2 + 4(A - iB)^2 - 4(\beta+1)(A - iB)\alpha h}\rvert}{2}$	
		$-i$	$b_1 = \frac{-\alpha h - \lvert\sqrt{(\alpha h - 2(A - iB))^2 - 4(\beta+1)(A + iB)\alpha h}\rvert}{2}$	

References

[1] A. Comtet, A. Bandrauk and D. Campbell, Phys. Lett. **B150**, (1985) 159: A. Khare, Phys. Lett. **B161,** (1985) 131.

[2] CM. Bender, K. Olaussen and P.S. Wang, Phys. Rev. **D6,** 1740 (1977).

[3] R. Adhikari, R. Dutt, and U.P. Sukhatme, Phys. Rev. **A38,** 1679 (1988).

[4] K. Raghunathan, M. Seetharaman aud S.S. Vasan, Phys. Lett. **B188,** 351 (1987).

[5] A. Khare and Y.P. Varshni Phys. Lett. **A142, 1** (1989).

[6] D.T. Barclay, A. Khare and U. Sukhatme, [UICHEP-TH/93-13] (Sept. 1993)

[7] E. Witten, *Nucl. Phys.* **B188,** 513 (1981); A. Jevicki and J.P. Rodrigues, *Phys. Lett.* **B146,** 55 (1984); T. Imbo and U.P. Sukhatme, *Phys. Rev.* **D33,** 3147 (1986); P.K. Panigrahi and U.P. Sukhatme, *Phys. Lett.* **A178,** 251 (1993).

[8] A. Inomata and G. Junker, in *Proc. Adriatic Research Conf. on path-integration and its applications, ICTP, Italy, 3-6 Sept.* (1991);

[9] R. Dutt, A. Gangopadhyaya, A. Khare, A Pagnamenta and U. Sukhatme, Phys. Rev **A48,** 1845 (1993).

[10] R. Dutt, A. Gangopadhyaya, A. Khare, A. Pagnamenta and U.P. Sukhatme, *Phys. Lett.* **A174,** 363 (1993).

[11] R.S. Bhalla, A.K. Kapoor and P.K. Panigrahi, MRI preprint. MRI-PHY/96-19 (1996).

[12] R.S. Bhalla, A.K. Kapoor and P.K. Panigrahi, MRI preprint. MRI-PHY/96-17 (1996).

[13] D. DeLaney and M.M. Nieto Phys. Lett. **B247,** 301 (1990).

[14] R.S. Bhalla, A.K. Kapoor and P.K. Panigrahi (under preparation).